INFORMATION TO USERS

This manuscript has been reproduced from the microfilm master. UMI films the text directly from the original or copy submitted. Thus, some thesis and dissertation copies are in typewriter face, while others may be from any type of computer printer.

The quality of this reproduction is dependent upon the quality of the copy submitted. Broken or indistinct print, colored or poor quality illustrations and photographs, print bleedthrough, substandard margins, and improper alignment can adversely affect reproduction.

In the unlikely event that the author did not send UMI a complete manuscript and there are missing pages, these will be noted. Also, if unauthorized copyright material had to be removed, a note will indicate the deletion.

Oversize materials (e.g., maps, drawings, charts) are reproduced by sectioning the original, beginning at the upper left-hand corner and continuing from left to right in equal sections with small overlaps.

ProQuest Information and Learning
300 North Zeeb Road, Ann Arbor, MI 48106-1346 USA
800-521-0600

Electrochemical Studies of Volume Phase Transitions of Temperature-Responsive Polymeric Gels

by

Weimin Zhang

A Dissertation submitted to the Graduate Faculty in Chemistry in partial fulfillment of the requirements for the degree of Doctor of Philosophy, The City University of New York

2004

UMI Number: 3115304

UMI Microform 3115304

ProQuest Information and Learning Company
300 North Zeeb Road
P.O. Box 1346
Ann Arbor, MI 48106-1346

This manuscript has been read and accepted for the Graduate Faculty in Chemistry in satisfaction of the dissertation requirement for the degree of Doctor of Philosophy.

12/29/2003

Date

Chair of Examining Committee

1/5/2004

Date

Executive Office

Supervisory Committee

The City University of New York

Abstract

Electrochemical Studies of Volume Phase Transitions of Temperature-Responsive Polymeric Gels

by

Weimin Zhang

Adviser: Professor Malgorzata Ciszkowska

The objective of this project is to study volume phase transition of polymeric gels utilizing electroanalytical techniques. Two types of gels, poly(*N*-isopropylacrylamide), (NIPA), and poly(*N*-isopropylacrylamide-*co*-acrylic acid), (NIPA-AA), were studied in our project.

The oxidation of electroactive probes, which include 1,1'-ferrocenedimethanol ($Fc(MeOH)_2$), 4-hydroxy-tempo (TEMPO), Ferrocenylmethyltrimethylammonium ion ($FcTMA^+$) and Hexaammineruthenium(III) ion ($Ru(NH_6)^{3+}$) was studied in aqueous solutions and swollen state NIPA and NIPA-AA gels using Pt microdisk electrodes. The diffusion coefficient (D) of $Fc(MeOH)_2$ in swollen state of gels is only about 15% - 55% smaller than that in aqueous solution. However, the viscosity of these gels is approximately 5 orders of magnitude greater than that of aqueous solution. The value of activation energy (E_a) for the diffusion of $Fc(MeOH)_2$ in aqueous solution and in NIPA and NIPA-AA gels was almost identical. These data suggest that microscopic viscosity of solvent trapped in swollen gel network is similar to that in aqueous solutions.

A decrease of the D of a probe in swollen gels was analyzed in terms of "obstruction effect" and "hydration effect". A new model was developed to explain this phenomenon and experimental results were compared with predictions of that model.

For NIPA gels, after the volume phase transition, the D of $Fc(MeOH)_2$ in collapsed gels decreased approximately 2 orders of magnitude when the gel collapsed. D of $Fc(MeOH)_2$ in collapsed NIPA-AA gels does not change significantly.

Voltammetric experiments were also carried out for positively charged $FcTMA^+$ and $Ru(NH_3)_6^{3+}$ in NIPA-AA gels with and without supporting electrolyte. After the volume phase transition occurs, a decrease of the D of both probes was observed. Such decrease is more pronounced in NIPA-AA gel without supporting electrolyte than that with supporting electrolyte.

UV-vis spectroscopy was used to study the distribution of $Fc(MeOH)_2$ between the collapsed polymer phase and released solution during the volume phase transition. The estimated concentration of $Fc(MeOH)_2$ in collapsed phase is 4.5 times higher than that in the original swollen gel and 6 times higher than that in released liquid.. The concentration of $Fc(MeOH)_2$ in collapsed NIPA-AA gel is about 20% higher than that in original swollen gels.

Dedication

This thesis is dedicated to my father and mother, Yong Zhang and Xiuqing Xu, who worked so hard in their lives so that my sisters and I would not have to. I would also like to thank my wife. Liya Ren. Without her constant moral support and help I would not have been able to complete this work.

Acknowledgment

I would like to express my deepest gratitude to Professor Malgorzata Ciszkowska for her guidance, her patience and her understanding throughout my long association with her.

Acknowledgment is also due to Brooklyn College of the City University of New York in the form of teaching assistantships and to the Office of Naval Research award program under grant number N00014-98-1-0244, and the PSC-CUNY Reach Award under grant number 62385 00 31

Table of Contents

List of Tables

List of Figures

CHAPTER 1 Introduction

1.1 Polymeric gels

Polymeric gels are commonly defined as three-dimensional polymer networks swollen by fluids.[1] The major component of a gel is a liquid; in some cases it can be as much as 99% of a gel. Since polymeric gels have properties of both solid and liquid phase, they are also called "solid liquids".

The unique properties of gels allow them to be useful in various applications. In biological systems, almost all reactions and activities occur in aqueous solutions; where the system needs to retain its shape. Nature uses polymeric gels as containers to retain water as an entity. Polymeric gels are the bases for multibillion dollar business that affect all areas of our lives. They are used in pharmaceutical industries as drug controlled-release media, bioadhesives and enteric dosage forms. Gels are inexpensive and indispensable materials for industrial separations, such as sewage treatment, membrane process, and protein and biological synthesis processes. Gels are also used to fabricate soft contact lenses, artificial lenses, artificial vitreous, and materials for plastic surgeries.

1.2 Phase transition of polymeric gels.

Numerous polymeric gels have been designed, synthesized and utilized in various sides of our lives from as early as the 1940's. The last two decades have witnessed a remarkable progress in the research on polymeric gels, and they are still

under intensive studies currently. One reason for such kind of thorough researches can be contributed to the discovery of smart gels. [2] The "intelligence" of smart gels arises from the gels' unique feature of existing in two states, the swollen and collapsed state. The transformation of a gel from one state to the other is generally defined as the volume phase transition. When phase transition of a gel occurs, the volume change of the system can be as large as 1000 times. The volume phase transition of a gel occurs when it is stimulated by chemical or physical factors, such as temperature, solvent composition, pH, ionic strength, and electromagnetic radiation.

Theoretical studies of phase transitions of polymeric gels can be tracked back to 1968. Dusek and Patterson [3] predicted that when external forces are applied to the gels, the volume of those gels might undergo discontinuous change. A similar phenomenon, known as coil-globule transition, also exists in linear polymers. In a sense, the phase transition of gels is a macroscopic manifestation of a coil-globule transition. The microscopic and macroscopic views of phase transition are shown in figure 1.1 and figure 1.2. In 1975, volume phase transition of polymeric gel was observed for the first time by Tanaka. [4] When he used quasielastic light scattering to study acrylamide gels in water, he found that at –17 °C the fluctuations of polymer network diverged. By measuring the refractive index of a gel, he eliminated the possibility of ice formation in gels at low temperature. Tanaka placed acrylamide gels in acetone-water mixtures with different concentrations of acetone at room temperature. After one day, he found half of the gels in swollen state and half of the gels in collapsed state. [5] Accidentally, he

discovered the volume phase transition of gels, and opened a new era of study of polymeric gels.

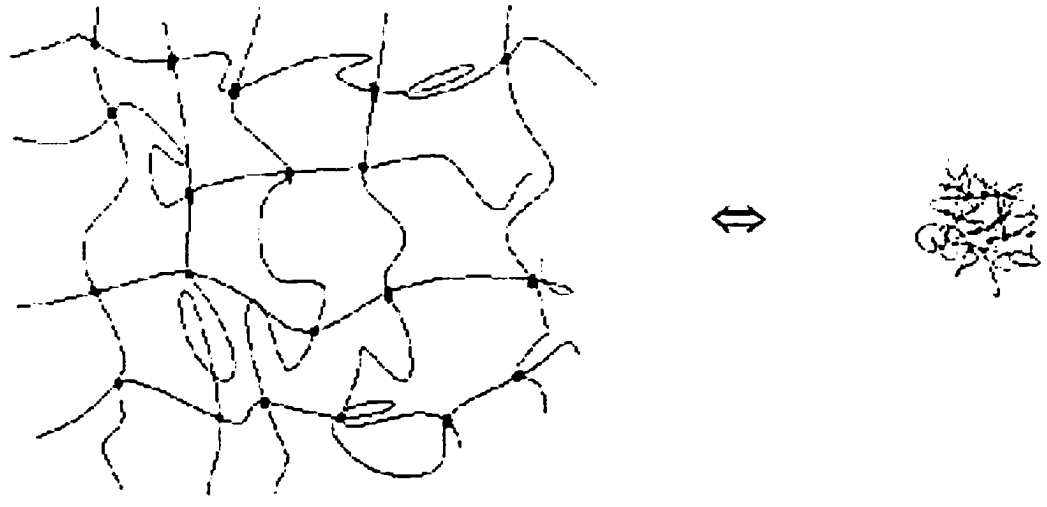

Swollen state of gels Collapsed state of gels

Figure 1.1 The microscopic view of phase transition of polymeric gel – unfolding and folding of polymer network

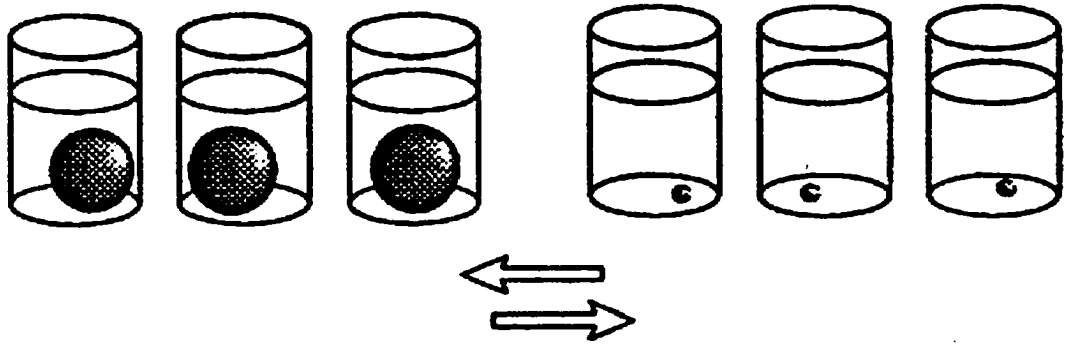

Figure 1.2 The macroscopic view of reversible phase transition of polymeric gel

1.3 Mechanism of volume phase transition of polymeric gels

The volume phase transition of a polymeric gel is a result of a competitive balance between repulsive forces that act to expand the polymer network and attractive forces that act to shrink the polymer network. The repulsive forces include the electrostatic interaction between the polymer charges of the same kind and the osmotic pressure by counter ions. The attractive forces include van der Waals, hydrophobic interaction, ion-ion interaction, and hydrogen bonding. The magnitude, temperature dependence, properties among these forces is quite different in gels.

Volume phase transition of partially hydrolyzed acrylamide gel is believed to be due to Van der Waals interaction. [2] The major attraction force between polymer chains is Van der Waals force. A poor nonpolar solvent must be added to solvent in order to increase this interaction large enough to induce volume phase transition of this gel.

Poly(N-isopropylacrylamide) and poly(N-isopropylacrylamide-co-acrylic acid) hydrogels are temperature responsive gels. The temperature sensitivity of these gels is due to the hydrophobic interactions between a polymeric network and water. These gels undergo a discontinuous, reversible volume phase transition; they are swollen at low temperatures and they collapse at higher temperatures. [6-9] Without ionizable acrylic acid, the phase transition temperature of poly(N-isopropylacrylamide) gels is 32°C. As the concentration of acrylic acid increases, the phase transition temperature increases. One simple explanation for this phenomenon is that, the polymer chain is less hydrophobic at low temperature and, therefore, the polymer chain has more water

molecules bonded around it. At high temperature, the polymer chain becomes more hydrophobic, and bonded water is excluded from the polymer network. As a result, (see Figure 1.3) the gel collapses and its volume decreases.

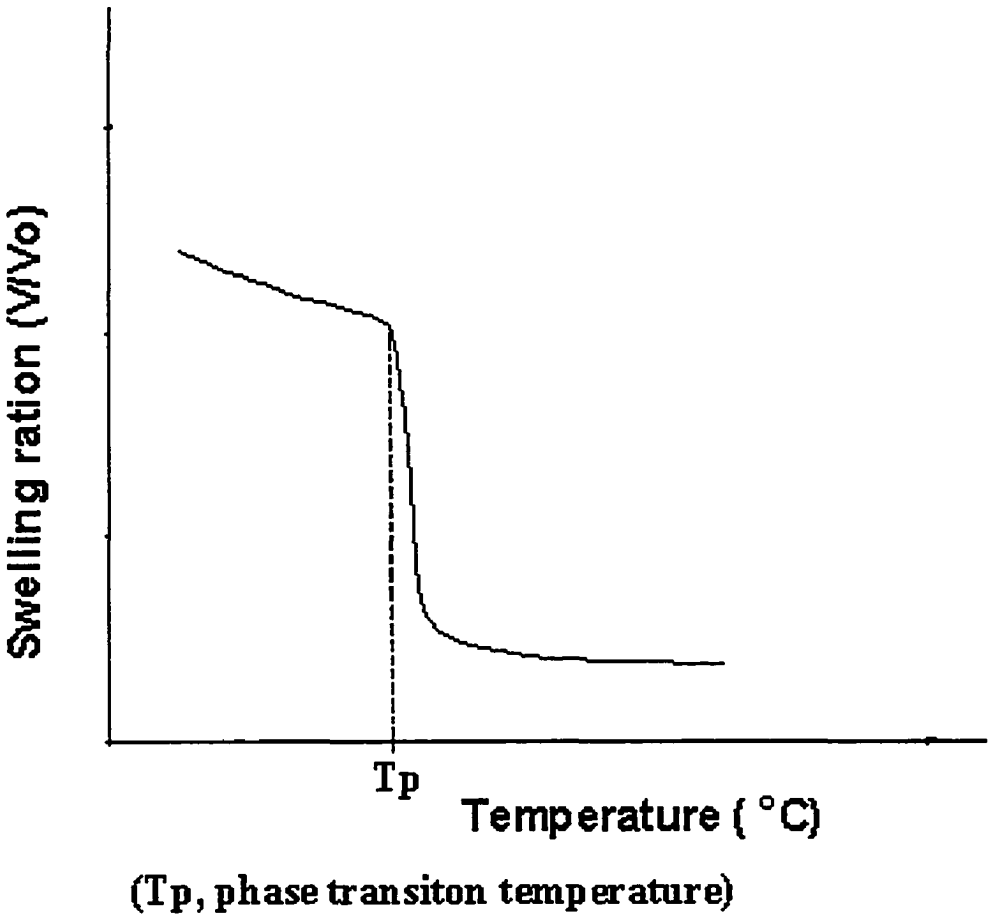

Figure 1.3 Schematic representation of the volume phase transition of a temperature responsive gel

The volume phase transition induced by hydrogen bonding was found in gels with an interpenetrating polymer network that consists of two independent polymer

networks. One example of such a gel formed by poly(acrylic acid) and poly(acrylamide) networks was found by Okano and his colleagues. [10] When swollen by water, this gel shrinks at low temperature and swells at high temperature.

Polymers having both cationic and anionic groups are called polyampholytes. Myoga and Katayama [11] studied such gels and found that the gel exists in a collapsed state at neutral pH because both cations and anions are ionized and they attract each other. At high or low pH, only one group of ions will be ionized. The most important interaction in these gels during the phase transition are the repulsive forces between the same charges on the polymer chains.

1.4 Phase transition of polymeric gels - Model

The volume phase transition of polymeric gels was quantitatively described in terms of "mean field theory" of swelling equilibrium of gels. [12] The theory gives the free energy of the gel in the form as

$$\Delta G = G_{mixing} + G_{rubber} + G_{counter\text{-}ion} \qquad (1.4.1)$$

$$\Delta G = kT[n\ln(1-\varphi)+\chi n\varphi]+\frac{3\nu kT}{2}(\alpha^2-1-\ln\alpha)-\nu fkT\ln(\frac{V_0\alpha^3}{n\upsilon_1}) \qquad (1.4.2)$$

where G_{mixing} represents the mixing free energy, G_{rubber} represents the free energy of rubber elasticity, $G_{counter\text{-}ion}$ is the osmotic pressure due to the counter ions, k is the Boltzmann constant, T is the absolute temperature, n is the number of solvent molecules in the gel, φ is the volume fraction of polymer network, χ is the polymer-solvent interaction parameter, ν is the total number of polymer chains in the gel, which can be

estimated from the amount of crosslinker used during the gel synthesis, α is the linear swelling ratio, V_o is the volume of the gel when polymer collective diffuses, υl is the molar volume of the solvent, and f is the number of counter ions per chain. In case of neutral gel, the term $G_{counter\text{-}ion}$ can be neglected.

In the equilibrium state, the osmotic pressure is zero (N is the Avogadro number).

$$\Pi = -\frac{N}{\upsilon 1}\left(\frac{\partial \Delta G}{\partial n_1}\right)_{T,P} = 0 \qquad (1.4.3)$$

Therefore, the osmotic pressure of a gel can be written as

$$\Pi = \Pi_{mixing} + \Pi_{rubber} + \Pi_{ion} =$$

$$= -\frac{NkT}{\upsilon 1}[\varphi + \ln(1-\varphi) + \chi\varphi 2] + \nu kT[\frac{\varphi}{2\varphi_0} - (\frac{\varphi}{\varphi_0})^{1/3}] + \nu fkT(\frac{\varphi}{\varphi_0}), \qquad (1.4.4)$$

where φ_0 is the volume fraction of polymers when the gel network has a random walk configuration, which can be estimated from the experimental asymptotic value of V/V_0, and ν is the number of polymer chains per unit volume of a gel at $\varphi = \varphi_0$. The polymer-solvent interaction parameter χ is temperature dependent, which can be expressed as:

$$\chi = \frac{\Delta F}{2kT} = \frac{\Delta H - T\Delta S}{2kT} \qquad (1.4.5)$$

where ΔF is the difference of the free energies of a polymer segment-segment, and polymer-solvent interaction, ΔH and ΔS are the corresponding enthalpy and entropy. Using the previous equations, the equation related to the equilibrium concentration of a gel to temperature can be expressed as

$$\frac{1}{T}=\frac{\Delta S}{\Delta H}+\frac{k}{\Delta H}[\frac{\upsilon_1 \nu}{N\varphi^2}((2f+1)(\frac{\varphi}{\varphi_0})-2(\frac{\varphi}{\varphi_0})^{1/3})-\frac{2}{\varphi}-\frac{2\ln(1-\varphi)}{\varphi_2}] \qquad (1.4.6)$$

where ν can be estimated from the amount of the cross-linker used during the gel preparation. Based on the equation 1.4.6, one can see that the transition temperature is primarily dependent on ratio of $\Delta H/\Delta S$. If ΔH and ΔS are determined, the curvature of a swelling curve can be resolved. [12] However, this theory fits poorly to the experiment result. When ΔH and ν were taken as variable parameters, the calculated curves reproduced the experimental data well. This modification created another question: the variable ΔH and ν are significantly larger than values from experiment. This discrepancy suggests that this model is too simplified. This theory should be reformulated by taking into account all various factors, such as free branches of polymer chain, non- Gaussian properties of chains, polydispersity of chains, etc. Therefore, several models were proposed to give a more precise description of the thermally induced discontinuous shrinkage of hydrogel. One of the models was suggested by Otake and his co-workers.[13] In their model, the free energy of a hydrogel is divided into four parts, the elastic free energy of polymer network, the osmotic pressure of dissociated counter ions in the gels, the free energy of interactions except for the hydrophobic interaction and the free energy of the hydrophobic interaction. Their new model is able to represent various types of volume phase transition including the "convexo" type. Sasaki [14-16] and Marchetti [17] also made significant contributions to the theory of volume phase transition of polymeric gels.

1.5 Smart gels

Many types of gels that respond to different kinds of stimuli have been designed and synthesized since the discovery of intelligent gels. In the following parts, some of the typical gel systems will be discussed.

- Light sensitive gels

Polymeric gels that undergo phase transition in response to light have been synthesized. Mamada and his colleagues [18] synthesized poly(N-ispropylacrylamide (NIPA)-co-bis(4-dimethylaminophenyl)-4'-vinylphenyl-methane-leucocyamide) hydrogels. At a fixed temperature, these gels discontinuously swell when exposed to ultraviolet light, and shrink when UV light is removed. The phase transition of these gels is induced by the cyanide ion created by the ultraviolet radiation, which changes the osmotic pressure of the system.

The second approach to prepare the light sensitive gel was to increase the local temperature within the temperature sensitive gels by absorbing energy of visible light. [19] The gel is a covalently cross-linked temperature sensitive N-ispropylacrylamide and chlorophylin copolymer network. The chromophore can absorb light, and subsequent thermal dissipation of light energy and the local temperature increment is proportional to the chlorophyllin density, thus proportional to the polymer density. The phase transition of this gel is presumably generated by local heating of the N-ispropylacrylamide polymer chain.

➢ Solvent sensitive gels

Some gels undergo phase transition as the solvent composition varies. For instance, acrylamide gel swells in water and gradually shrinks as acetone is added to the solution. [20]

➢ pH sensitive gels

pH-sensitive gels usually contain acidic or basic groups, such as carboxylic acids or primary amines which ionize in response to changes in pH, thus change the properties of the gels.[21,22] Poly(acrylic acid) and poly(methacrylic acid) hydrogels are among the first investigated ionic gels which swell when the pH of the solution increases.

➢ Biochemically sensitive gels

Biochemically sensitive gels undergo phase transition when particular molecules or ions are introduced. Biochemically active elements such as enzymes or receptors are incorporated into the gel network. When the target molecule or ion enters the gels, the active elements convert them into another compound or form a complex molecule. [23-26] Therefore, the equilibrium of the gel is disturbed and causes the gel to swell or collapse.

➢ Temperature-sensitive gels

Temperature responsive polymeric gels are the most intensively studied smart or intelligent gels. Many researchers have produced a variety of thermo-responsive gels and demonstrated that hydrophobic interactions play a very important role in the volume phase transition of these gels. In light of these findings, hydrogels whose monomers contain a hydrophobic group, usually an alkyl chain, and a hydrophilic group, usually an

amide function group, are expected to undergo temperature induced phase transition in water. Figure 1.4 shows some of monomers used for preparation of temperature responsive gels. The swelling behavior of these gels are quite different, due to the change of the side chain hydrophobilicity or copolymerization of hydrophilic/ hydrophobic monomers. The well known poly(N-ispropylacrylamide), polyNIPA, gel has a low phase transition temperature, 32-33 °C . With the incorporation of hydrophilic acrylic or sodium acrylate monomers, the phase transition temperature increases. [12, 27, 28] Temperature-sensitive hydrogels based on N-ethylacrylamide was prepared by Lowe and his colleagues. [29] The phase transition temperature of this gel is 78 °C for the homopolymeric gels. Poly(N-vinylisobutyramide) gel, an isomer of polyNIPA gel, in which the positions of the nitrogen and carbonyl are exchanged, has phase transition temperature of 40 °C. [30]

The relationship between a magnitude of hydrophobic interaction and swelling and shrinking behavior of a gel is still far from clear. For example, N-isopropylmeth-acrylamide contains one more methyl group than NIPA. Therefore, one might expect that N-isopropylmethacrylamide hydrogel would have a lower phase transition temperature than NIPA gel, which was reported as 32-33 °C. However, that is not the case; reported phase transition temperature for N-isopropylmethacrylamide hydrogel ranges from 39 to 47 °C, and further optical density experiments narrowed the value to about 45 °C. [31]

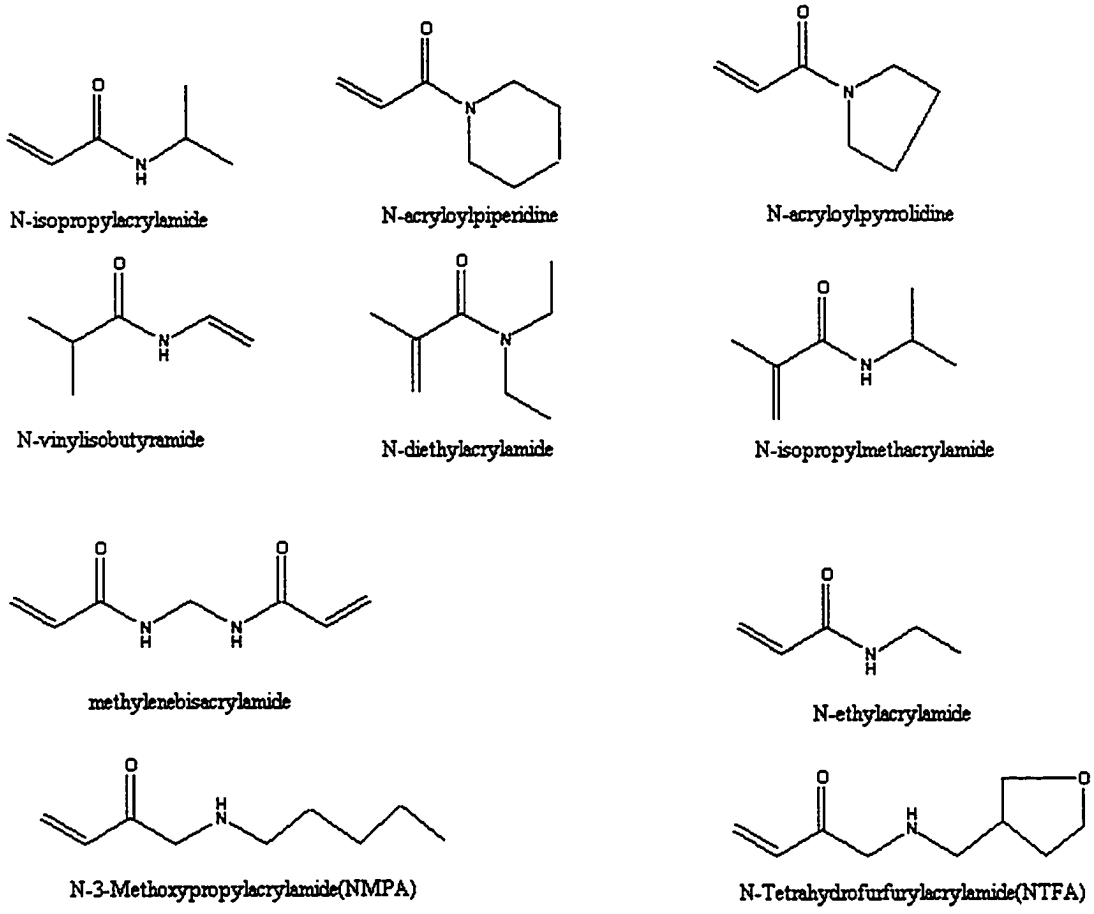

Figure 1.4 Monomers used in preparation of temperature responsive gels

Temperature responsive polymeric gels are very promising materials for drug-control-release-delivery system and actuator. One requirement for this kind of materials is a sharp and well-defined phase transition. However, a sharp phase transition may only occur at an optimum hydrophilic/hydrophobic balance, which was only found in the N-isopropylacrylamide networks. Other polymers,[32-37] such as poly N-ethylacrylamide, have a less abrupt phase transition. In contrast to the behavior of polyNIPA gels, the DSC scans showed that the transition of poly N-ethylacrylamide gels depends on concentration of polymer, and the transition is not reversible. Repeated measurements of the same sample were not identical. A series of N-Alkoxyalkylacryl-amide hydrogels (see figure 1.4) was studied by Naozumi Wada and his coworker. [34] These gels only gradually shrink upon heating within the temperature range 25-35 °C, and the volume of these gels does not change significantly within the temperature range studied. It is known that alkoxy groups have a hydrophilic property due to their oxygen atom possessing a lone pair electron. For this reason, they can form hydrogen bonding with water. This kind of a gel initially decreases in volume and then swells with the increasing temperature. One explanation for this was the thermal mixing which dominated the hydrophobic interaction.

Due to these unexpected discoveries, most of the current works on temperature responsive gels focus on poly(NIPA) and its copolymers. Water based poly(NIPA) gels have a low phase transition temperature of 32 °C, which is not very sensitive to the concentration of a polymer. Upon heating, poly(NIPA) gels undergo a distinct volume

phase transition by expelling water from gel network over a narrow temperature range.[38]

1.6 Kinetic of the volume phase transition

In some applications of smart gels such as drug delivery systems and actuators, quickly responsive gels are desired. Hence the kinetic process of the phase transition is a critical property of gels. The first theory of swelling and shrinking of spherical gel was developed by Tanaka and Fillmore (the TF theory), [39] whose theory was based on the equation of motion of gel network, which is regarded as the dynamics of thermal fluctuations of gel network.

According to TF theory, the speed of swelling of spherical gels is inversely proportional to the diffusion coefficient of gel network and to the square of the gel radius. The characteristic time of swelling of spherical gels is given as

$$\tau \equiv R^2/D \qquad 1.6.1$$

where R and D are the radius of the sphere shape gel and the cooperative diffusion coefficient of the gel, respectively, D is defined as $D = E/f$, where E is the longitudinal bulk modulus of the network, and f is the coefficient of friction between the network and the solvent in gel. The cooperative diffusion coefficient was introduced by Tanaka, Hocker, and Benedek, [40] and can be measured by laser light scattering spectroscopy. The TF theory was proposed for spherical gels only. In 1989, Li and Tanaka [41] introduced the shear modulus of the network into this model and made it suitable for the

swelling of cylinders and large disk gels. The nature of shear modulus is to keep the system in shape, for example minimize the nonisotropic deformation of gels. When the diameter of a spherical gel is the same as the diameter of a cylinder as the thickness of the disk, this model predicts that the effective diffusion constants of long cylinder and large disk gel are 1.5 and 3 times smaller than that of a spherical gel. The relaxation times of these long cylinder and large disk gels are approximately 2.0 and 5.7 times longer than that a sphere. This modified model had successfully predicted the swelling of long cylinder and large disk gel.

The TF theory suggests that the time of the volume phase transition of gels depend on the size of gels and cooperative diffusion coefficient of gel network. The smaller the gel the faster the gel can shrink or swell, the larger the cooperative diffusion coefficient the faster the gel shrinks and swells. For the bulky size NIPA gel, the volume phase transition is very slow. Recent differential scanning calorimetry (DSC) studies have shown that small size NIPA gel (0.3 mm in diameter) undergoes the volume phase transition in several minutes. However, for large size NIPA gel (3 mm in diameter), volume decrease was very slow, and the volume phase transition could not occur during the DSC experiment. [42]

According to the TF swelling theory, gels consisted of polymers with fast diffusion coefficients will have a fast swelling rate. Naturally, the first approach to obtain fast response gels is preparing gels with polymer network with a fast diffusion coefficient. Yuzo Kaneko and his coworkers [43,44] introduced a novel deswelling

mechanism to enhance the response rate of stimuli-responsive hydrogels. They used a NIPA cross-linked gel containing NIPA graft chains with a freely mobile end. In this graft-type NIPA gel, the graft chains undergo rapid dehydration in response to temperature increase due to the nature of the freely mobile end. In their experiment, they found that the normal-type NIPA gel in which both polymer ends are cross-linked shrinks slowly and took several weeks to reach its equilibrium state. On the other hand the graft-type hydrogel shrinks on the minute time scale and the time depends on the length of graft chain.

The diffusion coefficient of a typical polymer network is on the order of 10^{-7}-$10^{-6}$$cm^2/s$, [45] depending on the concentration of polymer, cross-link density, etc. However, it is not easy to increase the value of D by a factor of 10^2 or more. Therefore, a reduction of gel size has been an effective way to achieve quick response. One effective approach is to prepare microgels. The size of microgels ranges from single nm to several μm. Due to the small size of a microgel, the phase transition of micro-NIPA gel or its related copolymers can be completed in seconds. Temperature-sensitive aqueous microgels were first synthesized by Philip Chibante. [46] His method is described as a "surfactant-free emulsion polymerization" of aqueous NIPA monomer and methylenebisacrylamide. The polymerization was conducted at 60-70 °C in order to generate free radicals by decomposition of persulfate initiator. This simple polymerization procedure can produce remarkable uniform gel particles.

Microgels, unlike macrogels, exhibit very rapid phase transition in response to temperature change; this makes them very promising materials for a temperature-triggered drug or chemical release matrix. Therefore, considerable amount of work has been performed on this microgel system recently. [47-53] These gels have been characterized by standard colloidal techniques including electrophoresis, dynamic light scattering, rheology and electron microscopy.

Recent experimental studies have shown that designing special gel with a pathway in the polymer network in which water can go through when the phase transition occurred can accelerate the rate of gel shrinking and swelling. Ren-xi Zhou and his coworkers [54,55] synthesized a novel PNIPA gel using ethylene triethoxy silane (ETEOS) as the cross-linking agent. During the polymerization/cross-linking process, macroporous structure is formed in the polymer network. NIPA gels with incorporated siloxane show a dramatically rapid response rate when the external temperature changes. This macroporous structure can provide interconnected water release channels and prevent the formation of a dense, thick skin layer during the shrinking course. On the other hand, water can also diffuse into the polymer network through these channels during the reswelling process. Another approach to synthesis macroporous NIPA gels was designed by Mitsuru Akashi and his coworkers. [56] They introduced silica micro-particles during the gel preparation. These silica microparticles were removed later by an acid treatment. The deswelling rate was significantly enhanced compared to

conventional hydrogels. The thermoresponsive properties can be easily controllable by adjustments in the amount of silica.

1.7 The experimental studies of smart gels

After the discovery of the phase transition of gels, the NIPA based temperature responsive hydrogels have attracted considerable attention. They have been studied using variety of experimental techniques, and their properties have been systematically characterized. Usually these gels were prepared as cylinders with diameters as large as several mm [12,57, 58] or films with thickness of several mm. [18] The volume change of gels was determined by a calibrated microscopy or CCD camera.

The small-angle neutron scattering (SANS) experiment has been extensively employed to characterize polymeric gels. Toyoichi Tanaka and his coworkers [59,60] used deuterium water to label the polymer network and used SANS to study the static structure factor of nonionic crosslinked NIPA networks and ionic NIPA-AA polymer networks. They found that the static structure factor had a distinct scattering maximum even for the gels in swollen state, which indicates that polymer rich and poor regions were created in the system. They suggested that the polymer concentration fluctuations lead to a microphase separation between polymer rich and poor domains before the system undergoes the volume phase transition. This conclusion is consistent with the prediction by Borue and Erukhimovich [61] of a microphase separation structure in polyelectrolyte solutions in a solvent. Thermal analysis also probed the existence of the

microphase separation at a lower temperature than the macroscopic volume transition temperature. [42]

The volume phase transition has also been studied by other approaches, such as NMR, [62, 63] fluorescence spectroscopy, dynamic light scattering (DLS), [45, 64] differential scanning calorimeter (DSC), [42] and fluorescence spectroscopy. [65]

1.8 Applications of intelligent gels

The discovery of phase transition triggered intensive studies on polymeric gels. The ability of the gels to undergo huge but reversible changes in volume allows unique new systems to be made. Polymeric gels are recently under investigations for variety of applications, such as batteries, sensors, and artificial muscles. Most of these studies are focused on temperature or pH responsive hydrogels – gels that swell in aqueous solution. But researchers also have been probing gels response to other stimulus, such as glucose or ionic strength, etc.

An intelligent gel named Smart Hydrogel is currently being developed for drug delivery and skin care applications. [4] Smart Hydrogel is an entangled network of two randomly grafted polymers. One is pH -responsive poly (acrylic) (PAA). The other is a copolymer of poly(propyleneoxide) (PPO) and poly (ethylene oxide) (PEO). This copolymer forms gel when it is warmed to 37 °C. When Smart Hydrogel is dropped onto the eyes as a liquid, the temperature of the eyes will warm up the liquid and it

becomes a more viscous gel. The gel thus slowly releases medicine to the eyes over hours, instead of being diluted or washed away by tears.

A number of research groups have been exploring a device which releases insulin in response to glucose levels in blood using glucose response hydrogels. Bae and his coworkers [66] have been developing a biohybride artificial pancreas, which is a pouch with a semipermeable membrane that can be implanted into human body permanently. A polymer solution containing clumps of insulin releasing pancreatic cells called islets of Langerhans would be injected into the pouch. When the temperature of solution reaches 37 °C, the temperature-responsive polymer will form gel, immobilizing the islets in a stable state. In response to the level of blood glucose, the islets would release insulin to bring down the glucose. Other technological applications of intelligent gels including mass separation, [67-70] artificial muscles, [71-73] chemical valves,[74] injectable support tissue [75] and drug delivery [76-79] are also under rapid progress.

As we increasingly recognize natural resources are not unlimited, materials with better quality and higher functional performance become more wanted and needed. Soft and gentle materials are beginning to replace some of the hard mechanical materials in various industries. Now many scientists agree that smart materials will change the sensor and health industries with in next decades. However, smart gels are still an engineering oddity. Still a tremendous amount of work is needed to do to establish the principles underlying the individuality and specificity of these fascinating materials and to improve their properties and performance.

Chapter 2 Statement of Objective

2.1 Objective of project

The objective of this project is to develop robust methodology for continuous monitoring of volume phase transition of gels and study the volume phase transition of temperature responsive gels. We aimed to study the transport properties of ions and molecules in a variety of gel systems using electroanalytical techniques. The knowledge of mass transport properties of polymeric gels before, during and after phase transition is of great importance in applications such as polymeric gel electrolytes for batteries, sensors based on sol-gel technology, gels in separation techniques and polymeric gels as "solid-state" storage for liquids and their controlled release. The diffusion coefficient of selective probes in gel can also provide some information of the structure of gels, to mimic transport across natural and synthetic membranes, and to model flow through porous media. To our knowledge, there were no data on transport properties in polymeric gels that undergo volume phase transitions. Complete characterization of these materials requires these data.

Two types of temperature responsive polymeric gels, poly(*N*-isopropylacrylamide), NIPA, and poly(*N*-isopropylacrylamide-*co*-acrylic acid), NIPA-AA, are studied in our project. These gels undergo discontinuous, reversible volume phase transition as a response to temperature changes. These gels will swell at low temperature and shrink at high temperature. The phase transition temperature for NIPA gel and NIPA-AA hydrogel is 32 °C and 45 °C, respectively.

In the transport studies in polymeric gels we will focus on the following problems; (1) the influence of the phase transition of gels on the diffusion properties of probes with various charges and molecular weight, (2) the interpretation of macro- and microscopic viscosity of polymeric gels and their influence on the diffusion phenomena, and (3) the dependence of the transport of ions in gels on electrostatic interactions between polymers and ions.

We will apply a variety of electroanalytical techniques to follow local physical and chemical changes that occur during phase transitions. As a result of swelling or shrinking with significant volume changes, the concentration of probes might change and hence influence the monitoring current. Change of the volume of the gel will be coupled with the local viscosity and structure change of the polymer network. We will study it in detail.

Aggregation of polymer units to form gel networks results in dramatic changes of macroscopic viscosity. However, since gel systems consist of mainly fluid, the local, microscopic viscosity can be extremely different than its macroscopic viscosity. We will study this phenomenon in details in these polymeric gels by monitoring macroscopic viscosity of polymeric systems using classic viscometers and independently studying diffusion of neutral electroactive probes as a measure of microscopic viscosity.

The dependence of the transport of ions in gels on electrostatic interactions between polymers and ions is a very important issue for any devices based on gels as electrolytes since it influences ionic conductivity of those systems. It is also important

in the studies of gelation mechanism and gel structure. Most gels prepared from polyelectrolytes include ionic moieties such as carboxylic and sulfate groups. Therefore, the strength of the electrostatic interactions between the gel network and simple ions may depend very strongly on the charge of the ion as on the charge density of the polymer. We will determine diffusion coefficients of probe ions with various charges. By correlating the transport properties of these ions with their charges and charge densities of the polymers, we can gain information on changes of charge density of polymeric system due to the phase transition of gels.

The significance of this work is that the results will lead to a further and more detailed understanding of these interesting materials, which is needed for further progress in sensor development and other proposed applications of these materials.

2.2 Main research instrumentation

The transport properties of probes in gels have been studied using techniques, such as light scattering spectroscopy [80] radioactive tracer methods, [81] and pulsed-field-gradient-spin-echo NMR. [82] However, these techniques required relatively high concentration of diffusion species and the latter two are limited to NMR or radio-active probes. Electroanalytical techniques, such as transient generation-collection methods, [83] chronoamperometry, [84-86] scanning electrochemical microscopy, [87, 88] steady-state voltammetry, [89-92] for transport studies permit a decrease in the concentration of probes and extends the list of ions and molecules than can be investigated. The instrumentation is inexpensive and the method is very fast and accurate.

➢ Electrochemical techniques and microelectrodes

The principle technique we use is voltammetry with microelectrodes, whose size is in the range of micrometers. Microelectrodes originally were developed by independent works of Wightman and Fleischmann and their coworkers at about 1980. [93, 94] Electroanalytical methods using microelectrodes have been used to study mass transport of molecules in solutions and polymeric gels. [95-97] Microelectrodes have some unique advantages compared with the normal size electrodes. Current flowing at microelectrodes is very low, and even in solutions of very low conductivity such as low ionic strength aqueous solution or organic solutions, the ohmic drop is very small. Investigations of transport phenomena in various media have become possible due to these unique features of microelectrode. The other feature related to microelectrode is that steady state current can be obtained on microelectrode and this makes diffusion coefficient measurement using microelectrode very convenient.

The microelectrode is commonly defined as an electrode having at least one dimension, such as the radius of a disk or the width of a band, smaller than 25μm. The size of the electrode can be as small as 0.1μm to 10 nm. [98] Since only one dimension of an electrode must be small to obtain characteristic properties of microelectrode, there are various shapes of microelectrodes. They are spherical microelectrode, microdisk electrode, band shape electrode and cylindrical electrode.

Spherical microelectrodes can be made by plating Hg onto to a microdisk electrodes. [99-101] The active size in these electrodes is the radius of curvature, r_0. Disk

microelectrode is the most commonly used electrode, which is fabricated by sealing a fine wire in a glass or plastic resin and then the embedded wire is exposed and polished.

The band microelectrode is a quite unique electrode. The width of this electrode is usually in the range below 25μm. The length of electrode can be as long as in the centimeter range. Band microelectrodes are usually fabricated by embedding metallic foil or evaporated film between glass plates or in a plastic resin. The electrode is then exposed and polished.

Cylindrical electrodes can be as simple as a metal wire with radius smaller than 25 μm and length as several millimeters.

Two electrochemical methods will be applied in our experiments, cyclic voltammetry and chronoamperometry.

➢ *Cyclic voltammetry* (CV) and *steady state current*

In cyclic voltammetry, the potential is usually varied linearly with time (see figure 2.1). The sweep rate is in the range of mv/s to 10^6v/s for microelectrodes. The current is commonly recorded as the function of potential. Cyclic voltammetry is a very popular and useful technique for electrochemical studies in a new system.

The main properties related to voltammetry at microelectrode is a steady-state current, which is independent of time. Considering the general reaction $O + ne \rightarrow R$ in solution, when the potential applied on the electrode (see figure 2.2) is sufficiently negative, the reaction can be activated, regardless of the reaction kinetics process. The concentration of reagent O at the electrode surface will be quickly reduced to zero. To

calculate the diffusion current on microdisk electrode, one needs to consider two kinds of diffusion, linear diffusion and spherical diffusion.

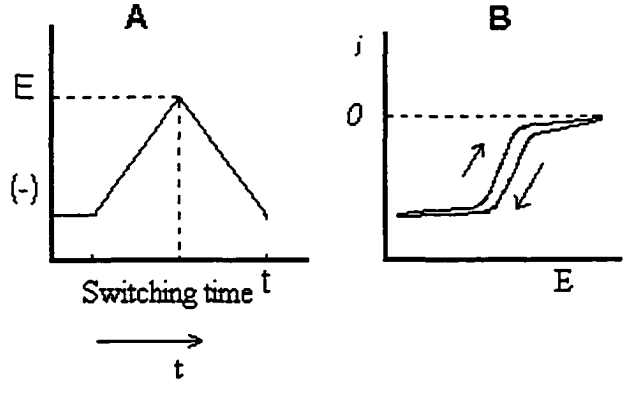

Figure 2.1 Potential change (A) and cyclic voltammogram with a microelectrode (B)

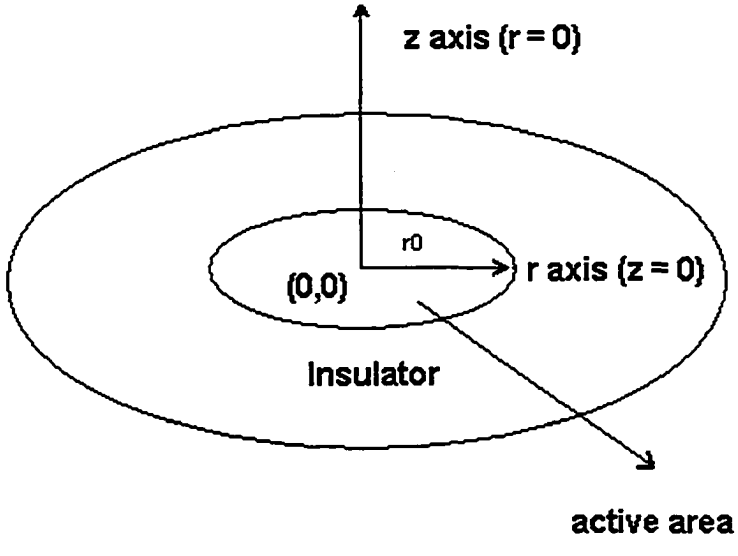

Figure 2.2 Geometry of diffusion at an microdisk electrode

The diffusion equation for species *O* can be written as follows:

$$\frac{\partial C_o(r,z,t)}{\partial t} = D\left[\frac{\partial^2 C_o(r,z,t)}{\partial r^2} + \frac{1}{r}\frac{\partial C_o(r,z,t)}{\partial r} + \frac{\partial^2 C_o(r,z,t)}{\partial z^2}\right] \tag{2.2.1}$$

where C_o is the concentration of *O*, t is time, r describes radial position normal to the axis of symmetry at $r = 0$, z is linear displacement normal to the plane of the electrode at $z = 0$.

Under the following boundary conditions:

$$C_o(r,z,0) = C_o^* \tag{2.2.2}$$

which shows that at the beginning of the experiment, $t = 0$, the solution is homogeneous, C_o^* is the initial concentration of reagent *O*.

$$\lim_{r\to\infty} C_o(r,z,t) = C_o^* \tag{2.2.3}$$

$$\lim_{z\to\infty} C_o(r,z,t) = C_o^* \tag{2.2.4}$$

these conditions express that the areas distant from the electrode are unperturbed by the experiment.

$$\left.\frac{\partial C_o(r,z,t)}{\partial z}\right|_{z=0} = 0 \qquad (r > r_0) \tag{2.2.5}$$

which expresses that there can no be flux of *O* into or out the insulator area ($r > r_0$), because there is no reaction there.

$$C_o(r,0,t) = 0 \quad (r \leq r_0, t > 0) \tag{2.2.6}$$

The last boundary condition expresses that when sufficient low potential is applied on the electrode, the concentration of reagent *O* will reduce to zero when the experiment begins. The solution to these equations is a very complex problem. Aoki and Osteryoung addressed it in terms of a dimensionless parameter $\tau = 4D_0t/r_o^2$, where D_0 is the diffusion coefficient of *O*, r_0 is the radius of a electrode. [102] For any specific instrument, τ is an index of time *t*. The solution for current-time they obtained is:

$$i = \frac{4nFAD_0C_o^*}{\pi r_0} f(\tau) \tag{2.2.7}$$

At a long time, when $\tau > 1$, the function $f(\tau)$ can be expressed as:

$$f(\tau) = 1 + 0.71835\,\tau^{-1/2} + 0.05626\,\tau^{-3/2} - 0.00646\,\tau^{-5/2} \ldots\ldots \tag{2.2.8}$$

When the τ becomes very large, the steady state current is established and eq. 2.2.7 reduces to the following formula:

$$i_{ss} = \frac{4nFAD_0C_0^*}{\pi r_0} = 4nFD_0C_0^* r_0 \tag{2.2.9}$$

where *n* is number of electrons transferred, *F* is the Faraday constant. Even in very complex media, the steady state current is independent of kinetics of the electrode process. Therefore, the diffusion coefficient can be determined from the steady state current in a straightforward way.

- Chronoamperometry

When the gels collapse, aqueous phase and gel phase separate, the concentration of a probe in the gel phase is not known. The steady state voltammetry is not a convenient technique to measure diffusion coefficient. Chronoamperometry is often used to determine the diffusion coefficient of probe molecules when their concentration is not known.

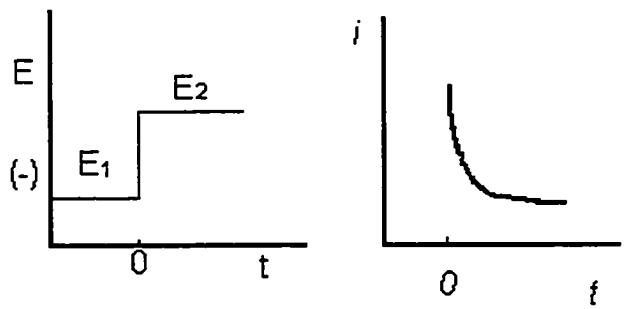

Figure 2.3 Diagram of the waveform applied in the chronoampermetry experiment.

For general reaction $O + ne \rightarrow R$, let E1 the potential region where faradaic processes do not occur. E2 is the potential region negative enough for the reaction to occur. The corresponding current is recorded as the function of time. (see figure 2.3)

The time dependence of current for microdisk electrode is rather complex, which spans three time regimes. The current-time curve is given by equation 2.2.8. Shoup and Szabo [103] provided a single empirical relationship covering the entire range of τ with an accuracy better than 0.6 % at all points.

$$\frac{i_{(t)}}{i_{ss}} = 0.7854 + 0.8862\tau^{-1/2} + 0.2146e^{-0.7823\tau^{-1/2}} \quad (2.2.10)$$

For the short time region, ($\frac{Dt}{r^2} < 10^{-4}$, for < 1% error), the diffusion layer remains thin compared to r_0, the radial diffusion does not manifest itself appreciable, and the diffusion has a semi-infinite linear character. Therefore, the corresponding current is Cottrell current. The normalized time dependent current, $\frac{I_t}{I_{ss}}$, within the 1 % of the deviation of equation 2.2.10 is given by: [85]

$$\frac{I_t}{I_{ss}} = 0.7854 + (\frac{\pi^{1/2}}{4})r_d(Dt)^{-1/2} \quad (2.2.11)$$

When the experiment enters into the intermediate time regime, the diffusion layer is getting thicker and its thickness is close to r_0 and radial diffusion become important. The current is larger than that of a pure linear diffusion. The current density on the electrode in not uniform anymore. The current density on the edge is larger than the central area because the edge is more accessible geometrically to the diffusing electroactive molecules and ions.

At a long time ($Dt/r^2 > 10^2$, for <1 % error), the diffusion field grows and its size is much larger than r_0. The current approaches to the steady state condition. The normalized time dependent current, $\frac{I_t}{I_{ss}}$, within the 1 % of the deviation of equation 2.2.8 is given by [85]

$$\frac{i_{(t)}}{I_{ss}} = 1 + \frac{2}{\pi^{3/2}} a(Dt)^{-1/2} \qquad (2.2.12)$$

where $I_{(t)}$ is the current at the time t, I_{ss} is the steady state current, a is the radius of the electrode. A plot of $I_{(t)}/I_{ss}$ *Vs* $\frac{1}{\sqrt{t}}$ yields a straight line, whose slope can be used to determine the D without knowing the concentration of electroactive probes.

Chapter 3. Experimental

3.1 Reagents

N-isopropylacrylamide (NIPA), Dimethylformamide (DMF), N,N'-methylenebisacrylamide (BIS), sodium chloride, N,N,N',N'-tetramethylethylene-diamine (TMED), acrylic acid (AA), ammonium persulfate and lithium perchlorate were purchased from Aldrich. 1,1'-Ferrocenedimethanol ($Fc(MeOH)_2$) was purchased from Fluka. 4-hydroxy-tempo (TEMPO) was purchased from Sigma. Ferrocenylmethyl-trimethylammonium ($FcTMA^+$) iodide was purchased from Strem Chemicals. Hexaammineruthenium (III) chloride ($Ru(NH_3)_6^{3+}Cl_3$) was from Alfa. Ammonium hexafluorophosphate was purchased from Acros. All chemicals except AA were used as received. The acrylic acid was purified by vacuum distillation (21 mm Hg, 52 °C) and was stored in refrigerator before use. All solutions were prepared using high purity water obtained from Milli-Q (Millipore Model RG) purification system.

3.2 Apparatus

The voltammetry measurements were carried out in a jacketed glass cell with a three-electrode system consisting of an Ag/AgCl reference electrode, a Pt wire counter electrode, and Pt microdisk working electrodes (Project Ltd., Warsaw, Poland). A refrigerated circulator (Isotemp model 1016P, Fisher Scientific) controlled the temperature of a cell. Staircase voltammetry and chronoamperometry were applied with a model 283 potentiostat (Perkin-Elmer, PARC) and controlled via a PC computer.

The working microdisk electrodes were 5.0 μm, 11μm and 12.0 μm radius Pt electrodes. The working electrodes were polished before measurement with Microcloth polishing cloth (Buehler) and 0.1 μm diamond suspension polishing solution (Buehler). Optical inspection of the state of the electrode surface was accomplished with an inverted microscope for reflected light (Nikon, Model Epiphot-200).

3.3 Synthesis of ferrocenylmethyltrimethylammonium hexafluorophosphate

For hexafluorophosphate iodide, both $FcTMA^+$ and I^- ions can be oxidized. The oxidation potential of these two ions is so close that only one oxidation wave can be observed in our experiment. Since we are only interest in the $FcTMA^+$ ion, the I^- should be replaced by an electrochemical inactive ion such as hexafluorophosphate. [104] Ferrocenylmethyltrimethylammonium hexafluorophosphate was synthesized by adding saturated ammonium hexafluorophosphate aqueous solution into Ferrocenylmethyltrimethylammonium iodide saturated aqueous solution. Yellow precipitate will be formed immediately at room temperature. This precipitate was collected by filtration and washed several times by distilled water. Ferrocenylmethyltrimethylammonium hexafluorophosphate synthesized by this method was purified by recrystallization using mixture of solvents of acetone and water. At last, the golden flak like ferrocenylmethyltrimethylammonium hexafluorophosphate will be obtained and saved in desiccators.

3.4 Gel preparation

The synthesis of a NIPA-AA copolymer cross-linked with BIS was modified from a previous procedure. [8] The polymer gel was synthesized by conventional radical polymerization method (see figure 3.1); 0.87 g of NIPA, 0.025 mL of acrylic acid (AA), and 0.0156 g of N, N' – Methylenebisacryl-amide (BIS) (cross-linker) were dissolved in 10 mL distilled water. The pregel solution was placed in a water bath and it was deoxygenated with argon for 20 minutes. 5 mg of ammonium persulfate (initiator) was added to the solution followed by 56 μL of N,N,N',N' - tetramethyl-ethylenediamine (TEMED) (accelerator). The polymerization occurs at 22 °C for 20 hours. The synthesis of NIPA gel was following the same procedure but without using acrylic acid. The gel formed quickly (less than 1 h) and was allowed to sit overnight before purification.

3.5 Gel Purification

Gel purification was necessary to simplify our interpretation of the diffusion behavior of electroactive probes in gels. The presence of reactive monomers or initiator might cause reaction with electroactive probes, change their concentration, and complicate determination of diffusivity of the probes. Purification of the gel consisted

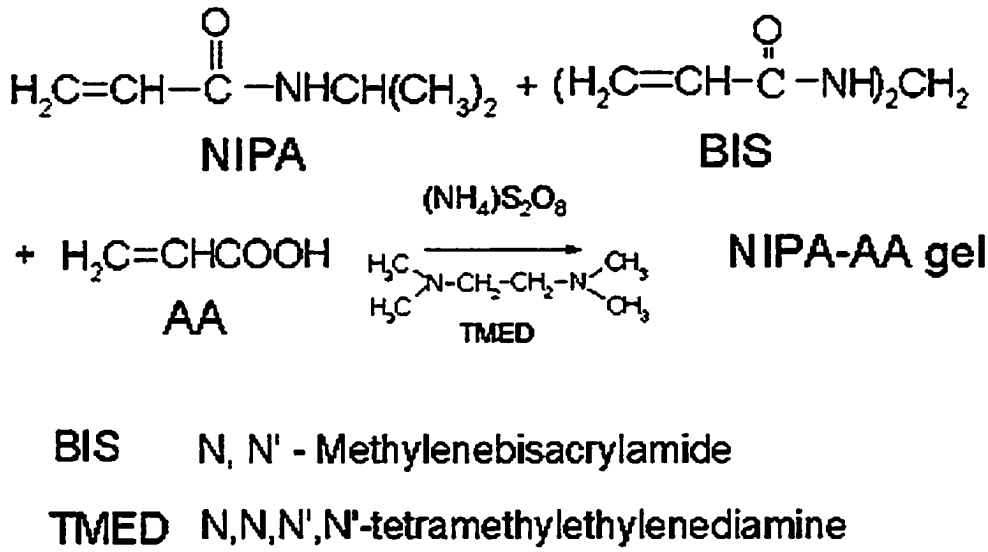

Figure 3.1 Schematic representation of synthesis of NIPA-AA gel

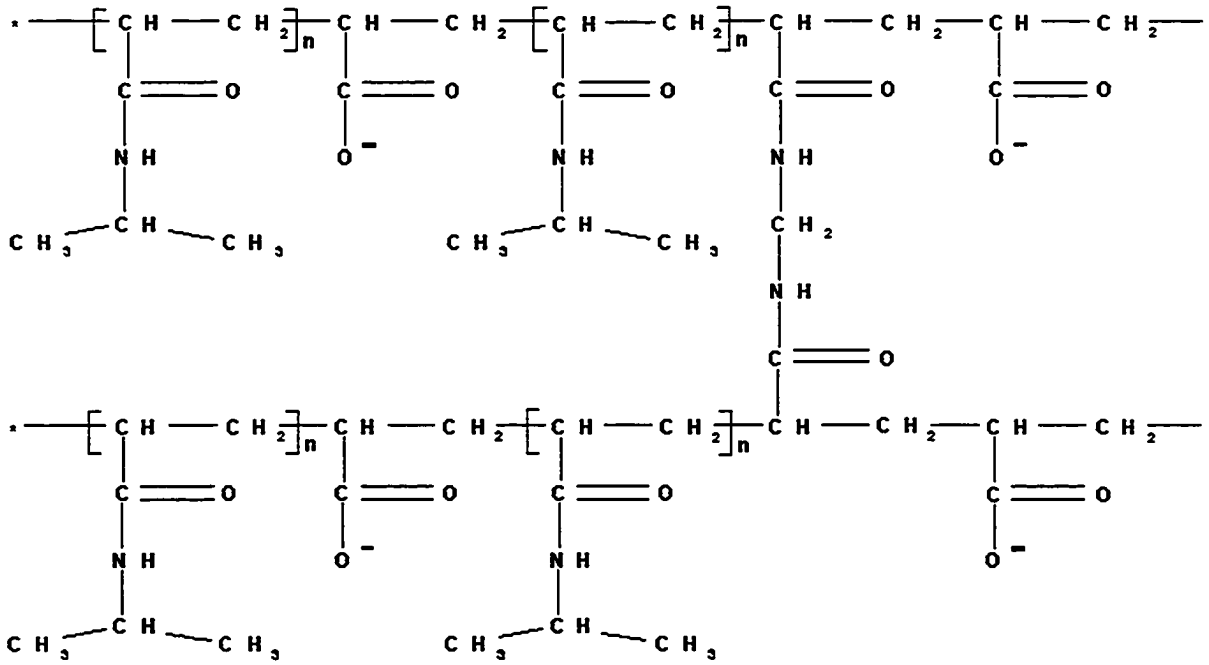

Figure 3.2 Schematic representation of cross linked NIPA-AA polymer

of three washing steps. Each of them consisted of collapsing the gel by heating it to approximately 80 °C, which is above the gel volume phase transition temperature. The expelled solution was poured off, and several hundred milliliters of water were added to the collapsed gel. The gel was allowed to swell by letting it sit at 20- 25 °C for a few hours. This washing procedure, which can be likened to the squeezing and refilling of a sponge, can be repeated several times without any significant changes in the amount of copolymer. Once washing was complete, the collapsed gel was placed in an oven and heated for 3 days at 80 °C. This step drives off any remaining solvent and results in a hard transparent to translucent polymeric material. The polymer was either used in pebble-sized pieces or ground to a fine powder. The schematic structure of NIPA-AA polymer is presented in figure 3.2.

FTIR spectroscopy was used to estimate the completeness of the polymerization reaction. The FTIR spectra of the two monomers (NIPA and AA), cross-linked NIPA-AA, cross-linked NIPA polymer are shown in Figure 3.3 - Figure 3.6. The best vibrational absorption bands to monitor the completeness of polymerization were considered to be those associated with the vinyl group present in the chemical structure of both monomers. Unfortunately, the C=C stretch (1623 cm^{-1}, NIPA; 1637 cm^{-1}, AA) was obscured by the strong and relatively broad amide I band at 1650 cm^{-1} in the copolymer FTIR spectrum. The remaining suitable vibrational absorption band to estimate the extent of polymerization is the trans CH=CH wag (994 cm^{-1}, NIPA; 984 cm^{-1}, AA). [105] In each of the monomer FTIR spectra, the trans CH=CH wag absorbance

peak is relatively strong. However, in the copolymer FTIR spectrum, the vibrational band at 984 cm^{-1} has almost completely disappeared, indicating that polymerization is essentially complete. There appears to be a very large, broad shoulder at 3700 cm^{-1} for the copolymer spectrum that is not observed in the NIPA spectrum. This shoulder could be from intermolecular hydrogen bonding between adsorbed water and acrylic acid segments. The effectiveness of the three gel washings on removing unreacted monomer molecules was characterized using FTIR. After each washing step, the expelled solution was collected and vacuum filtered with a 0.45 μm Millipore membrane filter. Monomers from the filtered washings were removed using liquid- liquid extraction with three 25 mL portions of diethyl ether. FTIR analysis of the extracted monomer was accomplished by evaporating 4 mL of the ether extract to dryness in a test tube, rinsing the inside of the test tube with 10 drops of diethyl ether, and evaporating the ether rinse onto the face of a NaCl plate. Figure 3.7 shows IR spectra of the residue from the ether extract for each wash. The spectra from each ether extract indicate the presence of unreacted NIPA. This is expected considering more than 94% of the polymer backbone consists of NIPA molecules. After each wash, it is apparent that a significant amount of unreacted NIPA is removed from the gel, and after three washes the unreacted NIPA has been removed from the gel.

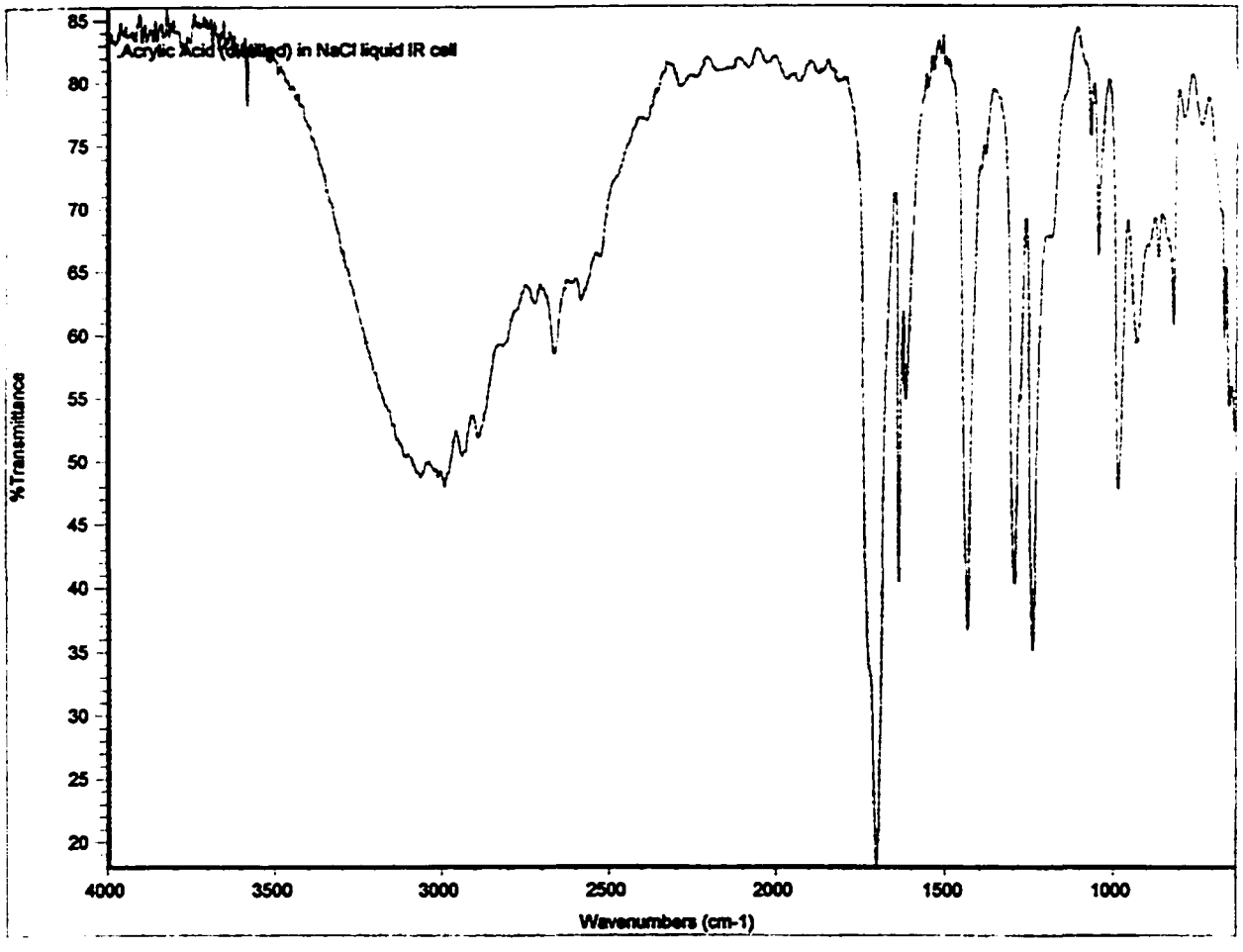

Figure 3.3 FTIR spectroscopy of acrylic acid, NaCl cell

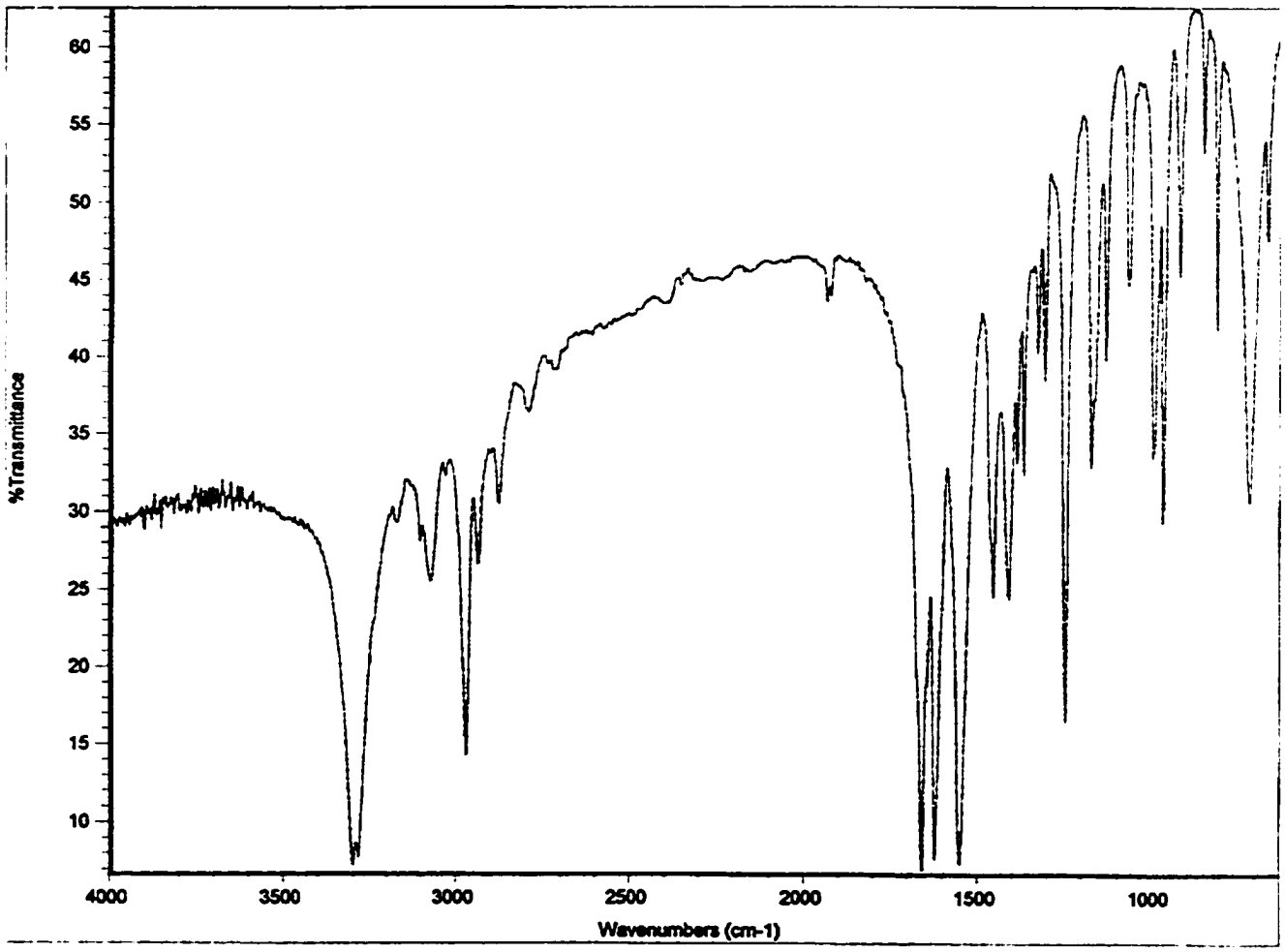

Figure 3.4 FTIR spectroscopy of *N*-isopropylacrylamide, KBr disk

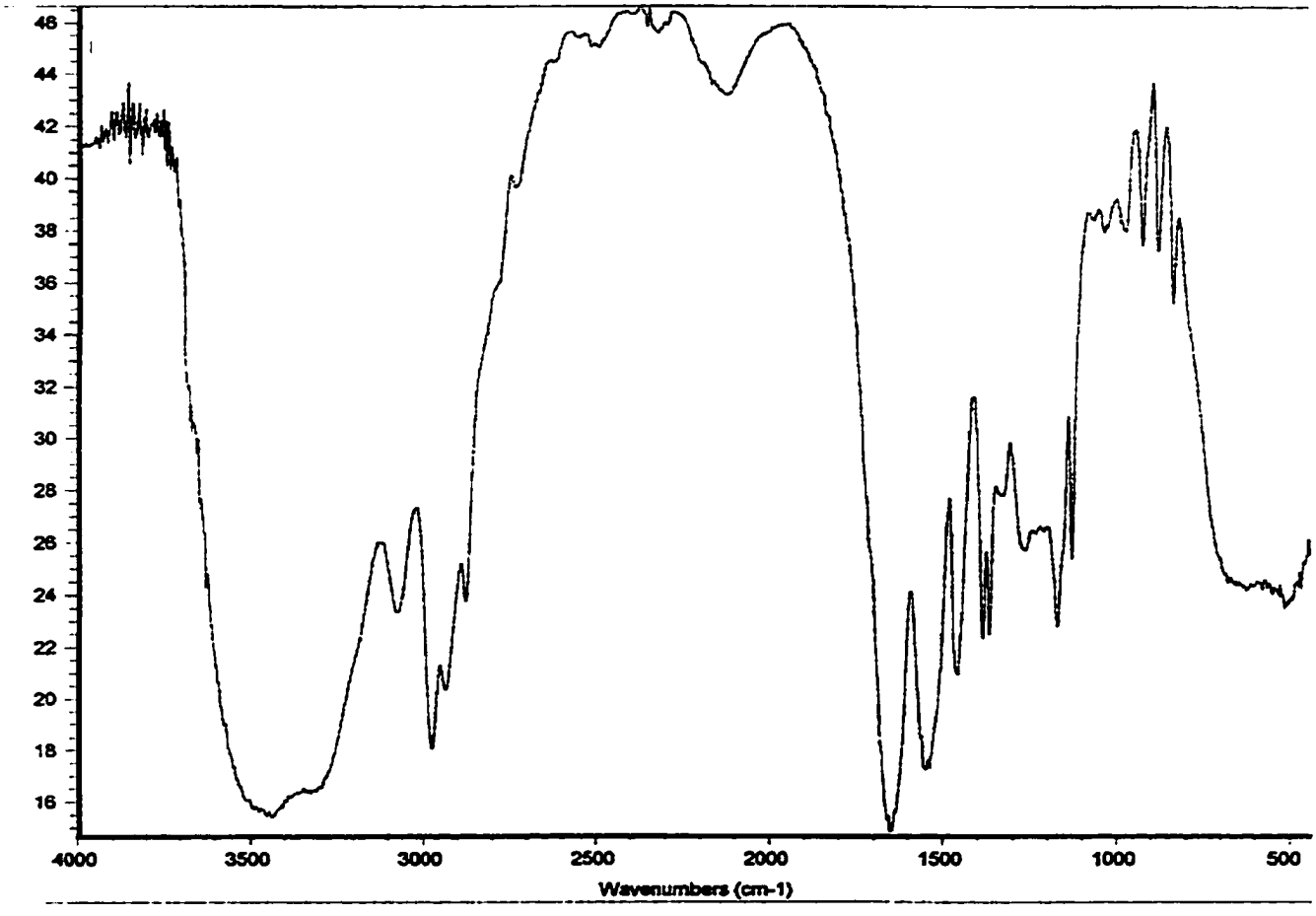

Figure 3.5 FTIR spectroscopy of NIPA-AA Co-polymer, KBr disk

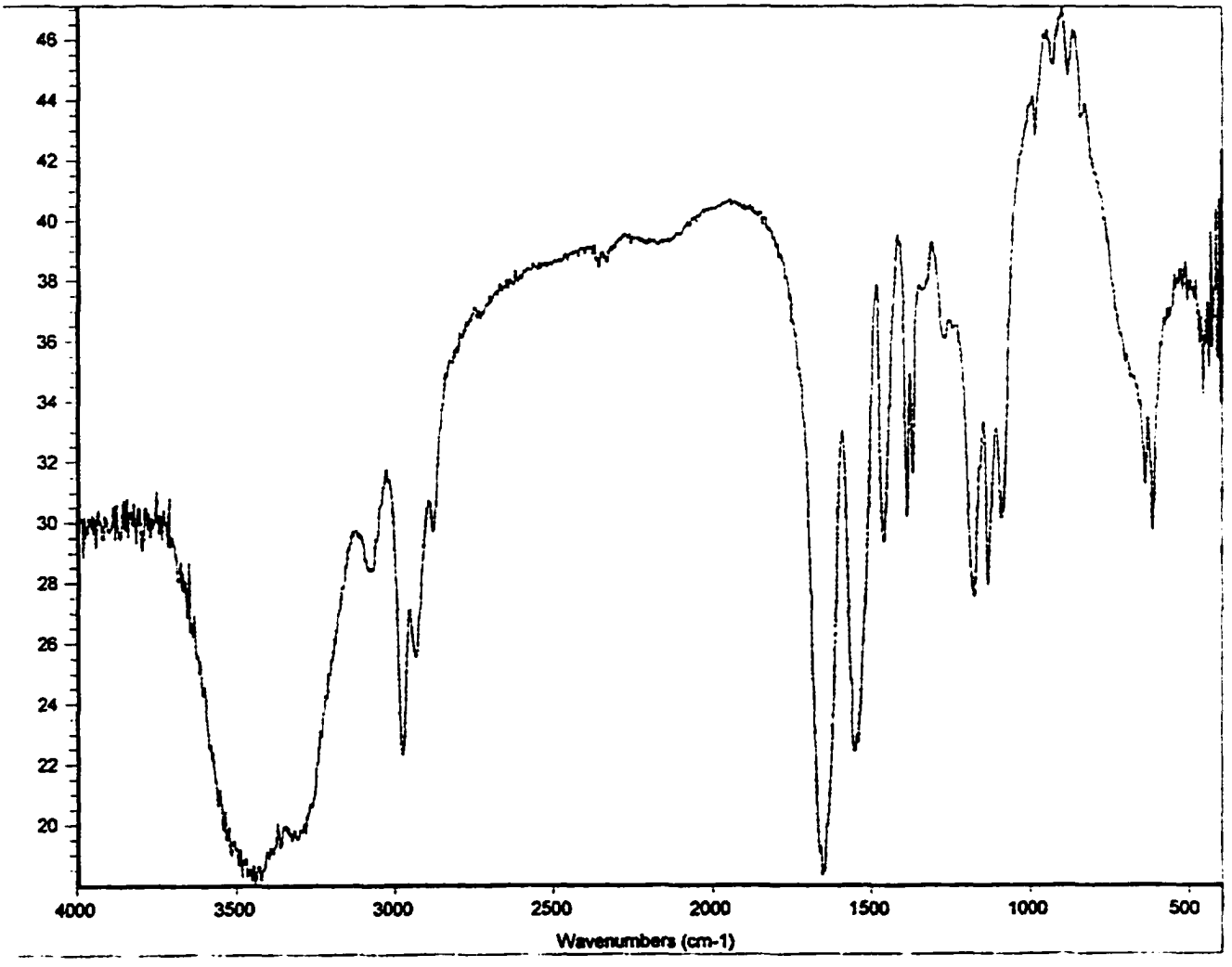

Figure 3.6 FTIR spectroscopy of NIPA polymer, KBr disk

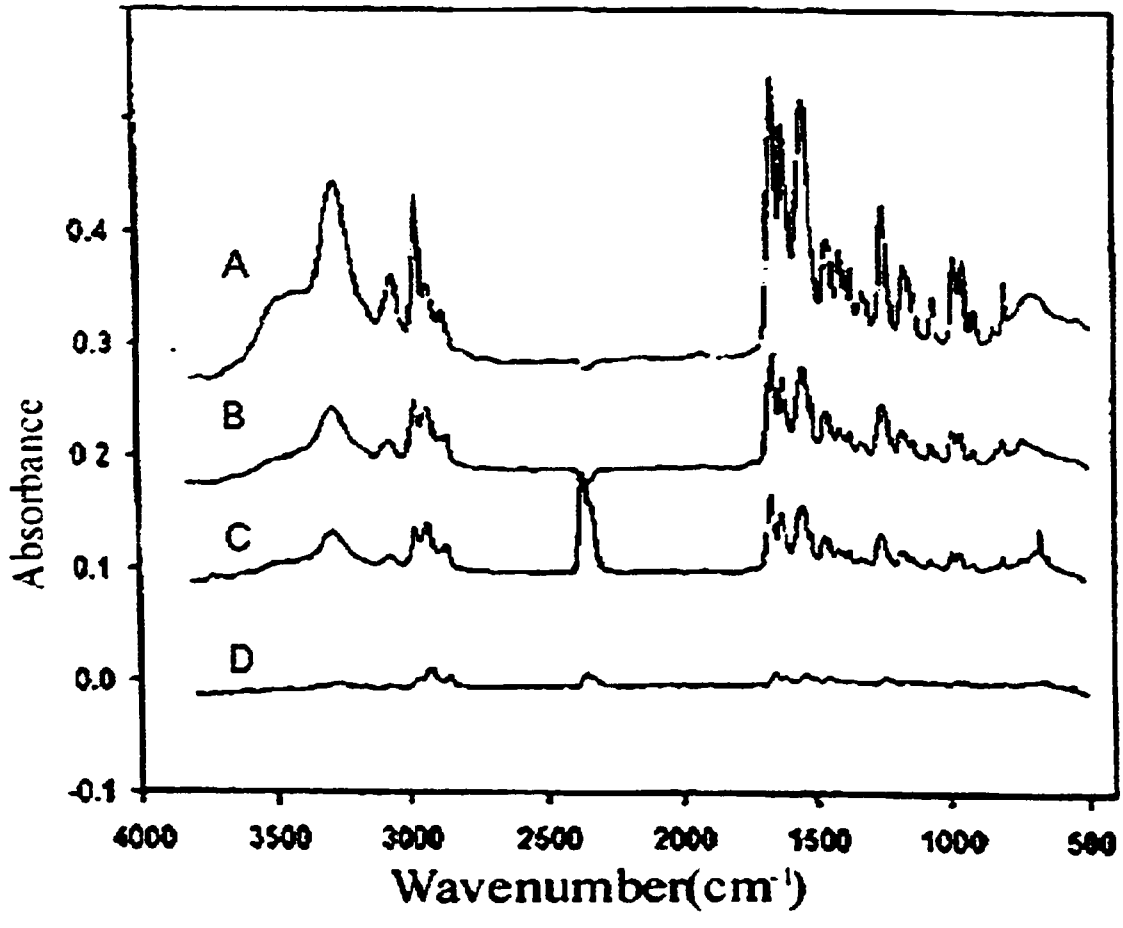

Figure 3.7 The efficiency of NIPA-AA gel purification process; (A) the spectra of impurity from the expelled solution before the first washing; (B) from the first washing solution; (C) from the second washing solution; and (D) from the third washing solution.

3.6 Preparation of gels with electroactive probes

Most electroactive probes cannot be introduced into a gel by mixing them with components of a polymerization mixture; they would react immediately. Our new procedure utilizes the fact that even after dehydrating the gel, the residual copolymer can be swelled by a solvent (or a solution) to reconstitute the gel. This is a reversible process and can be repeated several times. Since the purified copolymer can be swelled by a solution of a known and well controlled composition, this is a very convenient method to introduce any required probes into a gel. In our experiments, a known mass or volume of electroactive probe solution with or without 0.1 M $LiClO_4$ as the supporting electrolyte was added to a weighed amount of dry NIPA-AA or NIPA copolymer. After sitting overnight (ground polymer) or up to 3 days (pebble-sized polymer pieces) at room temperature, a gel with well-defined concentration of electroactive probe will be formed. The NIPA-AA gels prepared by this procedure exhibited a volume phase transition of 45 (±2.5) °C, which was determined visually. At this temperature a two-phase system exists, and approximately 40% of the solution mass will be expelled from the gel into this second phase. The NIPA gels have a phase transition temperature at 35 (±2) °C, and with approximately 90% of the solutions been expelled. This phase transition temperature appeared to be constant for the range of gel as formed with a well-defined polymer-to-solvent ratio. The molecular structures of electroactive probes in our experiments are presented in Figure 3.8.

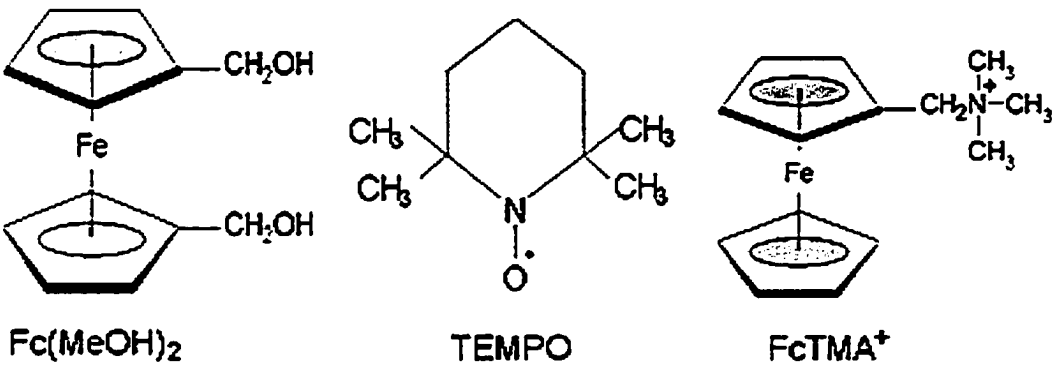

Figure 3.8 Electroactive probes used in experiments

3.7 UV-visible characterization

Once an electroactive probe is incorporated into a gel matrix, UV-visible spectroscopy may be used to estimate the concentration of the incorporated probe. All UV/vis experiments were run at room temperature. The only significant absorbance by the gel swelled using 0.1 M $LiClO_4$ without any electroactive probe is in the UV region below 300 nm. The optical transparency of this gel enables transition metal complexes serving as electrochemical probes to be quantified using visible spectroscopy. An example of this is shown in Figure 3.9, where a series of 2.5% (w/v) NIPA-AA gels containing different concentrations of $Fc(MeOH)_2$ were used to construct a calibration curve. The peak maximum of $Fc(MeOH)_2$ at 430 nm does not shift in the presence of the NIPA-AA matrix compared to the spectral response in aqueous solution, and there is a linear response between 0.6 and 5.0 mM $Fc(MeOH)_2$ for both matrixes. However,

there is a 15% increase in the sensitivity of the calibration curve obtained in a gel matrix compared with the sensitivity obtained in an aqueous matrix. This sensitivity increase may indicate a hyperchromic effect in the $Fc(MeOH)_2$ absorbance in the gel matrix. Hyperchromism, which is the result of increased dipole strength of the absorbing species,[106] may be a useful property for studying the interaction between an electroactive probe and the gel matrix. UV-vis spectroscopy seems to be a very useful technique for examination the spectroscopic properties of molecules in polymeric gels, and it provides a way to determine concentration of those molecules in gels.

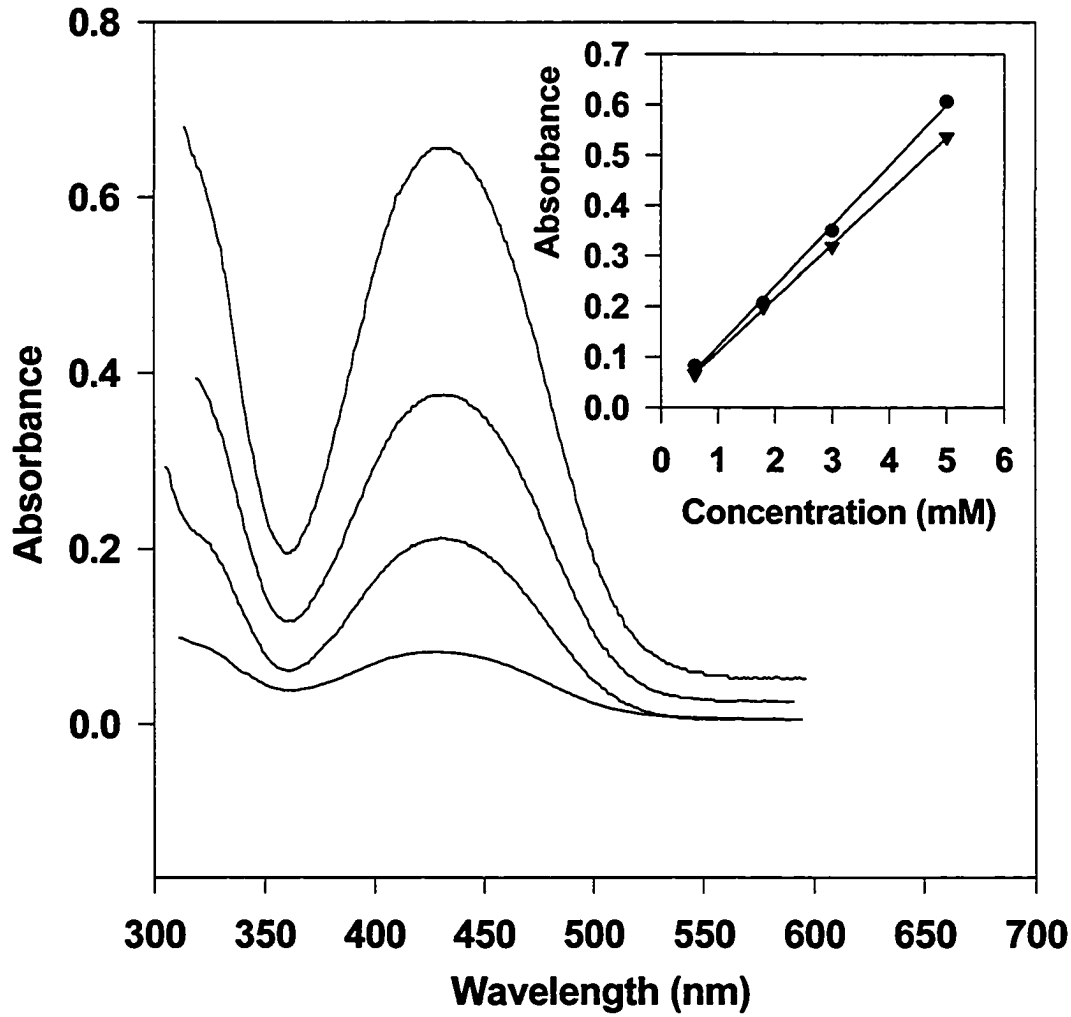

Figure 3.9 UV-vis spectra of $Fc(MeOH)_2$ in 2.5% (w/v) NIPA-AA gel with 0.1 M $LiClO_4$. Inset: calibration curves of $Fc(MeOH)_2$ in 0.1 M $LiClO_4$ (▲) and in 2.5% (w/v) NIPA-AA gel with 0.1 M $LiClO_4$ (●).

Chapter 4 Diffusion of probes in swollen state gels

4.1 Diffusion coefficient of electroactive probes in swollen NIPA-AA gels

The one-electron oxidation of $Fc(MeOH)_2$ and TEMPO was studied in aqueous solutions and NIPA-AA gels using Pt microdisk electrodes for a temperature range from 5 to 40 °C. Voltammograms for the oxidation of $Fc(MeOH)_2$ and TEMPO were well defined and reproducible, with a relative standard deviation less than 5% (calculated from 6 voltammograms). Typical steady-state voltammograms of $Fc(MeOH)_2$ oxidation obtained in an aqueous solution and 2.0% (w/w) NIPA-AA gel containing 0.1 M supporting electrolyte, $LiClO_4$, are presented in Figure 4.1. The diffusion coefficients of electroactive probes were determined according to eq. 2.2.9. Table 4.1 summarizes the temperature dependence of the diffusion coefficients of $Fc(MeOH)_2$ in aqueous solutions and NIPA-AA gels of various concentrations of the polymer. The values of diffusion coefficients of $Fc(MeOH)_2$ and TEMPO in aqueous solutions at 25°C were 6.35×10^{-6} cm^2/s and $6.64 \times 10^{-6} cm^2/s$ respectively. These values are well in agreement with those reported previously, 7.33×10^{-6} cm^2/s and 6.59×10^{-6} cm^2/s for $Fc(MeOH)_2$ and TEMPO respectively. The diffusion coefficient of $Fc(MeOH)_2$ in the NIPA-AA gel is approximately 20% - 50% smaller than that in aqueous solution. Additionally it decreases when the concentration of the co-polymer in the gel increases.

Although the same concentration of $Fc(MeOH)_2$ was used to prepare solutions and gels, the final concentration of $Fc(MeOH)_2$ in a gel can change due to the volume changes during gel preparation. To make sure that the concentration of an electroactive probe does

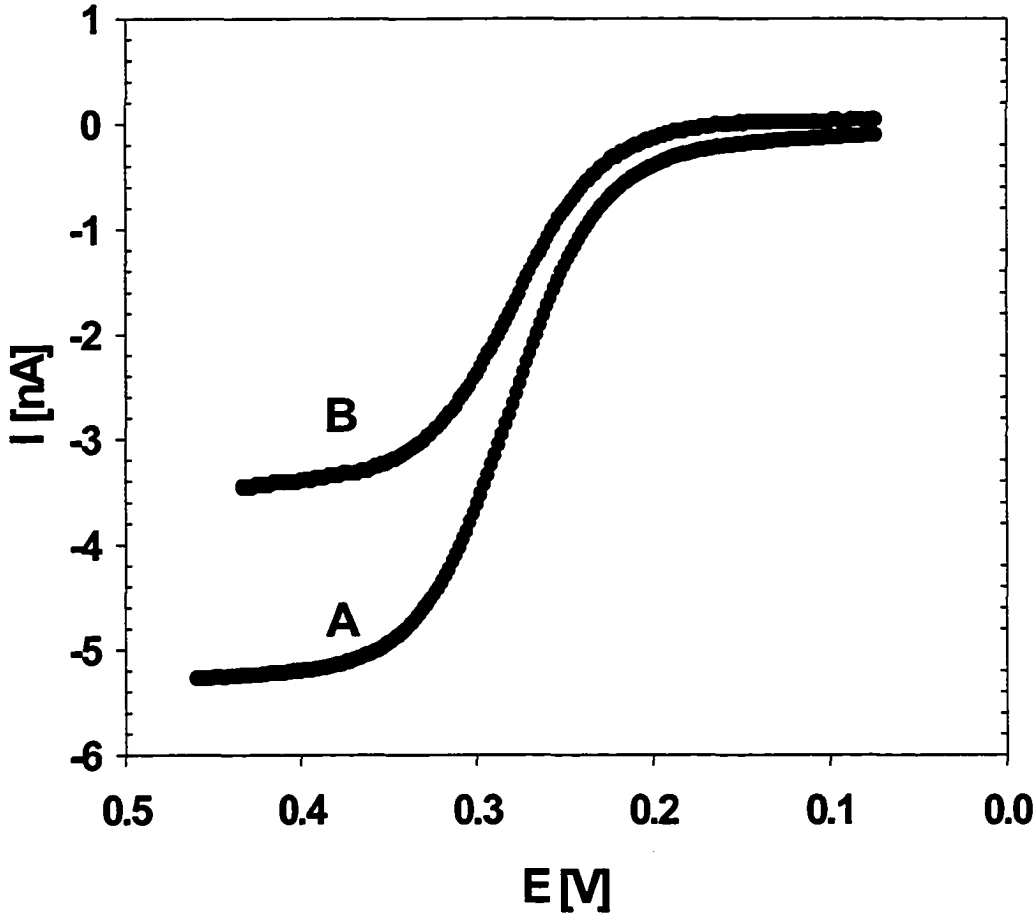

Figure 4.1 Steady-state voltammograms of oxidation of 1.8 mM $Fc(MeOH)_2$ in (**A**) aqueous solution and in (**B**) 2.0% (w/w) NIPA-AA gel; 0.1 M $LiClO_4$, Pt microdisk electrode , $r_d = 5$ μm.

Table 4.1 Temperature Dependence of the Diffusion Coefficient of $Fe(MeOH)_2$ in 0.1 M $LiClO_4$ Aqueous Solution and NIPA-AA Gels.

	$D(cm^2/s) \times 10^6$			
Temperature (°C)	Aqueous solution[1]	1.2% (w/w) NIPA-AA gel	2.0% (w/w) NIPA-AA gel	4.0% (w/w) NIPA-AA gel
25	6.35 ± 3.90	5.11 ± 0.00293	4.35 ± 0.00550	3.12 ± 0.00777
30	7.15 ± 0.367	5.70 ± 0.00773	4.94 ± 0.0866	3.50 ± 0.132
35	8.16 ± 0.139	6.43 ± 0.0186	5.48 ± 0.161	3.94 ± 0.0841
40	9.16 ± 0.138	7.29 ± 0.0680	6.21 ± 0.123	4.25 ± 0.150
45	1.02 ± 0.136	8.11 ± 0.00334	7.09 ± 0.163	4.57 ± 0.443

[1] reported value at 25 °C is $7.33 \times 10^{-6} \pm 3.6 \times 10^{-7}$ cm^2/s [107]

not change during swelling process, concentration independent determination of diffusion coefficient of $Fc(MeOH)_2$ was carried out by chronoamperometry on microelectrode. The normalized current, I_t/I_{ss}, was plotted as a function of $t^{-1/2}$ (see eq. 2.2.11) and presented in Figure 4.2. An average intercepts of the I_t/I_{ss} *versus* $t^{-1/2}$ plots was 0.7854, the value close to 0.7854 predicted by eq 2.2.11. The diffusion coefficient values of $Fc(MeOH)_2$ in 2.0% NIPA-AA gel calculated from short time region eq. 2.2.11 are compared with those from steady-state voltammetric experiments, and they are presented in Figure 4.3 for the temperature range from 20 to 38 °C. For this temperature range, diffusion coefficients of $Fc(MeOH)_2$ obtained by two methods are identical within the experimental error. This suggests that concentration of $Fc(MeOH)_2$ did not change significantly during the gel preparation and swelling process. Note that the concentration of polymer was very small, not higher than 4.0%.

4.2 Diffusion Coefficient of electroactive probe in swollen state of NIPA gels

Steady state voltammetry at microelectrodes was applied to determine the diffusion coefficient of $Fc(MeOH)_2$ in swollen NIPA gels according to eq. 2.2.9. The steady-state current for oxidation of $Fc(MeOH)_2$ was measured for temperatures from 20 to 30 °C, which is below the volume phase transition temperature. Voltammograms for $Fc(MeOH)_2$ oxidation in swollen gels as well as in solutions without the polymeric network were well defined and reproducible, with a relative standard deviation, *rsd*, less than 5% (calculated from 6 voltammograms). Figure 4.4 shows a typical voltammogram for oxidation of $Fc(MeOH)_2$ in NIPA gel with 0.1 M $LiClO_4$, and a background obtained

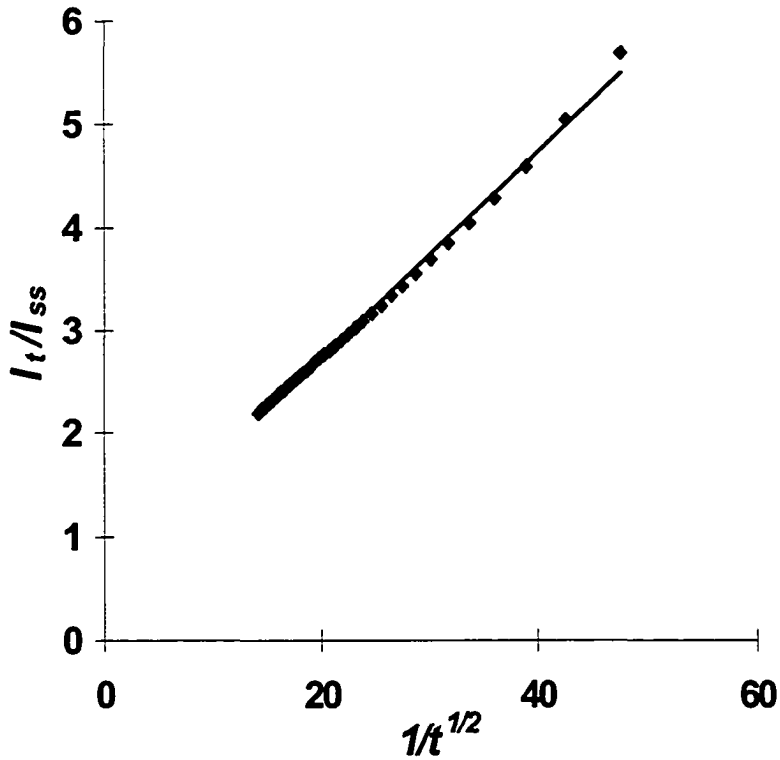

Figure 4.2 *I_t/I_{ss} versus. $1/t^{1/2}$* for the oxidation of 2.0mM $Fc(MeOH)_2$ in 2.0% (w/w) NIPA-AA gel containing 0.1 M $LiClO_4$; Pt microdisk electrode, r_d = 13 μm. Best fit:. $I_t/I_{ss} = 0.0993t^{-1/2} + 0.751$

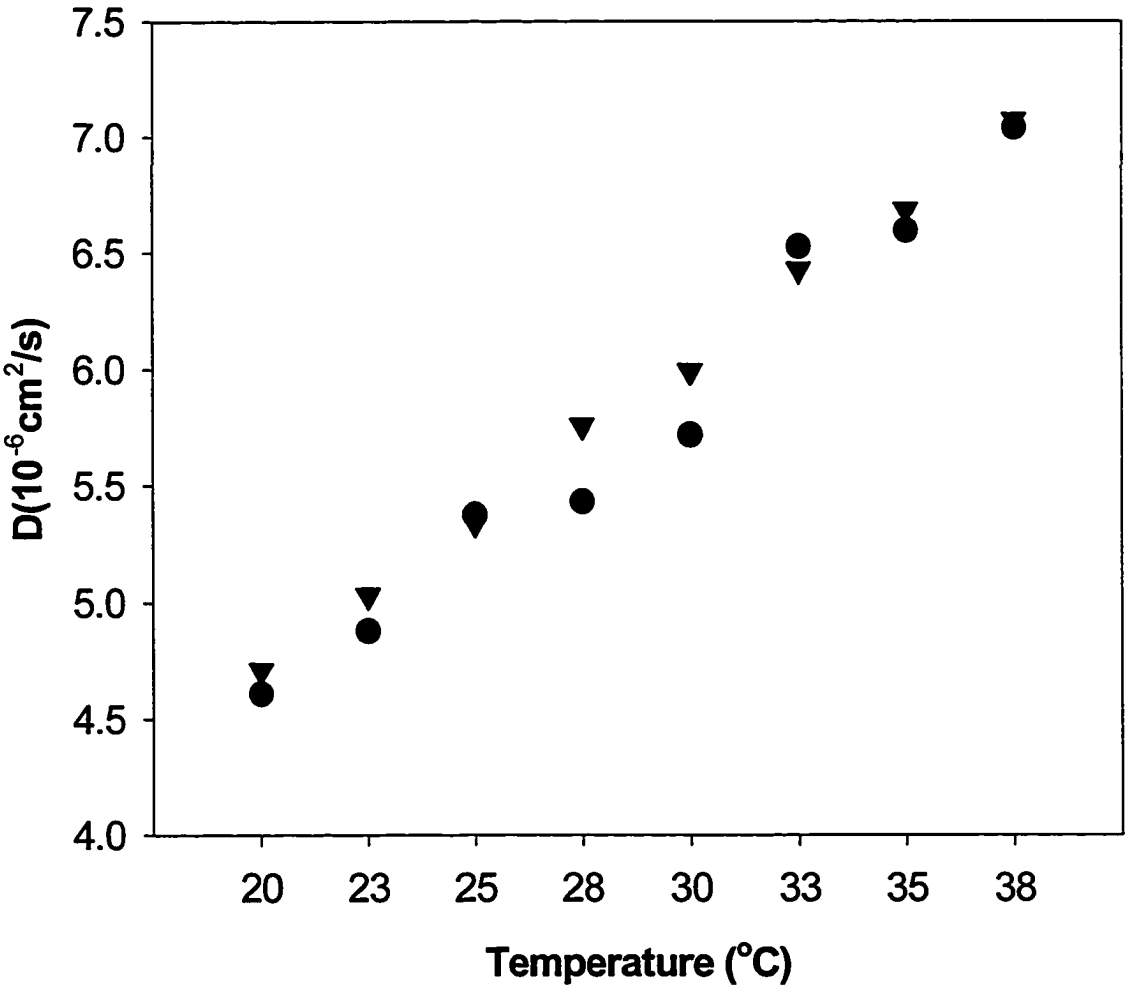

Figure 4.3 The diffusion coefficient of $Fc(MeOH)_2$ in 2.0% (w/w) NIPA-AA hydrogel containing 0.1 M $LiClO_4$; (•) measured by steady-state-voltammetry, (▼) measured by chronoamperometry.

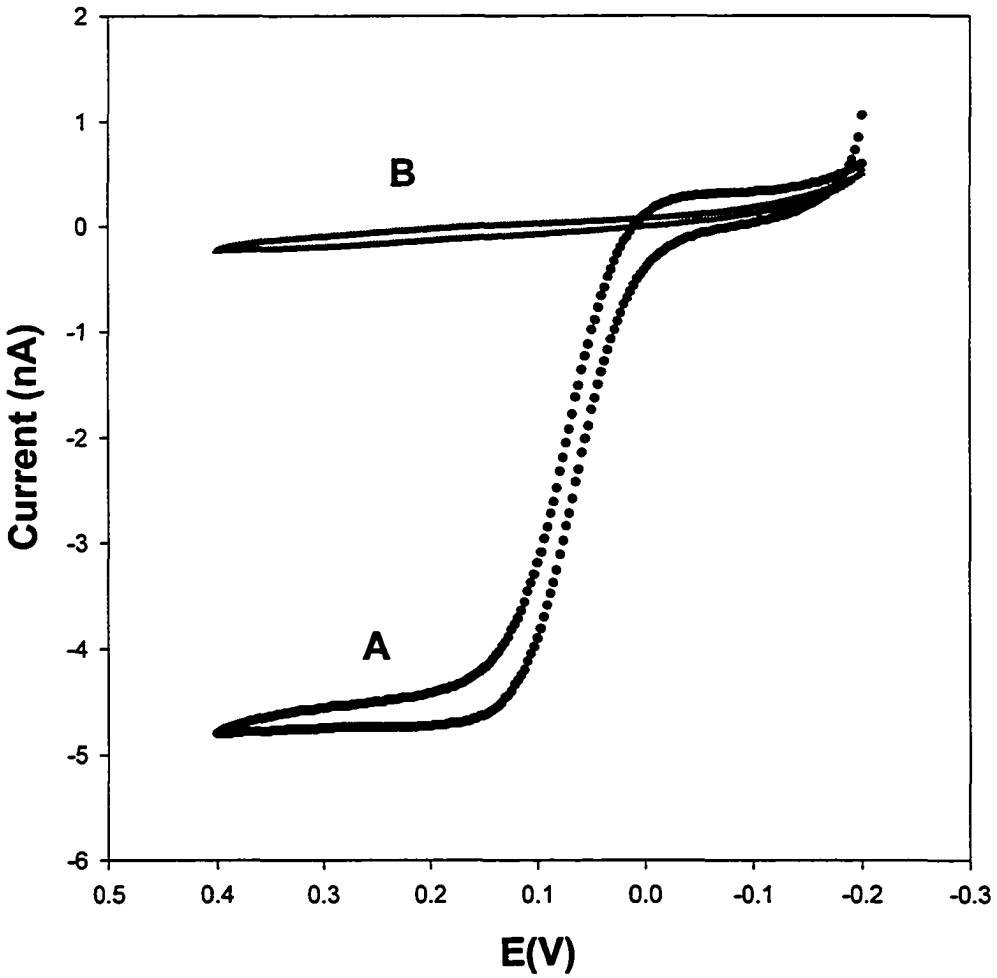

Figure 4.4 Steady-state voltammogram of the oxidation of (**A**) 2 mM $Fc(MeOH)_2$ in 3 % (w/w) NIPA gel, (**B**) background; 0.1 M $LiClO_4$, Pt microdisk electrode, r_d = 11 μm, 25 °C

for NIPA gel with 0.1 M $LiClO_4$. The diffusion coefficients of $Fc(MeOH)_2$ in the 1.7%, 2.4% and 3.0% NIPA gels at 25 °C were 5.8×10^{-6} cm^2/s, 5.5×10^{-6} cm^2/s and 5.4×10^{-6} cm^2/s respectively, which is smaller than that in aqueous solution, 6.4×10^{-6} cm^2/s. The following table (table 4.2) gives the diffusion coefficient of $Fc(MeOH)_2$ at different temperature and concentration of NIPA polymer.

4.3 Activation energy for diffusion – macroscopic and microscopic viscosity of gels

The diffusion of molecules in an ideal solution obeys Stokes-Einstein relationship:

$$D = kT/6\pi\eta r \qquad (4.3.1)$$

where D is the diffusion coefficient of diffusing species, k is Boltzmann's constant, T is the temperature, η is the solution viscosity, and r is the hydrodynamic radius of a molecule. It has been reported that the Stoke-Einstein relationship does not apply to diffusion in polymeric gels. [107,108] The macroscopic viscosity of NIPA-AA gels is always much larger than that of solutions (see Table 4.3), but the decrease of diffusion coefficient is relatively small. This is always attributed to the comparatively open structure of gels compared to the solid materials.

We studied the temperature dependence of diffusivity of $Fc(MeOH)_2$ in NIPA-AA gel, NIPA gel and in aqueous solution with supporting electrolyte, $LiClO_4$, in the

Table 4.2 Temperature Dependence of the Diffusion Coefficient of $Fe(MeOH)_2$ in 0.1 M $LiClO_4$ Aqueous Solution and NIPA Gels.

	$D(cm^2/s) \times 10^6$		
Temperature (°C)	1.7% (w/w) NIPA gel	2.4% (w/w) NIPA gel	3.0% (w/w) NIPA gel
20	5.09 ± 0.0664	4.86 ± 0.145	4.78 ± 0.0321
22.5	5.52 ± 0.0211	5.17± 0.194	5.03 ± 0.0416
25	5.9 ± 0.0153	5.51^6± 0.166	5.36 ± 0.0400
27.5	6.38 ± 0.0257	5.87 ± 0.127	5.6 ± 0.0624
30	6.73 ± 0.260	6.27 ± 0.193	5.88 ± 0.0600

Table 4.3 Viscosity and Diffusion Coefficients of $Fc(MeOH)_2$ in Various NIPA-AA Gels

Medium [a]	D ($cm^2 s^{-1}$) @ 25 °C	η_u (cP) @ 24 °C
0.1 M $LiClO_4$ solution	6.3×10^{-6}	9.4×10^{-1}
1% NIPA-AA gel	5.2×10^{-6}	N/A
2% NIPA-AA gel	4.3×10^{-6}	2.0×10^{5}
3% NIPA-AA gel	3.4×10^{-6}	2.4×10^{6}
4% NIPA-AA gel	3.2×10^{-6}	5.6×10^{6}

[a] All gels are prepared with 0.1 M $LiClO_4$

temperature range 20– 40 °C for NIPA-AA gel, 20 – 30 °C for NIPA gel. Note that this temperature range is below the volume phase transition for both gels, and those gels are in their swollen states. The results are presented in Figure 4.5. As predicted by Stokes-Einstein equation eq.4.1, the diffusivity of $Fc(MeOH)_2$ is proportional to the temperature of system.

The data from Table 4.1 and Table 4.2 were analyzed in terms of an Arrhenius-like equation $D = Ae^{-E_a/RT}$ (4.3.2)

where E_a is the activation energy of diffusion of the probe of interest in the aqueous solution or in a gel, A is the frequency factor, R is the gas constant, and T is the temperature. Figure 4.6 shows the data for the aqueous solution and these gels of various composition analyzed in the form of *lnD* vs. *1/T* plots, and table 4.4 shows values of E_a and A calculated from these data. The value of E_a for the diffusion of $Fc(MeOH)_2$ in aqueous solution and in NIPA-AA gels was in the range of 16.6 - 19.0 kJ/mol. The E_a for $Fc(MeOH)_2$ in the swollen state of NIPA were calculated following the same approach. The experimental activation energy of diffusion is 18.5, and 18.6 kJ/mol, for 1.1% and 2.4% NIPA gels, respectively. This agrees with the *Ea*-value of 19 ± 1.5 kJ/mol reported by Jacob [109] for diffusion of N,N,N',N' - tetramethylethylenediamine (TMED) in an aqueous solution. As pointed out by Jacob, the activation energy required for diffusion of a species reflects the viscosity of solvent in which that species diffuses. The similar activation energy of diffusion of $Fc(MeOH)_2$ i

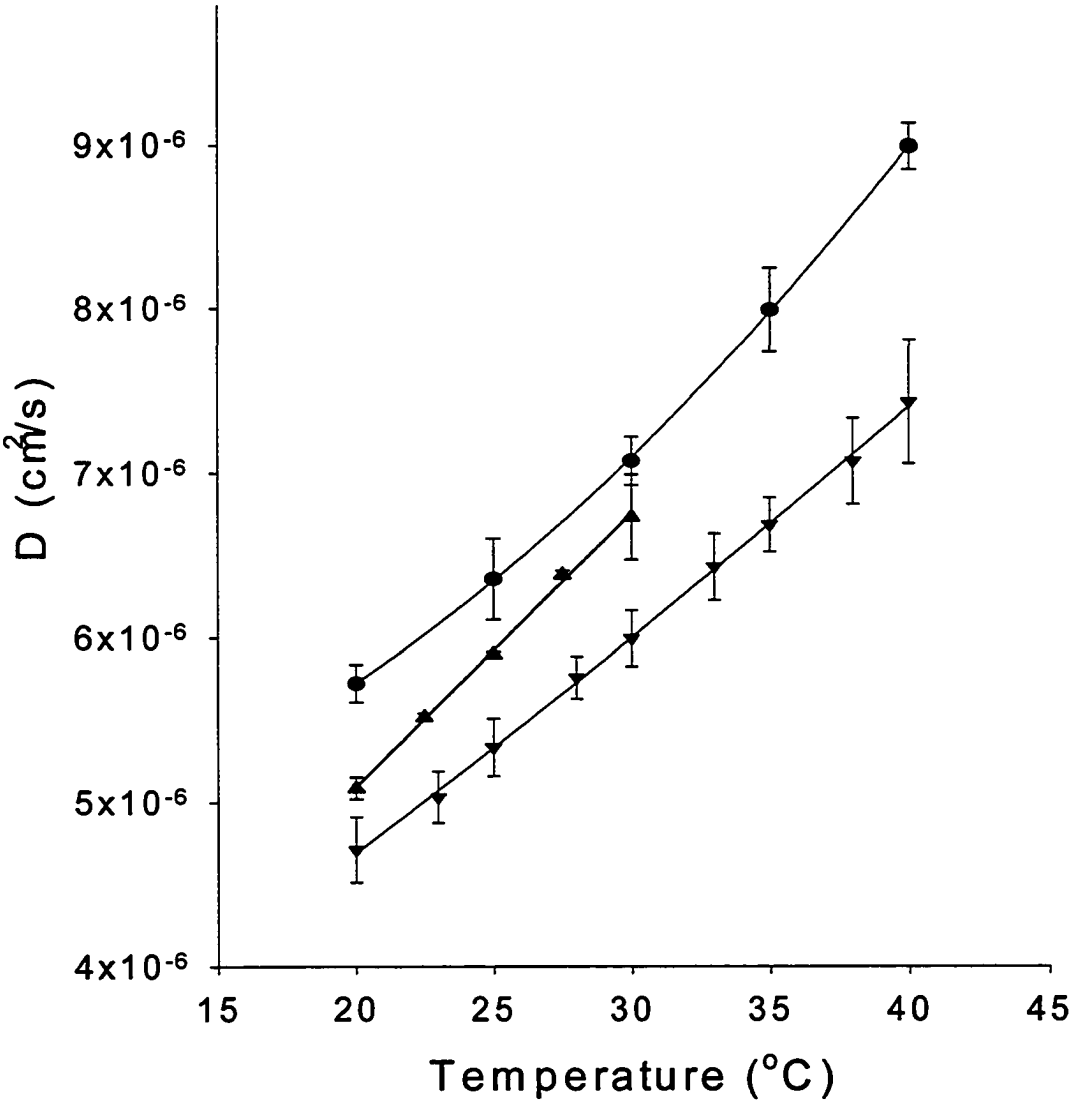

Figure 4.5 Temperature Dependence of Diffusion Coefficient of $Fc(MeOH)_2$, (●)Aqueous Solution; (▲) 1.7% NIPA Gel; (▼) 2.0% NIPA-AA gel; All with 0.1 M $LiClO_4$

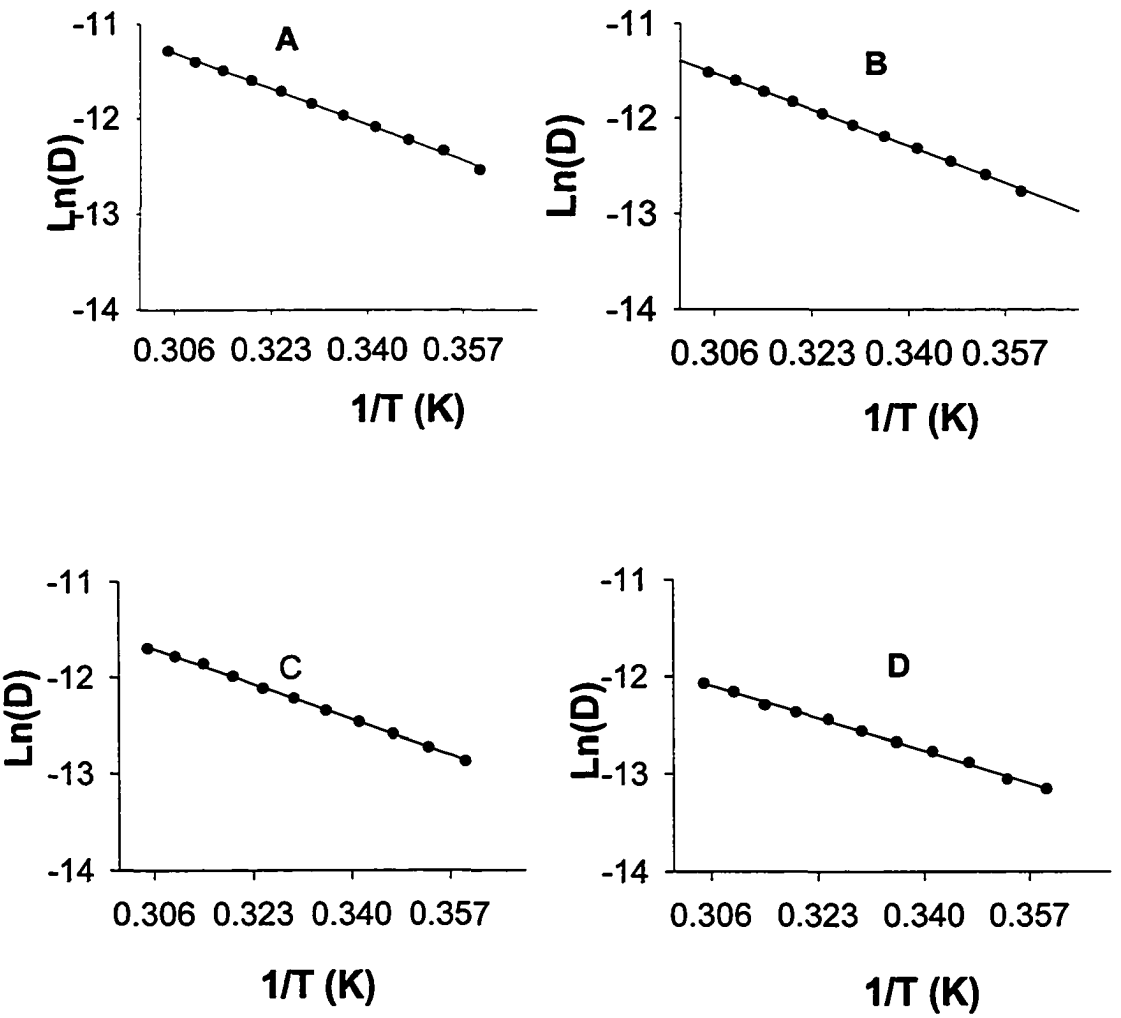

Figure 4.6 Arrhenius plots for the temperature dependence of the diffusion coefficient of Fc(MeOH)2 in aqueous solution (**A**), in 1.2% (w/w) NIPA-AA gel (**B**), in 2.0%(w/w) NIPA-AA gel (**C**), in 4.0% (w/w) NIPA-AA gel (**D**), all samples contain 0.1 M $LiClO_4$.

in aqueous solution and in the gels suggests that the microscopic viscosity of solvent trapped in NIPA-AA gels network is similar to that in aqueous solution due to the relatively open structure of gel system, although the macroscopically observed viscosity of gels is significantly larger than that for aqueous solution. For example the macroscopic viscosity of 3.0% (w/w) NIPA-AA hydrogel is 2.3×10^6 cP, which is approximately one million times larger than that of an aqueous solution. The smaller diffusion coefficient of $Fc(MeOH)_2$ in the gels may be attributed to change of the frequency factor A in an aqueous solution and gels. The frequency factors A for the diffusion of $Fc(MeOH)_2$ in various concentrations of gels are in the ranges of 1.1×10^{-2} - 2.6×10^{-3}, compare to 1.33×10^{-2} for and aqueous solution. However, the physical meanings of A is not clear yet.

These data suggests that E_a is a function of viscosity of solvent, the smaller the viscosity of the solvent, the smaller would E_a be expect to be. A series of experiments were designed to prove this idea. The temperature dependent D of $Fe(MeOH)_2$ in various concentration of sucrose aqueous solutions (20%, 40% and 60%) was measured. E_a was calculated by following the previously described approach. The viscosities of these solutions and the corresponding E_a shown in Table 4.5 indicate that solution with higher viscosity also has larger E_a. From our experiments, one can see that E_a is closely related to the viscosity of solution/solvent and it is very usefully to express the viscosity, especially in the case of gels, where the microscopic viscosity is totally different from the macroscopic viscosity and can not be measured by ordinary methods. However, both

Table 4.4 The Activation Energy of Diffusion of $Fc(MeOH)_2$ in Aqueous Solution and in the NIPA-AA Gels.

Polymer Concentration (W/W) %	Ea (kJ/mol)	A
0.00	18.9	1.33×10^{-2}
1.2	19.0	1.09×10^{-2}
2.0	18.0	6.35×10^{-3}
3.1	16.8	2.97×10^{-3}
4.0	16.6	2.58×10^{-3}

Table 4.5 The viscosity of different concentration of sucrose solution and activation energy (E_a) for diffusion of $Fc(MeOH)_2$ in these solutions

Concentration of sucrose	Viscosity (cP)(24(°C)	E_a (kJ/mol)
0	0.84	19.0
20%	1.40	19.9
40%	3.12	22.6
60%	6.65	24.0

NIPA-AA and NIPA polymers don't swell in sucrose solutions. Thus similar experiments can not be performed in gels.

Chapter 5 Diffusion in swollen gels - Model

5.1 Previous models

Several theoretical models have been proposed to describe the self-diffusion of solvent in colloidal suspension, gel systems and in protein solutions. These models include obstruction-scaling theory, [110, 111] free volume theory, [112,113] hydrodynamic theories. [114] None of these models is successful at explaining all the experimental observations. Therefore, the most appropriate model is still a controversial subject. We want to extend and apply an existing model [115, 116] for colloidal suspensions and protein solutions to thermosensitive polymeric gels, since the appropriate models to describe diffusion of molecules in polymeric gels are still not well developed. We assume that principles describing self-diffusion of solvents in polymeric systems should also be valid to describe diffusivity of any molecule, including our electroactive probes.

5.2 "Obstruction effect"

The decrease of the diffusion coefficient of water in the colloidal gel system and protein solution was analyzed in terms of two factors. The first factor is called the "obstruction effect". The colloidal suspension, polymer macromolecules, or micellar assemblies act as confinement and detour the diffusion of the molecules. The effective diffusion length is increased and diffusion coefficient is reduced as compared to the ideal solution. The second possible effect is the "hydration effect", when some water molecules

are bound to the surface of the colloidal objects or polymer molecules, and they form a temporally immobilized structured water layer. The volume of a polymer after hydration can be treated as several times larger, and it enlarges the "obstruction effect".

Wang [117] discussed the "obstruction effect" and its effect on diffusion of water in protein aqueous solutions. He proposed that the shape of ovalbumin molecules could be approximated by ellipsoids with principal semi-axes a, b, and c, respectively, as presented in figure 5.1. If only an "obstruction effect" is considered, the effective diffusion coefficient of water molecule in the protein solution, D', can be expressed as:

$$D' = D^{o}(1 - \bar{\alpha}\varphi) \tag{5.2.1}$$

where D^{o} and D' are diffusion coefficients of water in an ideal solution and in a protein solution, respectively, φ is the total volume fraction occupied by the hydrated protein molecules, which is defined as $\varphi = 1 - wg$, where w is the weight fraction of water and g

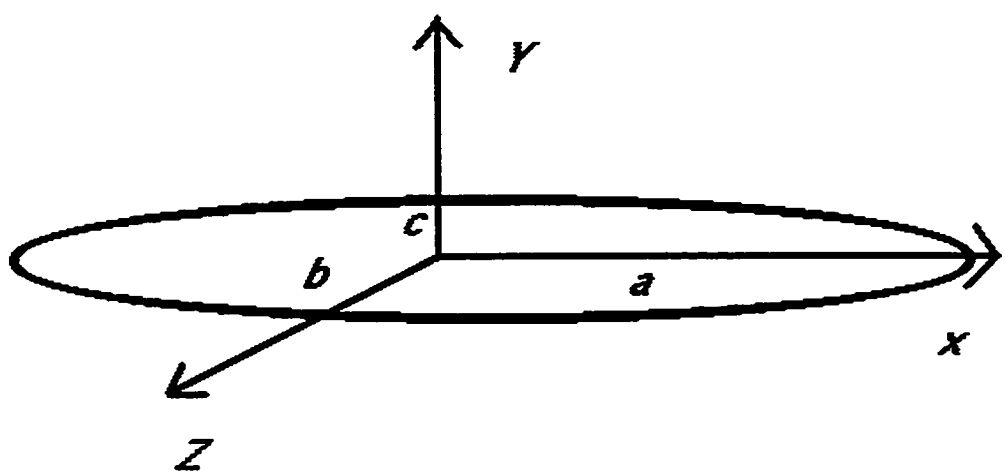

Figure 5.1 The schematic presentation of a macromolecule

is the specific gravity of the solution, and $\overline{\alpha}$ is a geometry related coefficient, which is defined as:

$$\overline{\alpha} = \frac{1}{3}(\alpha_a + \alpha_b + \alpha_c) \tag{5.2.2}$$

For prolate ellipsoids, if two of their principle axes are identical, that is $a = \rho b = \rho c$, where $\rho = a/b$ and $\rho > 1$, α_a and α_b can be obtained by the following equations:

$$\alpha_a = \frac{1}{\frac{\rho^2}{\rho^2 - 1} - \frac{\rho}{2(\rho^2 - 1)^{\frac{1}{3}}} \ln \frac{\rho + \sqrt{\rho^2 - 1}}{\rho - \sqrt{\rho^2 - 1}}} \tag{5.2.3}$$

$$\alpha_b = \frac{1}{\frac{\rho^2 - 2}{\rho^2 - 1} - \frac{\rho}{2(\rho^2 - 1)^{\frac{3}{2}}} \ln \frac{\rho + \sqrt{\rho^2 - 1}}{\rho - \sqrt{\rho^2 - 1}}} \tag{5.2.4}$$

As shown in figure 5.2, for a round shaped macromolecule, where the three axes are identical, the $\overline{\alpha}$ value is 1. If two axes of the macromolecules are identical and they are much larger than the third one. The $\overline{\alpha}$ value is $+\infty$. If one axis of a prolate ellipsoid, for example *a*, is significantly longer than the other two axes (*b* and *c*), the shape of molecule is like a rod cylinder. In this case, according to Wang's calculations (eqs. 5.2.2-5.2.4), the $\overline{\alpha}$

value is 1.667. Therefore, with proteins treated as cylindrical object, the effective diffusion coefficient of water molecules in the protein solution, D', can be expressed as:

$$\frac{D'}{D^o} = (-1.667\varphi + 1) \qquad (5.2.5)$$

One should be aware of the limitation of equation 5.2.5, it can be used only in very dilute gel systems. When the polymer fraction in the gel goes high, for example $\varphi > 1/1.667$, applying the equation 5.2.5 to explain experimental data will give the absurd result that the diffusion coefficient of a species in a gel has a negative value.

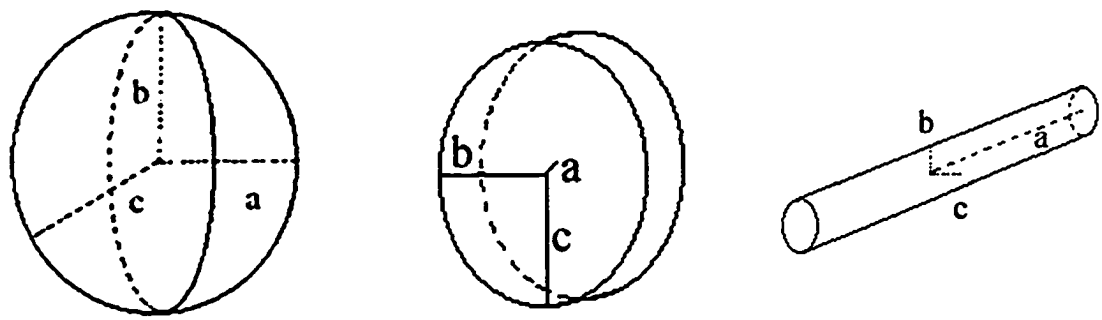

A
$a = b = c\ (\alpha = 1)$

B
$b = c >> a\ (\alpha = +\infty)$

C
$a >> b = c\ (\alpha = 1.667)$

Figure 5.2 The schematic presentation of different shapes of macromolecules

The eqs. 5.2.1 and 5.2.5 were originally used to describe the self-diffusion of water in protein aqueous solutions. We assume that the diffusion of electroactive probes should obey the same rules as those for solvent molecules in polymeric gels. In our experiment

NIPA-AA gel is a cross-linked polymer swollen by water or an aqueous solution. The diffusion coefficient of probes, such as $Fc(MeOH)_2$ in the swollen state of gels depends on the concentration of polymer in the gel. To develop an appropriate model describing the diffusion property in a gel, the gel can be simplified and treated as a system consisted of long rods swollen by a solvent. If the "obstruction effect" described by Wong is valid in a polymeric gel system, the diffusion coefficient of water, and consequently, all probe molecules in the gels should satisfy eq. 5.2.5. The total volume fraction occupied by polymeric units, φ, can be obtained experimentally by measuring weight fraction of water in the gels and the density of gels, which implies how much space in the gel is occupied by polymers. In our experiment, since the polymer concentration in gels was very small ($\leq 4.0\%$), the density of a gel was almost the same as aqueous solution. If we assume that polymer chain is not hydrated in hydrogels, the value φ may be treated as the weight concentration of polymer in the gels.

Table 5.1 gives the diffusion coefficient of $Fc(MeOH)_2$ in aqueous solution, D^o, and in NIPA-AA gel, D', for various values of φ, with φ defined as a weight concentration of the polymer in the gels. Experimental data presented in Table 5.1 are demonstrated in Figure 5.3, and they can be fitted to the linear dependent equation 5.2.6 with the correlation coefficients.

$$\frac{D'}{D^o} = -14.8\varphi + 0.990 \qquad (5.2.6)$$

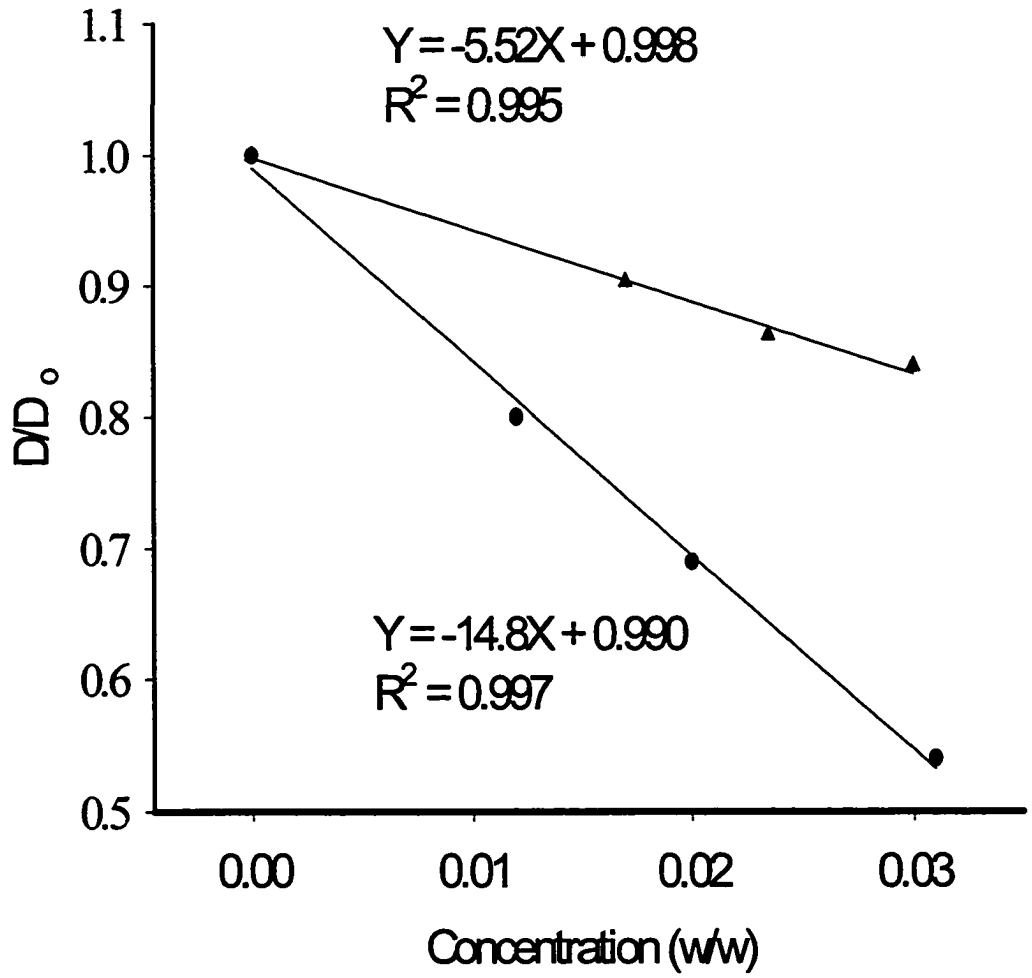

Figure 5.3 Dependence of the normalized diffusion coefficient (D/D_0) of $Fc(MeOH)_2$ in the NIPA-AA (●) and NIPA (▲) hydrogel on the concentration of polymer in the gel

Similar calculations also applied for NIPA gels (see Table 5.2) and the polymer volume fraction dependent of normalized diffusion coefficient was also plotted in Figure 5.3. They can be fitted to the linear dependent equation 5.2.7 with the correlation coefficients.

$$\frac{D'}{D^0} = -5.52\varphi + 0.998 \qquad (5.2.7)$$

Table 5.1 Diffusion Coefficient of $Fc(MeOH)_2$ in NIPA-AA Hydrogels

Polymer Concentration (W/W) %	***D* (cm^2/s) × 10^6 (25 °)**	***D/D°***	***φ***
0.0	6.32± 0.188	1.00	0.00
1.2	5.07± 0.293	0.80	0.012
2.0	4.35± 0.0555	0.69	0.020
3.1	3.42± 0.0281	0.54	0.031
4.0	3.12± 0.0777	0.50	0.040

Table 5.2 Diffusion coefficient of $Fc(MeOH)_2$ in NIPA hydrogels

Polymer Concentration (W/W) %	***D* (cm^2/s) × 10^6 (25 °)**	***D*/*D*°**	***φ***
0.0	6.40± 0.188	1.00	0.00
1.4	5.78± 0.0153	0.90	0.014
2.4	5.51± 0.116	0.86	0.024
3.0	5.36± 0.0399	0.84	0.030

5.3 "Hydration effect"

As presented in figure 5.3, one can see that diffusion coefficient of $Fc(MeOH)_2$ in gels is inversely proportional to the polymer concentration in the gel, as predicated by the "obstruction effect". As one can see the concentration dependence of the diffusion coefficient of $Fc(MeOH)_2$ in the NIPA-AA hydrogel system does not agree well with the "obstruction effect" model. If the weight concentration of the polymer in the gel is regarded as φ, the slope of plot in Figure 5.3 should be -1.667 as predicted by eq. 5.2.5. However, the experimental value is -14.8 and –5.52 for NIPA-AA and NIPA gel, which is 8.87 and 3.22 times larger than the predicted value individually.

If the geometry related coefficient, α, is correct, it seems that the volume fraction of the polymers in the hydrogel is expanded 8.87 and 3.22 times compared to the unhydrated state polymeric volume fraction. Such disagreement was also discovered previously in a colloidal system prepared by dispersing synthetic smectite clay in water. The value of the volume fraction of solid colloid measured from a self-diffusion of water experiment was 0.12, and it was six times larger than the actual solid volume fraction in the system, 0.02. The experimental value was "unrealistically high" according to the authors, because it would be related to a 3nm thick water layer on the surface of the clay platelets. The reason for this difference is not clear yet. Cheever, [115] Duval [118] and Von Meerwall [116] attributed this difference to the "hydration effect", which is related to the water molecules firmly attached to the polymer, forming a temporarily immobilized water film around the polymer chains due to hydration or another hydrodynamic effect.

The NIPA-AA co-polymer contains many carbonyl and amino functional groups. Polymeric chains in the hydrogels interact with water molecules through the hydrogen bond. Lee [119] proposed three states of water in gels in which the "bound" water is attached tightly to polymer, "non-bound" water is free to diffuse, and "intermediate" state water molecules interact weakly with the polymer chain. Since the "bound" state water and "intermediate" state water increases the volume of the polymer and can be treated as a part of the polymer in the hydrogel, we introduce a coefficient *H*, related to the degree of hydration of polymers. Now eq. 5.2.5 can be written as:

$$\frac{D'}{D^o} = (-1.667H\varphi + 1) \tag{5.3.1}$$

where -1.667 is a coefficient related to the shape of the polymer chain "obstruction effect". The experimental value of *H* can be obtained from equations 5.2.5 and 5.3.1. The *H*-value for NIPA-AA polymer in hydrogel is 8.77 according to our experiment. Since the diffusion coefficient of "bound" water is much smaller than the free state water, we treated the "bound" water as a part of the polymer chains and made an assumption that the electroactive probes do not diffuse freely in the "bound" water. We only focused on the diffusion of the probes in intermediate state and free state water in the gel. The *H*-parameter determined for NIPA polymer is 3.22, which is much smaller than that determined previously for poly(*N*-isopropylacrylamide-*co*-acrylic acid) hydrogel. This difference is easy to understand if one remembers that a polymer containing ionic groups like acrylate has a much larger degree of hydration than a nonionic polymer.

The hydration effect coefficient H should be characterized by the following properties. It is related to the properties of polymers and the interactions between the polymers and solvents. The interactions could be hydrogen bonding, specific absorption, and hydrodynamic effects. It is independent of the concentration of polymer in dilute gels. It is independent of the concentration of electroactive probes, if the probe concentration is low, and there is no interaction between the polymer and probes. Eq. 5.3.1 could be useful to describe the self-diffusion of any molecule in any polymeric gel system. If we know the diffusion coefficient of that molecule in an aqueous solution, the hydration H value of a polymer in its hydrogel, and weight concentration of polymer in that gel, the diffusion coefficient of that molecule in the gel can be predicted by eq. 5.3.1. The most important factor is the H value. For a given polymeric gel system, it can be determined by plotting D/D^0 vs. concentrations of polymer in gel.

To check if our model is correct, we performed a serial of experiments for TEMPO diffusing in NIPA-AA hydrogel. First we measured the diffusion coefficient of TEMPO in aqueous solution, D^o, and in 2.05% NIPA-AA hydrogel, D', using steady state voltammetry at disk microelectrode, and their dependence on temperature. The diffusion coefficient of TEMPO in 2.05% NIPA-AA hydrogel was calculated based on eq.5.3.1, using experimental D^o-values at various temperatures, the hydration coefficient $H = 8.77$ for NIPA-AA in hydrogel, and the volume fraction of the polymer in the gel, 0.021. Figure 5.4 compares calculated diffusion coefficients of TEMPO in 2.05% NIPA-AA gel with experimentally determined value. The difference between

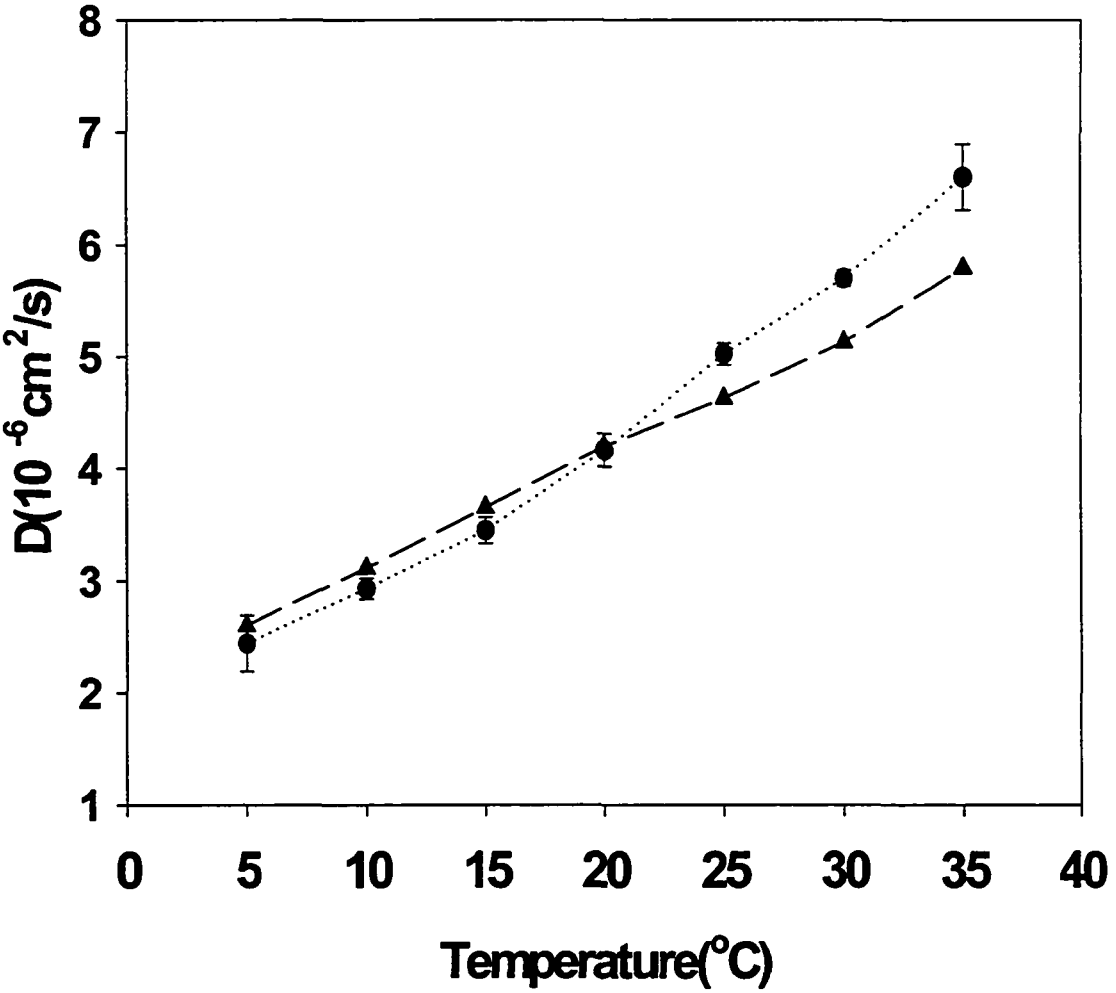

Figure 5.4. Temperature dependence of the diffusion coefficient of TEMPO in 2.0% (w/w) NIPA-AA gel; (▲) Calculated values, (●)

calculated values and experimental values was less than 7% for the temperature range 5 – 40 °C.

Eqs 5.2.5 and 5.3.1 could be very useful in many fields. For example, if we are interested in the diffusion coefficient of a target molecule in a polymeric gel, we know the diffusion coefficient of the molecule in an aqueous solution. We can estimate the diffusivity of that target molecule in a polymeric gel based on these equations. First, however we need the hydration coefficient value (H) of that polymer. The method is that we choose any molecule, which can be an electroactive probe, such as $Fc(MeOH)_2$. Its diffusion coefficient in polymeric gels can be easily determined using electrochemical experiments. From these diffusion coefficients, the hydration coefficient H for this polymer can be calculated as describe before. Then, the diffusion coefficient of the target molecule can be estimated by eq 5.3.1. As shown before, using the hydration coefficient, H, obtained from diffusion of $Fc(MeOH)_2$, we successfully predicated the diffusion coefficient of TEMPO in the NIPA-AA polymeric gel. This method should work well with small molecules diffusing in polymeric gels.

5.4 Limitations of our model

Since only the "obstruction effect" and the "hydration effect" were considered in our model (eqs. 5.2.5 and 5.3.1), this model is only valid for description of diffusivity of neutral probes in a diluted gel system. They may be valid to characterize transport of charged probes in non-charged gel system. However, it is not suitable to describe

transport of charged probes in polyelectrolytes systems and self-diffusion of large diffusion species such as polymeric molecules. Electrostatic interactions might be stronger than the "obstruction effect" and "hydration effect". In the gel, the cross-linked polymer chains define the passageway through which the molecules diffuse. The passageway constitutes the pores. The molecular weight of diffusing polymeric molecules and the pores of a gel affect the diffusion coefficient significantly. If the molecular weight of polymer is large enough, it will not penetrate the gel. The model we discussed above will not be valid for the gels during and after the volume phase transition. At the collapsed state, the polymer volume fraction of NIPA polymer phase could reach more than 0.9, irrespective of the NIPA and cross-linker concentration. These values are much beyond the assumption we made when we built the model for the diffusion, where only the dilute polymer gel was considered. In this situation, we would expect that the diffusion of molecules in the polymer phase would decrease dramatically due to the high polymer fraction in the gel phase.

5.5 Diffusion study in organic solvent

Recent progress in the investigations of transport phenomena in various media has become possible due to the unique features of micro or nanoelectrodes. Small measured currents and significant reduction of both ohmic potential drop and double-layer capacitance allow the exploration of new areas of electrochemistry inaccessible to

the classic approach, including measurements in highly resistive and concentrated redox systems, such as undiluted liquids. [120]

The diffusion of $Fc(MeOH)_2$ was also studied in gels swollen by organic solvent. The organic solvent used in our experiment was DMF with 50 mM $LiClO_4$ as supporting electrolyte. It should be pointed out that NIPA-AA polymer, which shows a temperature induced volume phase transition when swollen by water, does not show any sign of such a transition in the temperature range of 20 – 90 °C when DMF is used as the solvent. Similar behavior was also observed when methanol is used as solvent. [121] This may suggest that attractive interactions among the side chains of the NIPA-AA polymer, which induce the volume phase transition, become significantly weaker in nonaqueous media.

The oxidation of $Fc(MeOH)_2$ in NIPA-AA gels of various composition (2.1, 5.0, and 6.7 % of copolymer) was examined. $Fc(MeOH)_2$ gives well-defined, one-electron anodic wave at a platinum microelectrode. Voltammograms for the oxidation of $Fc(MeOH)_2$ in DMF solution and NIPA-AA/DMF gels studied over the temperature range 5-30 °C were very reproducible, with a coefficient of variation less than 5%. Diffusion coefficients for this probe were determined from steady-state, transport-limited currents, I_{ss}. Figure 5.5 presents temperature dependencies of $Fc(MeOH)_2$ diffusivity obtained in liquid and gel. As one can see, the D of $Fc(MeOH)_2$ in the gels are very close to those in pure DMF solvent. The change in the composition of the gel

from 2.1 to 6.7 % results in only a small change of the D of $Fc(MeOH)_2$ (less than 30% at 25 °C).

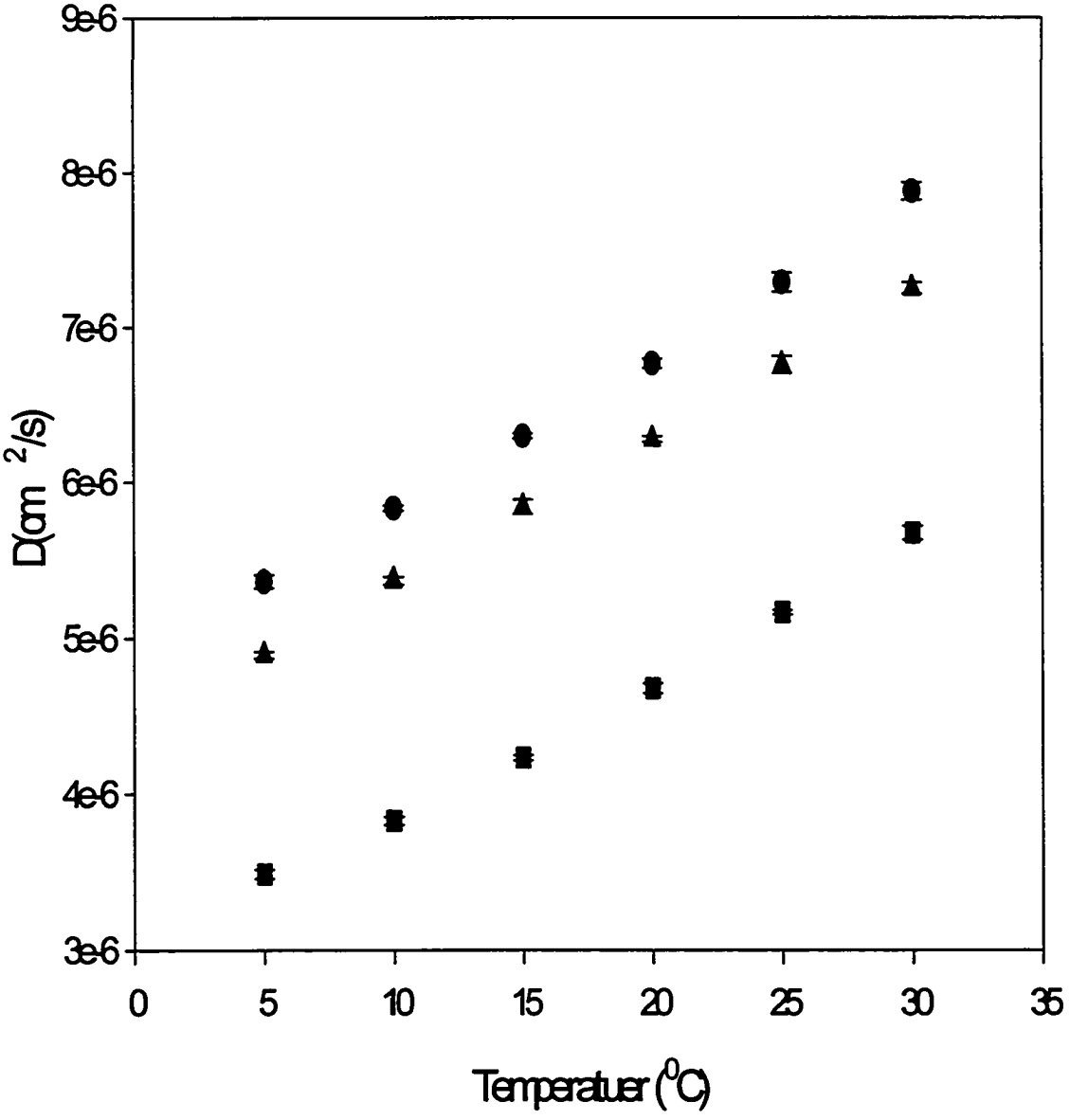

Figure 5.5 Temperature dependence of $Fc(MeOH)_2$ in DMF solvent (●), 2.1% NIPA-AA gel(▲), 6.7% (■)NIPA-AA gel.

The data presented in Figure 5.5 were analyzed in terms of the Arrhenius-like equation. The determined activation energies, E_a are 10.7, 10.9, 11.3 and 13.8 kJ/mol, for DMF solution, 2.1, 5.0, and 6.7% NIPA-AA/DMF gels, respectively. Similarly to DMF, the smaller values of E_a obtained for the gels may suggest a slight decrease in local viscosity in this medium compared to methanol solution. Note that the E_a value for $Fc(MeOH)_2$ in DMF, NIPA-AA/DMF gel is smaller those in aqueous solution and NIPA-AA hydrogel, which is in the range of 16.6-19.0 kJ/mol. However, it is very close to E_a in menthol and NIPA-AA/menthol, which are in the range of 11.6-13.5 kJ/mol. [121]

The dependencies of D of $Fc(MeOH)_2$ on the concentration of NIPA-AA polymer in NIPA-AA/DMF gels were also studied. Table 5.3 summarized the D of $Fc(MeOH)_2$ and normalized diffusion coefficient in various volume fractions of polymer. One can see that the concentration of NIPA-AA has a smaller effect on the decrease of the D of molecules in NIPA-AA/DMF gels than that in hydrogels. In 6.7% NIPA-AA/DMF gel, the D of $Fc(MeOH)_2$ decreases less than 30% compared with D in DMF solvent. The data in Table 5.3 was fitted with our newly developed diffusion model (Figure 5.6). The H coefficient measured from figure 5.6 is 2.67, which is much smaller than the H coefficient of NIPA-AA in hydrogels, which is 8.77. But in the case when organic solvent is used, the term "hydration coefficient" is not valid anymore and "solvation coefficient" is more appropriate. The small H coefficient suggests that the interaction between NIPA-AA polymer and DMF solvent is very weak. One reason for this effect may be lack of hydrogen bonding between the NIPA-AA polymer and DMF.

Table 5.3 Dependence of Diffusion Coefficient of $Fc(MeOH)_2$ in NIPA-AA/DMF gel on the Concentration of the Polymer in the Gel.

Polymer Concentration (W/W) %	D (cm^2/s) × 10^6	D/D^o	φ
0.0	7.3 ± 0.061	1.00	0.00
2.1	6.8 ± 0.051	0.93	0.021
5.0	5.7 ± 0.12	0.78	0.050
6.7	5.2 ± 0.013	0.71	0.067

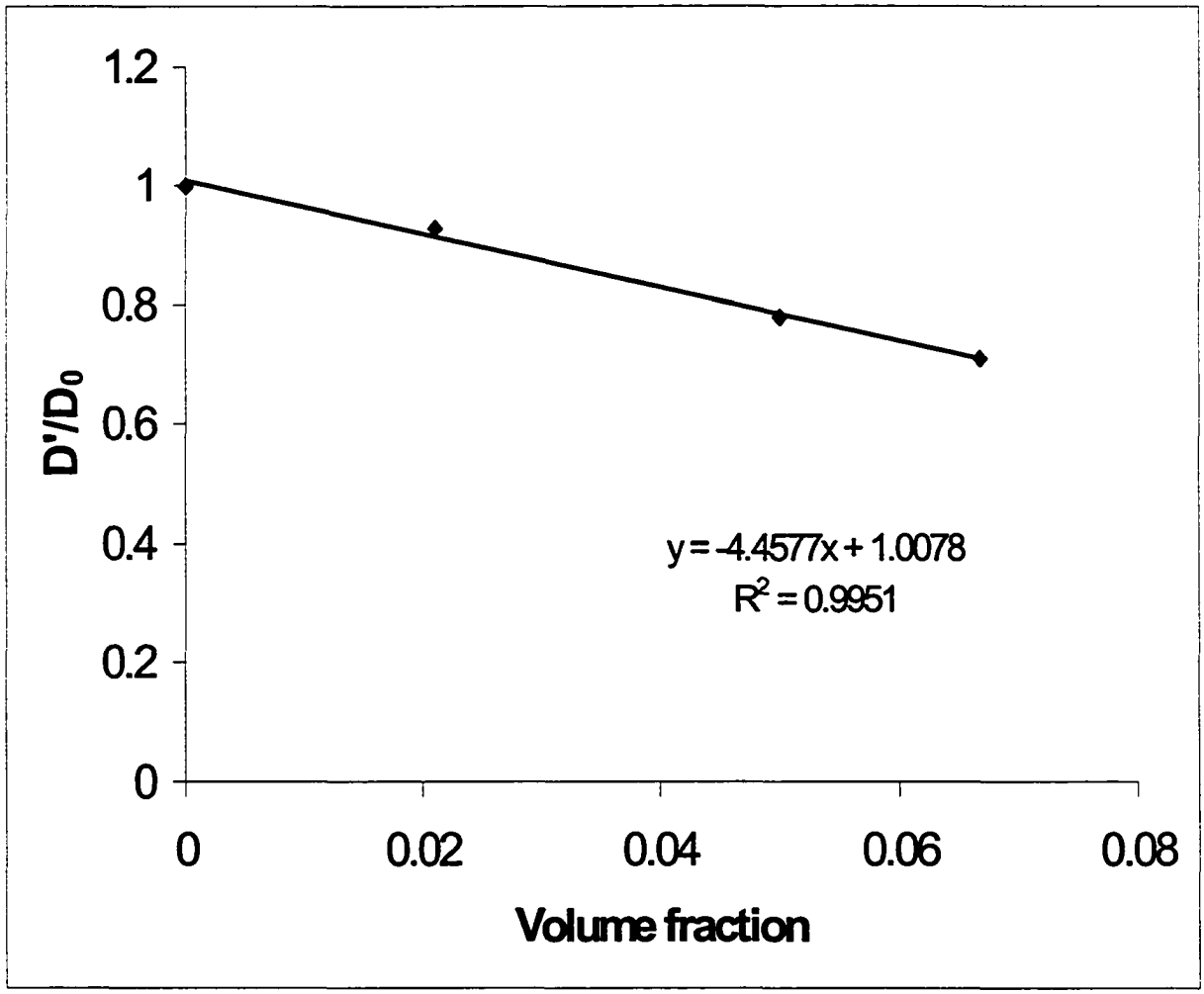

Figure 5.6 Dependence of the normalized diffusion coefficient (D/D_0) of $Fc(MeOH)_2$ in NIPA-AA/DMF on the volume fraction of NIPA-AA polymer.

Chapter 6 Diffusion in collapsed gels

6.1 Kinetics of gel collapsing

Tanaka-Fillmore (TF) theory suggests that the time-scale of the volume phase transition of gels depends on the size of gels, i.e., the smaller the gel the faster the gel can shrink or swell. [39] Recent differential scanning calorimetry (DSC) studies have shown that the small size NIPA gel (0.3 mm in diameter) undergoes the volume phase transition in several minutes. However, for a larger size NIPA gel (3 mm in diameter), the volume decrease was very slow, and the volume phase transition could not occur during the DSC experiment. [42]

In our experiment, when bulky sized gel (thickness >3mm) is used, the dynamic effect of the volume phase transition of gel can be clearly observed. When the volume phase transition occurred, the steady-state oxidation current gradually decreased. This fact also proves that the electrochemical approach using microelectrodes is a very sensitive method for gel studies, and it can be used to continuously monitor the phase transition of gels. The steady-state current for oxidation of $Fc(MeOH)_2$ in 2.6 % NIPA hydrogel was measured and plotted in Figure 6.1. It is obvious that the phase transition of NIPA gel occurs in two stages. During the first 120 minutes, the volume of the gel decreases relatively fast and the steady state current drops to approximately half of the original value. In the second stage, the steady state current changes very little, which suggest that the phase transition take place very slowly. As indicated in figure 6.1, at 55

°C, even after 660 minutes, the steady state current still decreases. At the second state of phase transition, the change of the gel is so small that the gel can be regard as in

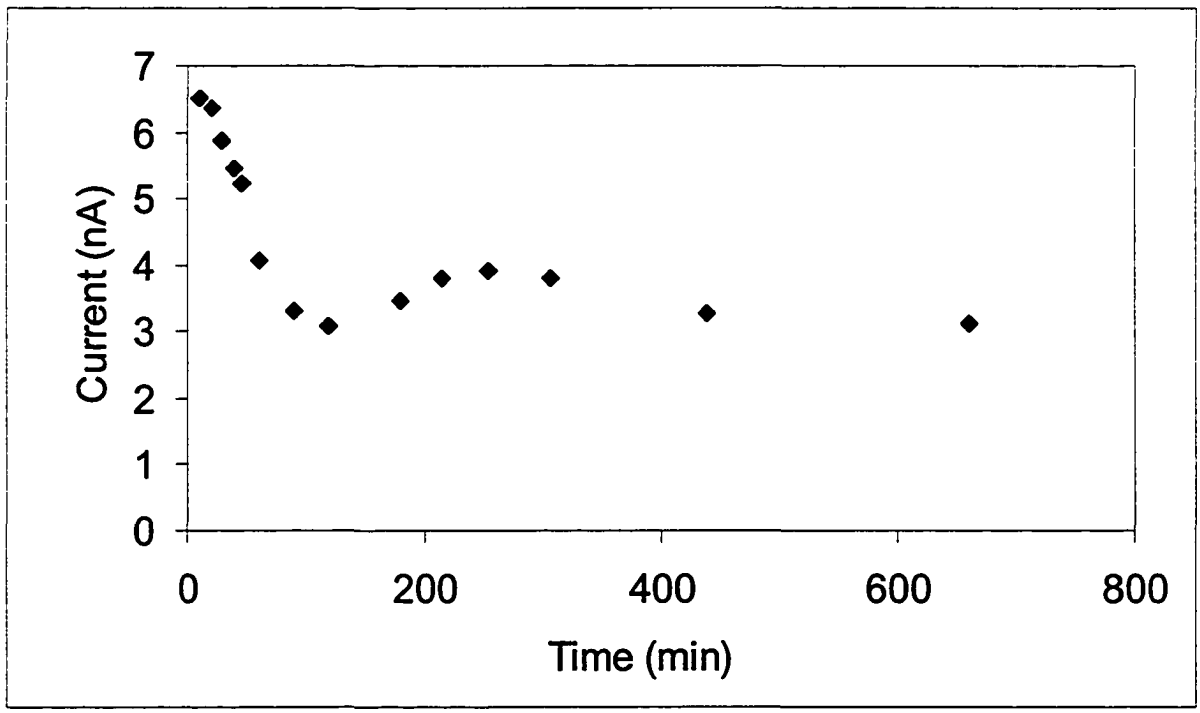

Figure 6.1 The steady state current of oxidation of 2 mM $Fc(MeOH)_2$ in 2.6 % NIPA gel (prepared using pebble size dry polymer)obtained at different of time. (r = 11μm Pt electrode, 0.1 M $LiClO_4$, 55 °C)

pseudo steady state. Therefore, some researchers who used relatively large sized NIPA gels reported that when the phase transition of their NIPA gels is completed, the volume of gels shrunk to half of the original size. [28, 122] Figure 6.2 shows the temperature dependent steady state current in large sized NIPA gels. At each temperature, which is above 32 °C, we waited 120 minutes before each scan was performed. One can see that when the phase transition occurred, the steady state current drops to approximately half of that at 30 °C. Then, the current will increase again due to the increase of temperature.

To minimize the uncertainties caused by the kinetic effect of the volume phase transition, dry crosslinked NIPA polymer was ground using a micro-mill to get very fine NIPA polymer powder. An inverted microscope was used to determine the size of the polymeric particles. The major fraction of these particles (approximately 90%) had a radius smaller than 0.1 mm. The NIPA hydrogel with small gel size was prepared using this ground polymer. After the swelling process, separation of a single swollen particle of the gel, and a measurement of the size of that particle was not possible. The NIPA gel prepared by this method undergoes a volume phase transition at a temperature of 32 ± 1 °C, and this transition results in a release of approximately 93% of the solvent from the polymeric phase. After the volume phase transition, the small-size NIPA gel particles did not separate; the polymer phase collapsed forming one large piece of a rubber-like polymeric phase.

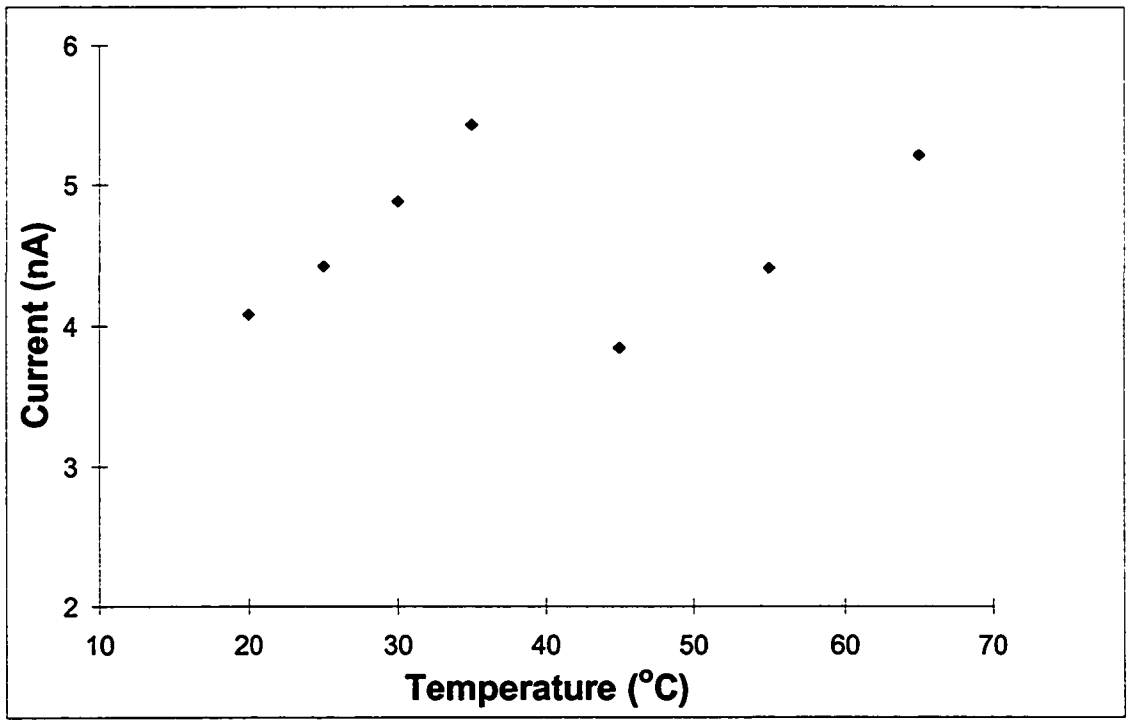

Figure 6.2 The steady state current of oxidation of 2 mM $Fc(MeOH)_2$ in 2.6 % NIPA gel as the function of temperature. (r = 11μm Pt electrode, 0.1 M $LiClO_4$, 55 °C)

6.2 Diffusion in collapsed NIPA gel

Transport of $Fc(MeOH)_2$ in collapsed NIPA gels was first studied using steady state voltammetry. We found that when the volume phase transition occurred, the oxidation current of the $Fc(MeOH)_2$ probe in collapsed NIPA gels dropped significantly. Therefore, a very slow scan, such as 1mv/s, was applied in steady state voltammetry experiments to make sure the current reached the steady state. Figure 6.3 compares two voltammograms of the oxidation of 2 mM $Fc(MeOH)_2$ and 4 mM in 3 % NIPA gel at 27.5 and 55 °C, and Figure 6.4 shows the dependence of the limiting current on the temperature, from 20 to 65 °C. As one can see, after the volume phase transition, the steady state current drops almost to zero. This suggests that the D of $Fc(MeOH)_2$ decreases significantly. The decrease of the limiting current in collapsed gels might also due to the change of the concentration of $Fc(MeOH)_2$ in the collapsed gel phase (see eq. 2.7.9). At the same time, the reproducibility of the limiting current is much worse than that for swollen gels. The relative standard deviation, *rsd*, of limiting currents after the phase transition is 42 %, while for swollen gels the *rsd* is less than 5%. This can be attributed to the inhomogeneous distribution of an electroactive probe in the collapsed polymeric phase or due to inhomogeneity of the collapsed polymeric phase. Since the concentration of the probe in the collapsed gel is not known, chronoamperometry was applied to measure the diffusion coefficient of electroactive probes in collapsed gels. According to eq. 2.2.11, the plot of a normalized current as a function of $1/t^{1/2}$ should be linear with a slope $s=\pi^{1/2}r_d/4D^{1/2}$. Therefore, the diffusion coefficient of probes can be calculated using the following dependence:

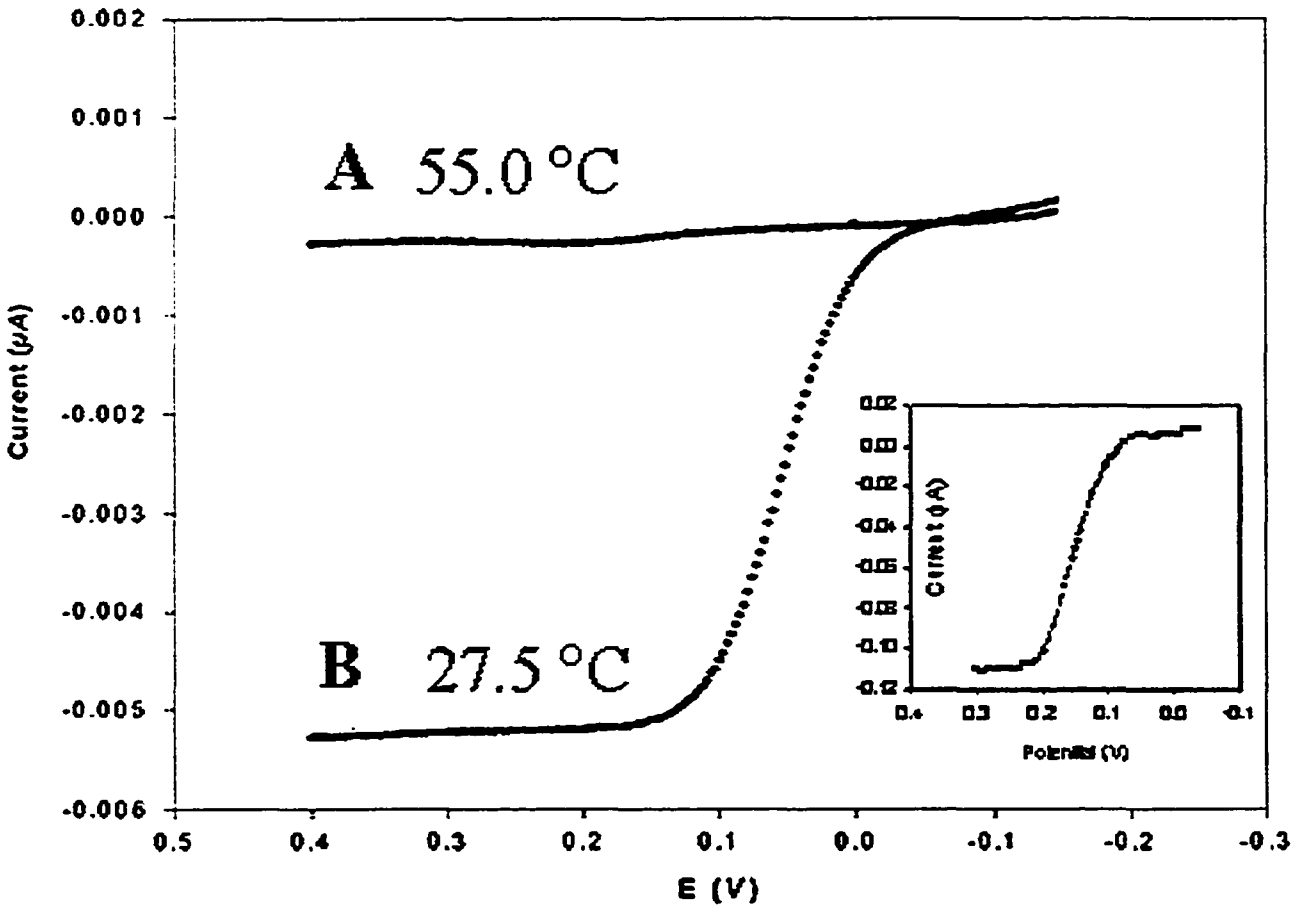

Figure 6.3 Steady-state voltammograms of oxidation (A) 4.0 mM $Fc(MeOH)_2$ in collapsed 3.0% NIPA gel at 55 °C. (B) 2 mM $Fc(MeOH)_2$ in 3 % (w/w) NIPA Gel at 27.5 °C. Inset: Enlarged voltammogram at 55 °C.

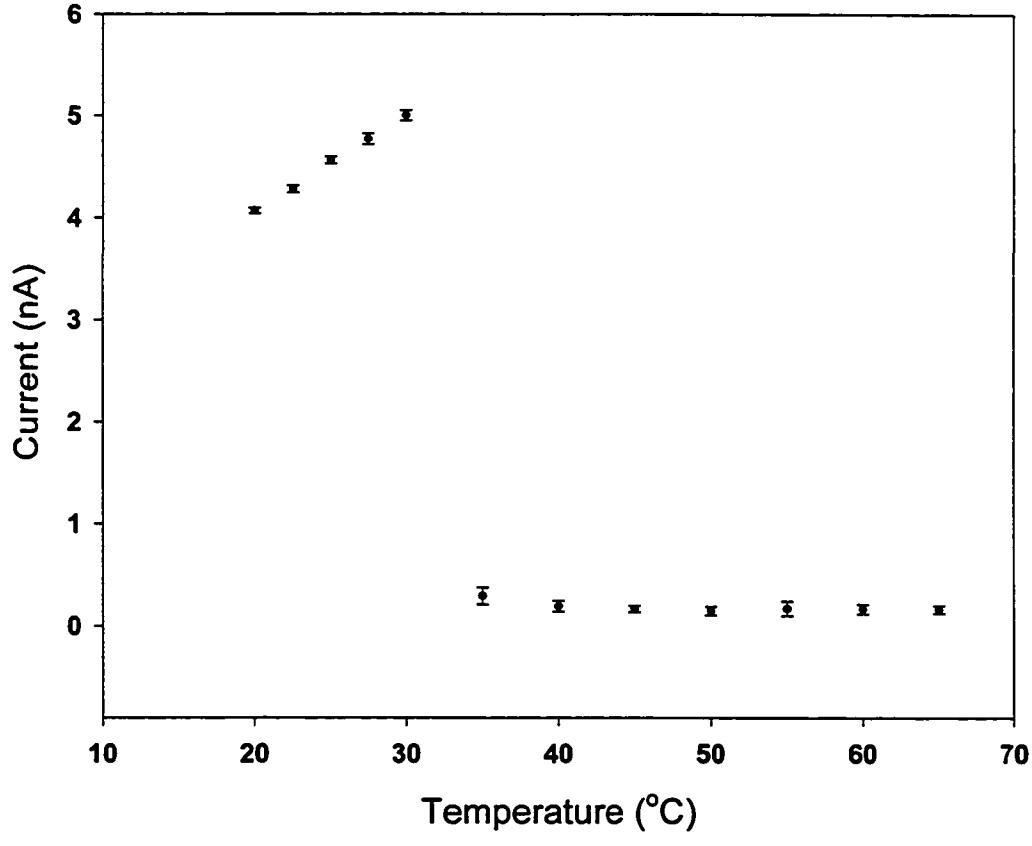

Figure 6.4 Temperature Dependent Steady State Current of $Fc(MeOH)_2$ in 3.0% NIPA Gel (prepared using grounded polymers), r = 11 μm Pt electrode, 0.1M $LiClO_4$.

$$D = (\frac{\pi^{1/2} r_d}{4s})^2 \qquad (6.2.1)$$

Figure 6.5 shows the transient current, I_t, as a function of $t^{-1/2}$. Linear dependence was obtained as predicted by eq. 2.7.11. The pulse time of chronoamperometry was set to 200 ms. Diffusion coefficients of $Fc(MeOH)_2$ in 3% NIPA collapsed gels were calculated based on eq. 6.2.1 and are listed in Table 6.1. From the data obtained from these experiments, we found that the diffusion coefficient of $Fc(MeOH)_2$ in collapsed gel was at the magnitude of $10^{-8}cm^2/s$.

As one can see, the diffusion coefficient of $Fc(MeOH)_2$ in collapsed gels is approximately 2 orders of magnitude smaller than that in 3% NIPA swollen gels, 5.4×10^{-6} cm^2/s at 25 °C. One reason for such a decrease is that, after a loss of 93% of the solvent during the volume phase transition; the polymer phase is very dense and the liquid channels for molecular/solvent transport are considerably restricted.

Since $Fc(MeOH)_2$ in aqueous solution has an absorption band in the UV-vis range with a maximum absorbance at 430 nm, UV-vis spectroscopy can be used to study the distribution of $Fc(MeOH)_2$ between the collapsed polymer phase and the released solution and to determine changes of its concentration as a result of the volume phase transition. The calibration plot was prepared using standard $Fc(MeOH)_2$ aqueous solutions with the concentration range from 1 to 6 mM. Three NIPA hydrogels with various polymer concentrations were prepared. Each gel contained 2 mM $Fc(MeOH)_2$. After the gel collapsed, the solution expelled from the gel was collected. The absorbance

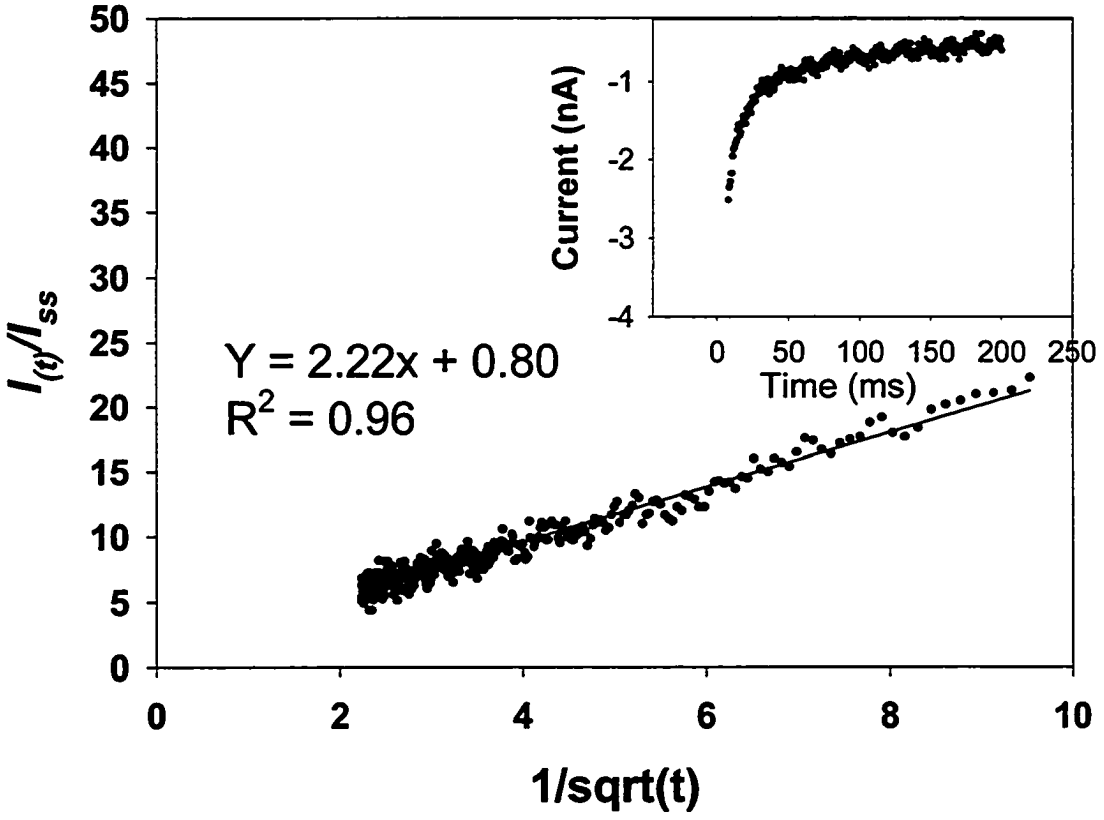

Figure 6.5 Plot of the experimental I_t/I_s *vs.* $t^{-1/2}$ for the oxidation of $Fc(MeOH)_2$ in 3% NIPA gel at a r_d = 5 μm Pt electrode at 40 °C; the transient current is also shown.

Table 6.1 Diffusion Coefficient of $Fc(MeOH)_2$ in Collapsed NIPA Gel (r = 5μm Pt electrode, 0.1 M $LiClO_4$)

Temperature (°C)	Diffusion Coefficient (cm^2/s)
35	7.5×10^{-9}
40	1.1×10^{-8}
45	1.2×10^{-8}
50	1.5×10^{-8}
55	2.1×10^{-8}
60	1.9×10^{-8}
65	2.7×10^{-8}

of that solution was measured and the concentration of $Fc(MeOH)_2$ was determined based on the concentration calibration plot. Table 6.2 presents concentrations of $Fc(MeOH)_2$ in expelled solutions for several compositions of NIPA gels. As one can see the concentration of $Fc(MeOH)_2$ in the released solution is lower than that in the original swollen gel. This means that the concentration of $Fc(MeOH)_2$ in the collapsed gel is higher than that in swollen gel. This indicates strong interactions between $Fc(MeOH)_2$ and the NIPA polymeric network. These might be due to hydrophobic interactions and/or van der Waals interactions. For the 3% NIPA gel with 2 mM $Fc(MeOH)_2$ in the swollen state, we found that after the volume phase transition, the concentration of the probe in the released solution is 1.5 mM. Based on the volume and the mass of the released solution and the mass of the collapsed gel, with the assumption that the density of polymeric phase is close to that of aqueous solution, we can estimate the concentration of $Fc(MeOH)_2$ in the collapsed gel as 9 mM, which is 4.5 times higher than that in the original swollen gel and 6 times higher than that in released liquid.

The distribution of inorganic salts between N-isopropylacrylamide collapsed gels and aqueous phase has been studied by the Kawasaki group. [123] All of the salts they studied are various alkali metal salts. They reported that the phase transition of NIPA hydrogel has a significant effect on the distribution of inorganic salts. Some salts were completely excluded from the gels phase after the phase transition. This exclusion depends on the character of the salts. However $LiClO_4$, which was used in our

Table 6.2. Concentration of $Fc(MeOH)_2$ in swollen NIPA-AA gels and expelled solutions.

	Concentration of $Fc(MeOH)_2$ (mM)		
NIPA (w/w) %	Swollen Gel	Expelled Solution	Collapsed Gel (Estimated concentration)
1.7%	2.0	1.7	12
2.6%	2.0	1.6	10
3.0%	2.0	1.5	9

experiments as supporting electrolyte, was not in their research list. We studied a series of Cu and Ni salts, including $Cu(NO_3)_2$, $CuSO_4$ and found the same tendency. Although, there are no data for $LiCO_4$, it is reasonable to believe that the concentration of $LiClO_4$ in the collapsed gel was smaller than that in swollen gel. The possibility that there was redox material trapped in the collapsed gel is small. The collapsed gel is just partially dehydrated and the gel phase still contains about 50% of the solvent.

6.3 Diffusion of neutral probes in collapsed NIPA-AA gels

The small amount of acrylic acid in NIPA-AA has a significant effect on the phase transition of gels. The volume phase transition temperature of NIPA-AA gels is about 45 °C. For NIPA gels, it is 32 °C. NIPA-AA gels lose approximately 40% of the solvent. NIPA gels lose more than 90% of the solvent. This difference causes a distinct consequence on the collapsed gel phases. The swelling ratio, $W_{solvent}/W_{polymer}$, of the gels, is about 1-2 and 20-30 for NIPA and NIPA-AA, respectively. The open structure for diffusion still exists in NIPA-AA gels, but not in NIPA gels. Figure 6.6 shows the temperature dependent D of $Fc(MeOH)_2$ in NIPA and NIPA-AA gels. One can see that there is a distinct diffusion behavior after the volume phase transition occurred. For NIPA-AA gels, the diffusion coefficient of $Fc(MeOH)_2$ was measured for the temperature range 5 – 55 °C. As the open structure is still persevered in the gel phase, no significant change in D of $Fc(MeOH)_2$ was observed in gel phase before and after the volume phase transition. Diffusion coefficients of $Fc(MeOH)_2$ in 3% NIPA-AA

collapsed gels were 5.5×10^{-6}, 9.3×10^{-6}, and 10.0×10^{-6} cm^2/s at 25, 50 and 55 °C, respectively.

The UV/vis studies were carried out in the 3.0% NIPA-AA gel with 1.5 mM $Fc(MeOH)_2$. The collapsed NIPA-AA gel phase retains $Fc(MeOH)_2$. But this effect is much weaker than in the NIPA gel. The released solution contained 1.1 mM $Fc(MeOH)_2$. The concentration of $Fc(MeOH)_2$ in collapsed NIPA-AA gel is estimated as 1.8mM, which is about 20% higher than that in original swollen gels. One possible reason could be that 0the NIPA-AA polymer chain is less hydrophobic than NIPA polymer chain.

6.4 Diffusion of charged probes in NIPA-AA gels

Since NIPA-AA gels are weakly negatively charged, we expect attractive electrostatic interactions with cations. Therefore, two electroactive cationic probes, ferrocenylmethyltrimethylammonium, $FcTMA^+$, and hexaammineruthenium(III), $Ru(NH_3)_6^{3+}$, cations were selected for these studies. We studied how the ionic strength, composition of the gel, and the discontinuous volume phase transition of the NIPA-AA hydrogels effect the diffusion coefficients and the concentration of electroactive probes.

6.4.1 Diffusion of monocharged probe in the gel

Steady-state voltammetry at a platinum disk microelectrode was used to study transport of $FcTMA^+$ in NIPA-AA gels of various concentrations. Steady-state oxidation waves of $FcTMA^+$ were very well defined. The reproducibly of limiting currents in NIPA-AA gels was excellent, with relative standard deviation, *rsd*, not higher

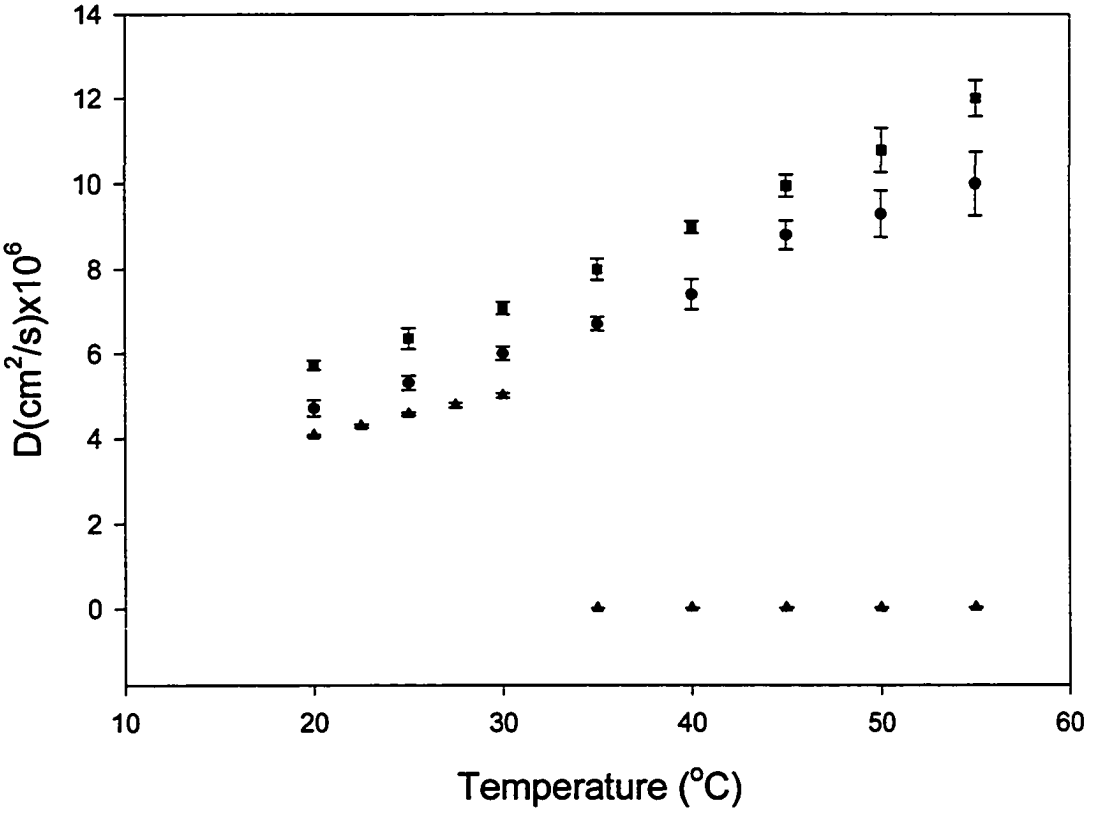

Figure 6.6. Diffusion coefficients of 1,1'- ferrocenedimethanol, ■ in 0.1M $LiClO_4$ solution, ● in 2% NIPA-AA gel supporting electrolyte, ▲ in 3% NIPA gel with 0.1M LiClO4 as supporting electrolyte

than 1.4% (calculated from 15 voltammograms). The shape of the steady-state voltammograms of $FcTMA^+$ oxidation was almost identical in NIPA-AA gels with and without $LiClO_4$, in pure water without a gel, and in aqueous solutions of $LiClO_4$. The reproducibility of the limiting currents, *rsd* was 2.1% and 2.5% in 0.1 M $LiClO_4$ and pure water, respectively.

Table 6.3 shows the dependence of the viscosity of a gel and the diffusion coefficient of $FcTMA^+$ on the concentration of a NIPA-AA copolymer in the gel, the latter was measured by steady state voltammetry. The diffusion data in NIPA- AA gels is compared with those in electrolyte solution. Note that these results are for swollen gels at temperatures below the discontinuous volume phase transition. As one can see, the decrease of the diffusion coefficient of $FcTMA^+$ in gels is very small compare to changes of viscosity of the system. As we discussed before, the reason is that the macroscopic and microscopic viscosity of gels are quite different and that the transport of $FcTMA^+$ in NIPA-AA gels at temperatures below the volume phase transition is controlled by the local microscopic viscosity of the system. This very low dependence of diffusion of ionic probes on macroscopic viscosity of polymeric networks indicates the potential usefulness of these gels as semi-rigid electrolytes for electrochemical applications.

Figure 6.7 shows the dependence of the diffusion coefficient of $FcTMA^+$ on temperature in $LiClO_4$ solutions and NIPA-AA hydrogels of various compositions and ionic strengths. For the temperature range below the volume phase transition of NIPA-

AA gels, diffusion coefficients of $FcTMA^+$ increase with an increase of temperature, as predicted by Stokes-Einstein relation. Note that these gels are in swollen state. The temperature range of increasing diffusion coefficient narrows for higher concentration of a copolymer in a gel, and it decreases from 5 - 45 °C to 5 - 25 °C with concentration of copolymer changing from 1% to 4%.

The activation energy of diffusion can be determined from the slope of the linear dependence of ln$D$ on $1/T$ as discussed before. The calculated values of activation energy of diffusion of $FcTMA^+$ in NIPA-AA hydrogels of various compositions are presented in Table 6.3. The E_a-values are in the ranges of 18.2 $kJmol^{-1}$ to 19.2 $kJmol^{-1}$ for 0.1 M NaCl solution and NIPA-AA gel with 0.1 M NaCl. As one can see from Table 6.2, E_a values for gels and solutions do not differ significantly. These data are slightly larger than those in NIPA gels, which are in the ranges of 16.5-17.4 kJ/mol for 1.1% to 4.0% NIPA gels. One possible reason for this different is the electrostatic interactions between the positive charged probe and negative charged polymer network.

When NIPA-AA gels undergo discontinuous volume phase transition, transport of $FcTMA^+$ in collapsed NIPA-AA gels is very different from that in the swollen gel. As shown in Figure 6.7, the D of $FcTMA^+$ decreases significantly as a result of the volume phase transition, and this decrease is more pronounced for larger concentrations of copolymer in the gel. For example, the D of $FcTMA^+$ determined from experiments at 50 °C is 2.39×10^{-6} $cm^2 s^{-1}$ in 4% NIPA-AA gel, only 20.6% of that in 0.1 M $LiClO_4$ solution (11.6×10^{-6} cm^2 s^{-1}), while for 1.0 % NIPA-AA gel at the same temperature,

Table 6.3. Diffusion Coefficients of $FcTMA^+$ and Viscosity of NIPA-AA Gels

Medium [a]	D ($cm^2 s^{-1}$) @ 25 °C	Ea (kJ/mol)	η_u (cP) @ 24 °C [12]
0.1 M $LiClO_4$ solution	6.3×10^{-6}	18.8	9.4×10^{-1}
1% NIPA-AA gel	5.5×10^{-6}	19.1	2.0×10^{4}
2% NIPA-AA gel	5.4×10^{-6}	19.2	2.0×10^{5}
3% NIPA-AA gel	4.8×10^{-6}	18.2	2.4×10^{6}
4% NIPA-AA gel	4.7×10^{-6}	18.5	5.6×10^{6}

[a] All gels are prepared with 0.1 M $LiClO_4$

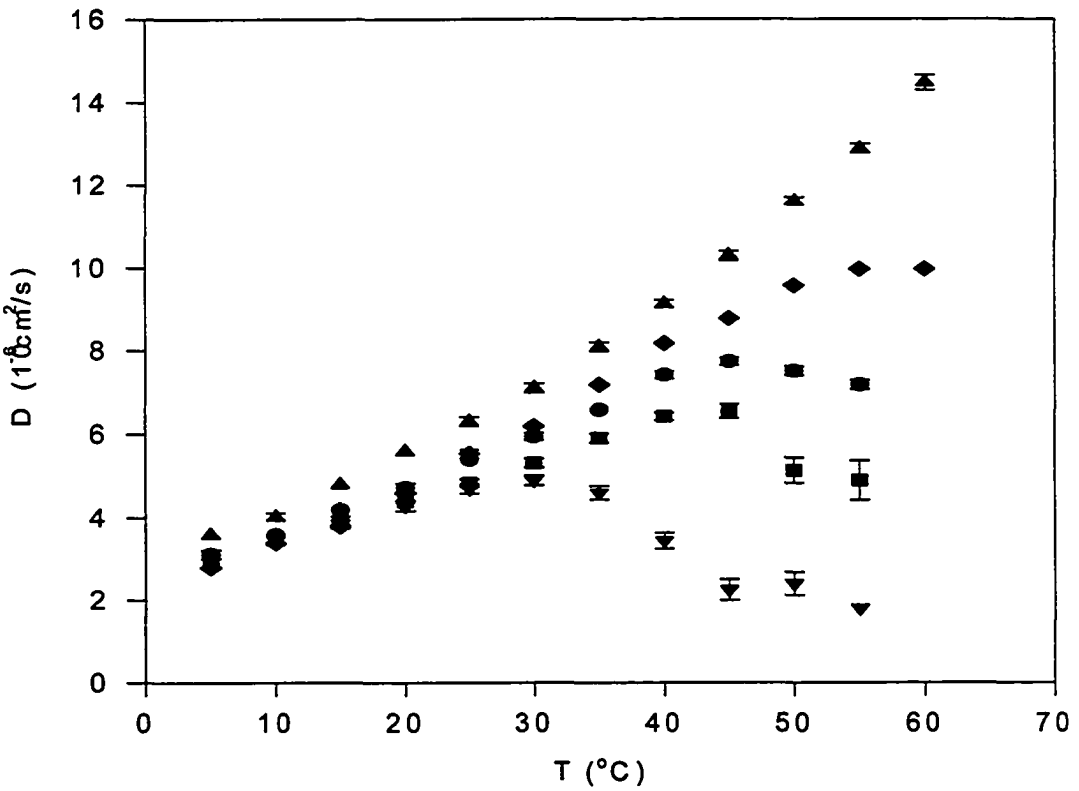

Figure 6.7 Diffusion coefficients of 1mM FcTMA determined by stair-case voltammetry in NIPA-AA gels and solution. ▲ in 0.1 M $LiClO_4$ solution ◆ in 1% gel ● in 2% gel ■ in 3% gel ▼in 4% gel. All gels with 0.1 M $LiClO_4$ as supporting electrolyte.

The diffusion coefficient of $FcTMA^+$ is 9.57×10^{-6} cm^2 s^{-1}, 82.5% of that in 0.1 M $LiClO_4$ solution. It should be pointed out here that these diffusion coefficient values were determined from steady-state voltammetry according to eq 2.2.9, with the assumption that the concentration of $FcTMA^+$ in the gel does not change during the discontinuous volume phase transition. To find out if our assumption was correct and to determine the diffusion coefficient of $FcTMA^+$ in collapsed NIPA-AA gels independent of concentration, we performed chronoamperometric experiments and determined the diffusion coefficient of $FcTMA^+$. The comparison of the temperature dependence of the diffusion coefficient of $FcTMA^+$ in 2.0 % NIPA-AA gel from chronoamperometric and steady-state voltammetric results shows that, for temperatures below the volume phase transition, the diffusion coefficient values obtained by both methods are very close. This means that the concentration of $FcTMA^+$ does not change with temperature for swollen gels. However, near and above the volume phase transition temperature, approximately 45 °C, the diffusion coefficients of $FcTMA^+$ determined from steady-state voltammetry are different compared with those determined from normalized chronoamperometry. This effect can be seen even for a lower temperature, approximately 30 °C, for 4% NIPA-AA gel. For example, the diffusion coefficients of $FcTMA^+$ in the collapsed NIPA-AA gels determined from normalized chronoamperometry at 55 °C were 9.6×10^{-6} and 5.3×10^{-6} cm^2 s^{-1} for 2.0 % and 4% gels, respectively. They are 1.34 and 2.94 times those determined from steady-state voltammetry, and 0.74 and 0.41 of those determined in 0.1 M $LiClO_4$ solution of the same temperature. The difference between

diffusion coefficient values determined by steady-state voltammetry and chronoamperometry indicates the change in the concentration of $FcTMA^+$ in NIPA-AA gel near and above volume phase transition temperature. Like $Fc(MeOH)_2$, $FcTMA^+$ ion also has absorption in a UV-Vis band, therefore, the method, determining the change of concentration of $Fc(MeOH)_2$ after phase transition of NIPA gel, is also valid for measuring the concentration $FcTMA^+$ in NIPA-AA gels. Two batches of NIPA-AA gels, 2.0% and 4.0% were prepared, both contained 5 mM $FcTMA^+$. When phase transition occurred, the released solutions were collected and their composition was analyzed by UV-Vis spectrophotometer. It was found that the release solutions contained 4.3 and 4.0 mM $FcTMA^+$ for 2.0% and 4.0% gels respectively, which suggests that the polymer rich gel phase absorbs $FcTMA^+$ due to the hydrophobic and electrostatic interactions.

Since NIPA-AA gels are weakly negatively charged, attractive electrostatic interactions can be expected between negatively charged carboxylic moieties of the NIPA-AA polymeric network and any cations in the system. Those interactions should be the strongest in systems of very low ionic strengths. A series of experiments has been performed in solutions and gels without added supporting electrolyte; the results are presented in Figure 6.8. As one can see, the transport coefficient of $FcTMA^+$ in pure water, calculated according to eq 2.2.11, is slightly lower than that with electrolyte, with an average value of 0.885 of that in 0.1 M $LiClO_4$ solution. This is due to the migration

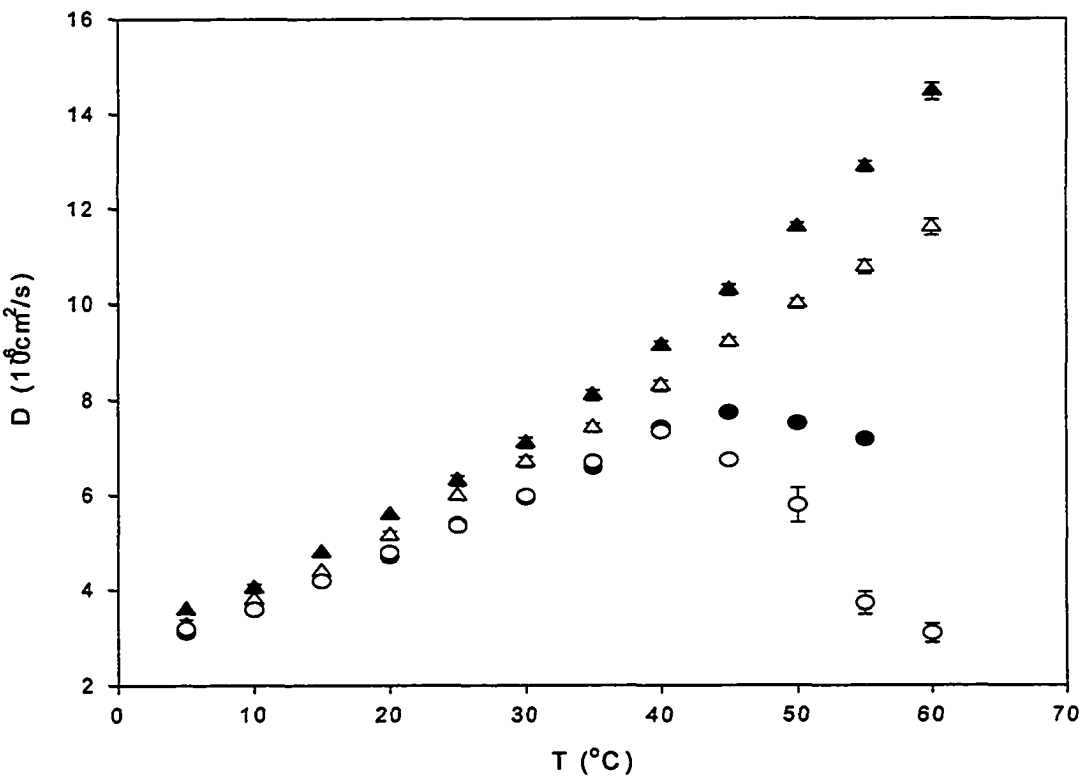

Figure 6.8 Diffusion coefficients of 1 mM FcTMA determined by stair-case voltammetry in NIPA-AA gels and solutions: ▲ in 0.1M $LiClO_4$ solution, △ in water, ● in 2% gel with 0.1 M $LiClO_4$ as supporting electrolyte, O in 2% gel without supporting electrolyte.

of $FcTMA^+$; the direction is opposite to that of diffusion, and therefore, decreases the total flux and oxidation current of $FcTMA^+$. According to theoretical predictions, [124] the total steady-state current for 1-electron oxidation of a monocharged cation should be 0.849 of the purely diffusional current. For temperatures below the volume phase transition of NIPA-AA gels, there is no difference between the diffusion coefficients of $FcTMA^+$ in 2.0% gel with and without 0.1 M $LiClO_4$; in both cases they increase with an increase of temperature. However, after the volume phase transition occurs, a decrease of the diffusion coefficient of $FcTMA^+$ in 2.0% gel without supporting electrolyte is more significant than that in 2.0% gel with 0.1 M LiClO4. For example, at 55 °C the diffusion coefficient was 7.2×10^{-6} and 3.7×10^{-6} cm^2s^{-1} for 2.0% gels with and without electrolyte, respectively. The *D* value in 2.0% gel without electrolyte is only 0.51 of that in 2% gel with electrolyte. Diffusion coefficients obtained by chronoamperometry at the same temperature were 9.6×10^{-6} and 6.2×10^{-6} cm^2s^{-1} for 2% gels with and without electrolyte respectively; the *D* value for the gel without electrolyte was 0.65 of that with electrolyte. This indicates that there are strong electrostatic attractive interactions between $FcTMA^+$ and the negatively charged polymeric network without electrolyte, and those interactions are much stronger than those with high concentrations of $LiClO_4$.

To compare the diffusivity of cations in NIPA-AA gels with diffusivity of neutral molecules, we studied the diffusion of $Fc(MeOH)_2$ as an electroactive probe. No

difference can be seen between systems with and without electrolyte; since $Fc(MeOH)_2$ is an uncharged probe, there are no electrostatic interactions between the gel network and the uncharged electroactive probe (see Figure 6.9).

6.4.2 Diffusion of trivalent cationic probe, $Ru(NH_3)_6^{3+}$

Voltammetric and chronoamperometric experiments were performed for a trivalent positively charged probe, hexaaminеruthenium(III) cation, $Ru(NH_3)_6^{3+}$, in NIPA-AA gels in their swollen state and during volume phase transitions. The one electron reduction of $Ru(NH_3)_6^{3+}$ at Pt microelectrodes results in a very well-defined voltammetric wave. The reproducibility of limiting currents was excellent, with *rsd's* (calculated from 15 voltammograms) of 0.48%, 0.70%, 0.77%, and 0.87% in 2% NIPA-AA gel with 0.1 M NaCl, 2% gel without electrolyte, 0.1 M NaCl solution, and water, respectively. Diffusion coefficients of $Ru(NH_3)_6^{3+}$ in solutions and in NIPA-AA gels were calculated according to eq 2.2.9, and their dependence on temperature in 0.1 M NaCl solution and NIPA-AA gels with 0.1 M NaCl is presented in Figure 6.10. As expected for a simple solution, the diffusion coefficient of $Ru(NH_3)_6^{3+}$ increases with an increase of temperature in 0.1 M NaCl solution.

In NIPA-AA gels with 0.1 M NaCl, it increases with temperature before the phase transition occurs and then decreases at temperatures close to the volume phase transition and above. For NIPA-AA gels in theirs swollen state, diffusion coefficients of

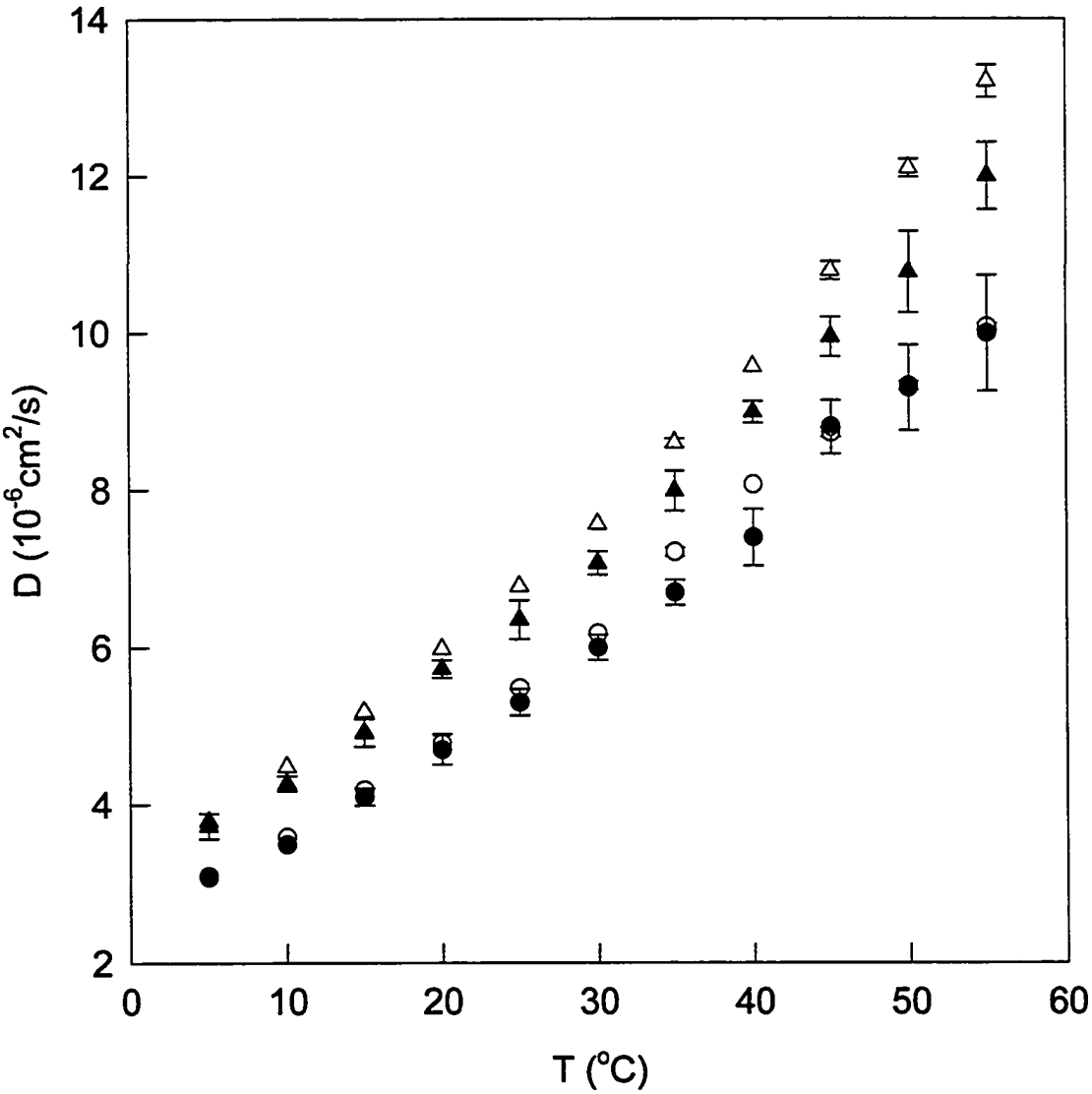

Figure 6.9 Diffusion coefficients of $Fc(MeOH)_2$ determined by stair-case voltammetry in NIPA-AA gels and solutions: △in 0.1M $LiClO_4$ solution, ▲ in water, ○ in 2% gel with 0.1 M $LiClO_4$ as supporting electrolyte, ● in 2% gel without supporting electrolyte.

$Ru(NH_3)_6^{3+}$ are only slightly lower than those in an aqueous solution. For example, at 25 °C (see Table 6.4) the D of $Ru(NH_3)_6^{3+}$ in 4.0% gel with 0.1 M NaCl is only 26.7% smaller than that in 0.1 M NaCl solution. This behavior is very similar to that of the monocharged cation, $FcTMA^+$. The activation energies of diffusion, E_a, of $Ru(NH_3)_6^{3+}$ were calculated using the Arrhenius-like equation, and are presented in Table 6.4. Similarly to $FcTMA^+$ and $Fc(MeOH)_2$, there are no significant differences in E_a values for the probe ions between gels and an aqueous solution. As one can see from Figure 6.10, the diffusion coefficient of $Ru(NH_3)_6^{3+}$ in NIPA-AA gels decreases significantly after the volume phase transition occurs, and this effect is more pronounced than that for $FcTMA^+$ (compare with Figure 6.7). This difference is probably due to electrostatic interactions of multicharged cations with the polymeric network in its collapsed state.

Apparently, there is a significant difference in interactions of the NIPA-AA polymeric network with molecules of a solvent, and other species present in the system between gels in their swollen and collapsed state. Tokuhiro [125] has determined the number and distribution of water molecules in swollen NIPA gels by measuring the densities of those gels using a specially designed pycnometer. His measurements verified the earlier findings that the physical state of water in gels is not identical to that of the liquid water. For ionic NIPA gels modified with acrylic acid groups, he found that acrylic acid residues could retain water molecules more than 9 times that of NIPA residues. It might be that these bound water molecules hinder interactions of probe

Table 6.4. Diffusion Coefficients of $Ru(NH_3)_6^{3+}$ and Viscosity of NIPA-AA Gels.

Medium [a]	D (cm^2s^{-1}) @ 25 °C	Ea (kJ/mol)
0.1 M $LiClO_4$ solution	7.9×10^{-6}	14.8
1.0%NIPA-AA gel	7.1×10^{-6}	16.1
2.0%NIPA-AA gel	6.3×10^{-6}	15.6
3.0%NIPA-AA gel	6.3×10^{-6}	16.0
4.0%NIPA-AA gel	5.8×10^{-6}	16.5

[a] All gels are prepared with 0.1 M NaCl

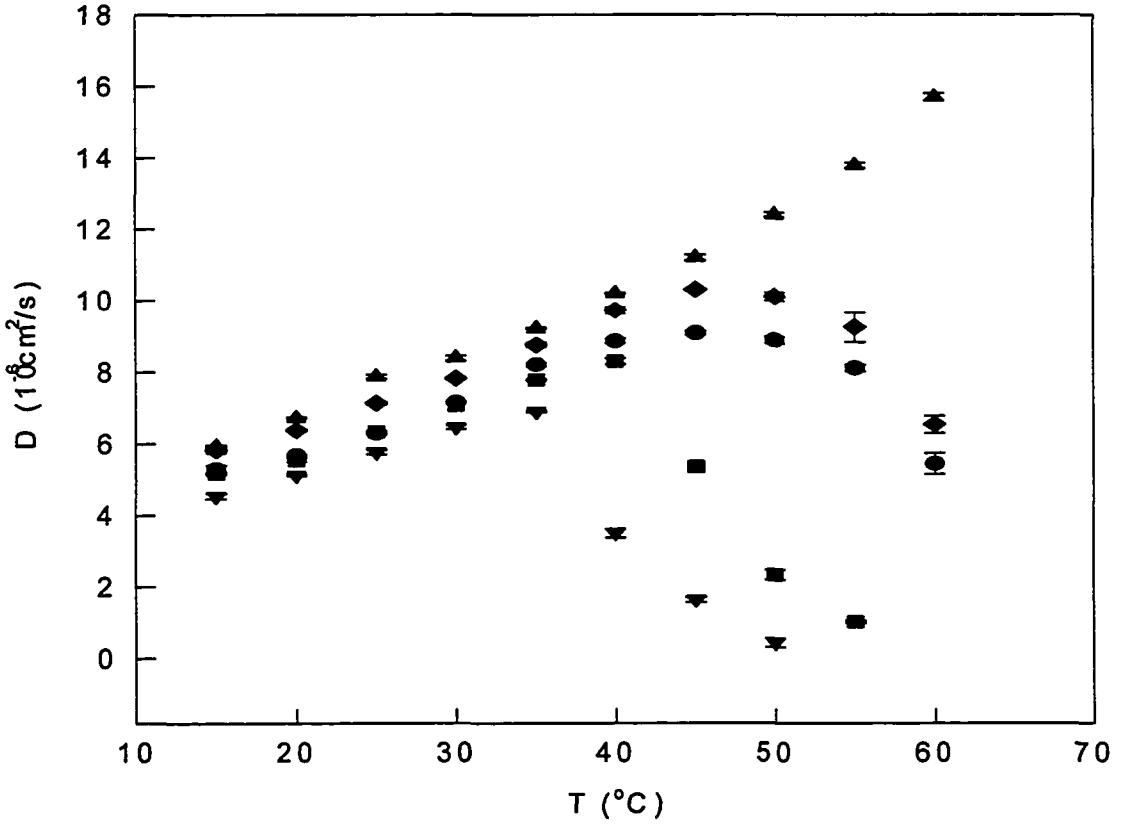

Figure 6.10 Diffusion coefficients of 4mM $Ru(NH_3)_6^{3+}$ determined by stair-case voltammetry in NIPA-AA gels and solution: ▲ in 0.1 M NaCl solution and in, ● 1%,◆2%, ■ 3%, ▼ and 4% gel. All gels with 0.1 M NaCl as supporting electrolyte

cations with acrylic acid groups of swollen NIPA-AA gels. However, with increasing temperature, the hydrogen bonds between water molecules, and between water molecules and polymer networks, will gradually be destroyed because of vigorous thermal motions of water molecules. This leads to loss of water molecules that are loosely bound to the polymer network. It induces a decrease in the total volume of the polymeric gel and brings various chemical groups of the NIPA network closer to each other. For NIPA-AA gels, negative acrylic groups are much closer to each other in collapsed gels than in the swollen state and as a result the total charge density of the NIPA-AA collapsed gel is much higher than that of a swollen network. Since $Ru(NH_3)_6^{3+}$ is a trivalent cation, it should be strongly attracted by negative acrylic groups. As a consequence, the diffusion movement of $Ru(NH_3)_6^{3+}$ is slowed by such interactions. Its diffusion coefficient in collapsed NIPA-AA gels decreases more than that of $FcTMA^+$ ion.

Figure 6.11 presents results obtained by chronoamperometry, according to eq 2.2.11. As one can see, the diffusion coefficient of $Ru(NH_3)_6^{3+}$ decreases when the temperature reaches the volume phase transition. However, it does not decrease as significantly as indicated by steady-state voltammetry (compare with Figure 6.10). It has been demonstrated [126] that NIPA gels in the collapsed state strongly adsorbed the organic molecule (e.g., benzoic acid) dissolved in water while NIPA-SSNa gels exclude salts (e.g., LiCl, CH_3COONa, KSCN) from their collapsed state above the transition

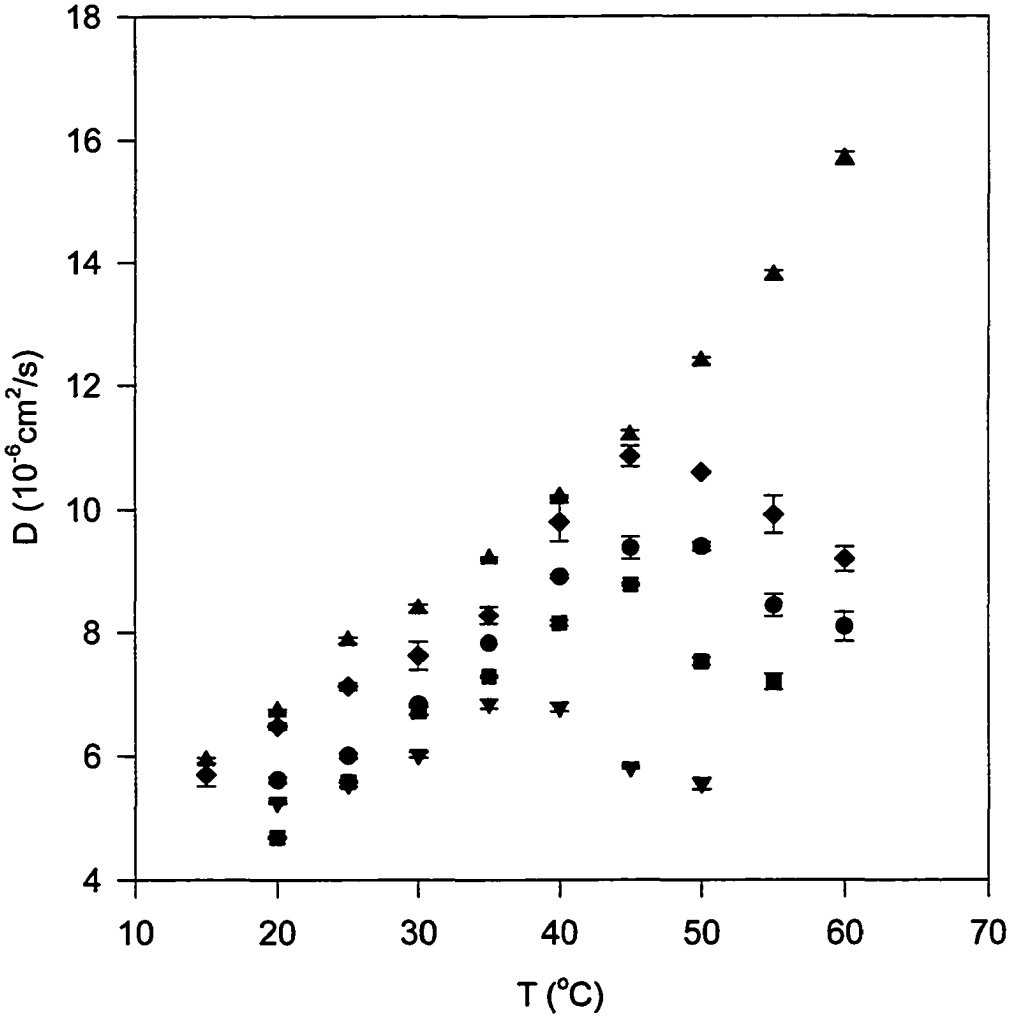

Figure 6.11. Temperature dependence of the diffusion coefficient of $Ru(NH_3)_6^{3+}$ determined by chronoamperometry in NIPA-AA gels and solution: (▲) 0.1 M NaCl solution, in (◆) 1%, (●) 2%, (■) 3%, and (▼) 4% NIPA-AA gel. 4 mM $Ru(NH_3)_6^{3+}$, all gels with 0.1 M NaCl.

temperature. Since $Ru(NH_3)_6Cl_3$ is an inorganic salt, it may be excluded more effectively from the collapsed NIPA-AA gel.

To study electrostatic interactions between the $Ru(NH_3)_6^{3+}$ probe and the polymeric network, 2.0% NIPA-AA gel without electrolyte was prepared. Figure 6.12 shows the temperature dependence of the transport of $Ru(NH_3)_6^{3+}$ in water and 2.0% NIPA-AA gel without supporting electrolyte, and for comparison in 0.1 M NaCl solution and 2.0% gel with 0.1 M NaCl. The transport coefficients of $Ru(NH_3)_6^{3+}$, calculated according to eq 2.2.9, are higher in pure water than those in 0.1 M NaCl solution. This is due to migration contributing to the total flux of $Ru(NH_3)_6^{3+}$ in solution without electrolyte, and consequently higher limiting current compared to purely diffusion current. According to theoretical prediction [124], the total limiting current for one electron reduction of +3 charged ion should be 1.173 times of the diffusion current. Our experimental value is 1.19, very close to that theoretically expected.

For temperatures lower than 25 °C, well below the volume phase transition temperature, there is no difference in the transport coefficients of $Ru(NH_3)_6^{3+}$ in 2.0% gel without electrolyte and those in 2.0% gel with 0.1 M NaCl. Transport of $Ru(NH_3)_6^{3+}$ in the gel without electrolyte begins to slow above 25 °C, and this effect is more significant at higher temperatures. For example, transport coefficients in 2.0% gel without electrolyte, calculated from eq 2.2.9, is 42% and 12% of that in pure water at 35 and 55 °C, respectively, and 56% and 24% of that in 2% gel with 0.1 M NaCl at 35 and 55 °C, respectively. At 55 °C the transport coefficient of $Ru(NH_3)_6^{3+}$ in 2.0% collapsed

NIPA-AA gel without electrolyte determined by chronoamperometry is 5.8×10^{-6} cm^2s^{-1}, only 35% of that in water without polymeric network (we assume the same ionic strength of both media). Note that for monovalent cation, $FcTMA^+$, the transport coefficient in 2% NIPA-AA gel without electrolyte was 58% of that in water, and for an uncharged probe, $Fc(MeOH)_2$, it was 76% of that in water under the same conditions determined by chronoamperometry. As one can see, the transport coefficient of the trivalent cationic probe in collapsed gels without electrolyte decreases more significantly than that of the monocharged cationic probe, and the transport of cations is significantly slower than that of uncharged probes.

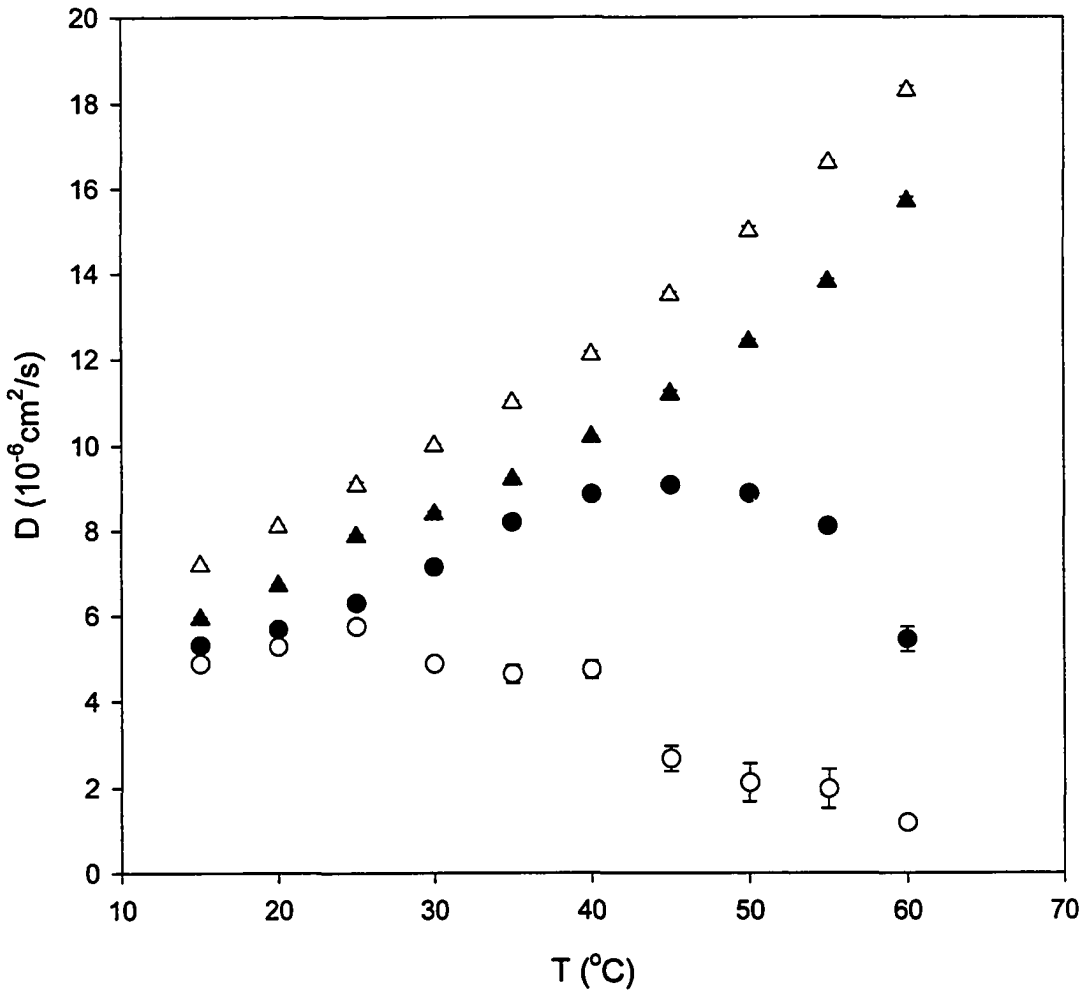

Figure 6.12 Temperature dependence of the diffusion coefficient of $Ru(NH_3)_6^{3+}$ determined by steady-state voltammetry in NIPA-AA gels and solutions (▲) 0.1 M NaCl solution, (Δ) water, (●) 2% gel with 0.1 M NaCl, and (O) 2% NIPA-AA gel without electrolyte.

Conclusions

Temperature responsive NIPA and NIPA-AA gels were synthesized by a free radical polymerization procedure. These gels were purified by a new procedure developed by us. Once washing was complete, a gel was formed with a well-defined polymer-to-solvent ratio and a known concentration of the electroactive probe following the new procedure developed by us.

The oxidation of electroactive probes, which include 1,1'-ferrocenedimethanol ($Fc(MeOH)_2$), TEMPO, $FcTMA^+$ and $Ru(NH_6)^{3+}$ was studied in aqueous solutions and the swollen state NIPA and NIPA-AA gels using steady state voltammetry on Pt microdisk electrodes. The diffusion coefficient of these probes was calculated based on the corresponding steady-state current.

The diffusion coefficient of $Fc(MeOH)_2$ in the gels is only about 15% - 55% smaller than that in aqueous solution. However, the viscosity of gels is approximately 5 orders of magnitude greater than that of aqueous solution. The value of activation energy (E_a) for the diffusion of $Fc(MeOH)_2$ in aqueous solution and in NIPA and NIPA-AA gels was almost identical. These data suggest that the microscopic viscosity of solvent trapped in swollen gel network is similar to that in aqueous solution.

A decrease of the diffusion coefficient of a probe in swollen gels was analyzed in terms of the "obstruction effect" and "hydration effect". In our mode, the diffusion coefficient of probes in swollen gels, D', can express by: $D'/D^0 = -1.667H\varphi+1$. The H-values determined by us for NIPA and NIPA-AA hydrogels are 3.22 and 8.77,

respectively. Theoretical *D* values for TEMPO in NIPA-AA gels calculated by our model have been compared with those measured using steady-state voltammetry. The difference between calculated values and experimental values was less than 7%, which means that they were identical within experimental error.

For NIPA gels, after the volume phase transition, the diffusion coefficient of $Fc(MeOH)_2$ in the collapsed gels decreased approximately 2 orders of magnitude when the gel collapsed. This significant decrease is due to the compact polymer structure formed after loss of 93% of the solvent during the volume phase transition. In addition the liquid channels for molecular/solvent transport are considerably restricted.

Transport of $FcTMA^+$ in a collapsed NIPA-AA gel is quite different from that in swollen gel. The diffusion coefficient of $FcTMA^+$ decreases significantly in NIPA-AA collapsed gels compare to an aqueous solution. After the volume phase transition occurs, a decrease of the diffusion coefficient of $FcTMA^+$ in NIPA-AA gel without supporting electrolyte is more pronounced than that in NIPA-AA gel with electrolyte. This indicates that there are stronger electrostatic attractive interactions between $FcTMA^+$ and the negatively charged polymeric network without an excess of electrolyte.

Voltammetric experiments were also carried out for trivalent positively charged $Ru(NH_3)_6^{3+}$ in NIPA-AA gels with supporting electrolyte. When the phase transition occurred, the diffusion coefficient decreased much more than those for $FcTMA^+$. In NIPA-AA gel system without supporting electrolyte, this effect is even more significant. Since $Ru(NH_3)_6^{3+}$ is a trivalent cation, it should have stronger electro-attractive

interaction with the negative charged acrylic acid groups in NIPA-AA networks. As a consequence, the diffusion movement of $Ru(NH_3)_6^{3+}$ is hindered by such interactions.

UV-vis spectroscopy was used to study the distribution of $Fc(MeOH)_2$ between the collapsed polymer phase and released solution during the volume phase transition. We found that the polymer phase absorbs $Fc(MeOH)_2$ during the phase transition of gels. An estimate of the concentration of $Fc(MeOH)_2$ in the collapsed gel is 4.5 times higher than that in the original swollen gel and 6 times higher than that in released liquid. The collapsed NIPA-AA gel phase absorbs $Fc(MeOH)_2$, but this effect is much weaker than in NIPA gel. The concentration of $Fc(MeOH)_2$ in collapsed NIPA-AA gel is about 20% higher than that in the original swollen gels.

Bibliography

[1] Tanaka; T. Phase Transition of Gels. *In Polyelectrolyte Gels. Properties, Preparation and Application*, Harland, R. S., Prud'homme, R. K., Eds.; ACS Symposium Series, Vol.480; American Chemical Society; Washington, DC, **1992**;

[2] Tanaka, T.; Fillmore, D.J.; Sun, S. T.; Nishio, I..; Swislow, G., Shah, A. *Phys. Rev. Lett.* **1980**, *45*,1636

[3] Dusek, K.; Patterson, D. *J. Poly. Sci.* **1968**, *part A-2*, 6, *1209.*

[4] Dagani, R. *C&EN.* **1997**, *June 9*, 26.

[5] Hirokawa, Y.; Tanaka, T.; Sato, E. *Macromolecules* **1985**, *18*, 2782.

[6] Hirotsu, S.; Hirokawa, Y.; Tanaka, T. *J. Chem. Phys.* **1984**, *81*, 1392.

[7] Kawasaki, H.; Sasaki, S.; Maeda, H. *Jour. Phy. Chem. B* **1997**, *101*,5089.

[8] Shibayama, M.; Fujikawa, Y.; Nomura, S. *Macromolecules* **1996**, *29*, 6535.

[9] Ilmain, E.; Tanaka, T.; Kokufuta, E. *Nature* **1991**, *349*, 400

[10] Bae, Y.H.; Okano, T.; Kim, S. W. *J. Controlled Release* **1989**, *9*, 271

[11] Myoga, A.; Katayama, S. *Polym. Prep. Japan* **1987**, *36*, 2852

[12] Hirotsu, S.; Hirokawa, Y.; Tanaka, T. *J. Chem. Phys.* **1987**, *87*, 1392

[13] Otake, K.; Inomata, H.; Konno, M.; Saito, S. *J. Chem. Phys.* **1989**, *91(2)* 1345

[14] Sasaki, S.; Kawasaki,H.; Maeda, H. *Macromolecules* **1997**, *30*,1847

[15] Sasaki, S.; Maeda, H. *Phys. Rev. E* **1996**, *54*, 2761

[16] Sasaki, S.; Kawaski, H.; Maeda, H. *Langmuir* **1999**, *15*, 4266

[17] Marchetti, M.; Cussler, E. L. *Macromolecules* **1990**, *23*, 1760

[18] Mamada, A.; Tanaka, T.; Kungwatchakun, D.; Irie, M. *Macromolecules* **1990**, *24*, 1605

[19] Suzuki, A.; Tanaka, T. *Nature* **1990**, *346*, 345

[20] Gudeman, F. L.; Peppas, F. N. *J. Appl. Poly. Sci.* **1995**, *55*, 919

[21] Zhang, X.; Takegochi, K.; Hikichi, K. *Polymer* **1992**, *46*, 1967

[22] Ricka, J.; Tanaka, T. *Macromolecules* **1984**, *17*, 2916

[23] Kokufuta, E.; Zhang, Y-Q.; Tanaka, T. *Nature* **1991**, *351*, 302

[24] Hoffman, A. S. *J. Controlled Release* **1987**, *6*, 297

[25] Okano, T.; Bae, Y. H.; Jacobs, H.; Kim, S. W. *J. Controlled Release* **1990**, *11*, 255

[26] Hoffman, A. S. Afrasiabi, A., Dong, L. C. *J. Controlled Release* **1986**, *4*, 213

[27] Inomata, H.; Nagahama, K.; Saito, S. *Macromolecules* **1994**, *27*, 6459

[28] Shibayama, M.; Ikkai, F.; Inamoto, S.; Nomura, S. *J. Chem. Phys.* **1996**, *105(10)*, 4358

[29] Lowe, J. S.; Chowdhry, B. Z.; Parsonage, J.; Snowden, M.J. *Polymer* **1998**, *39* 1207

[30] Akashi, M.; Nakano, S.; Kishida, A. *J. Polym. Sci., Part A: Polym. Chem.* **1996**, *34*, 301

[31] Duracher, D.; Elaissari, A.; Pichot, C.; *J. Polym. Sci., part A Polym. Chem.* **1999**, *27 (12)*, 1823

[32] Fujishige, S.; Kubota, K.; Ando, I. *J. Phys. Chem.* **1989**, *93*, 3311

[33] Bae, H. Y.; Okano, T.; Kim, S. W. *J. Polym. Sci., Part B: Polym. Phys.* **1990**, *28*, 923

[34] Wada, N.; Yagi, Y.; Inomata, H.; Saito, S. *Macromolecules* **1992**, *25*, 7220

[35] Inomata, H.; Wada, N.; Yagi, Y.; Saito, S. *Polymer 1995, 36*, 875

[36] Jin, M. R.; Wu, C. F.; Lin, P. Y.; Hou, W. *J. Appl. Poly. Sci.* **1995**, *56*, 285

[37] Wada, N.; Yagi, Y.; Inomata, H.; Saito, S. *J. Polym. Sci., part A Polym. Chem.* **1993**, *31*, 2647

[38] Heskins, M.; Guillet, J. E. *J. Macromol, Sci. Chem.* **1968**, *A2(8)*, 1441

[39] Tanaka, T.; Fillmore, J. D. *J. Chem. Phys.* **1979**, *70*, 1214

[40] Tanaka, T.; Hocker, L. O.; Benedek, G. B. *J. Chem. Phys.* **1973**, *59*, 5151

[41] Li, Y.; Tanaka, T. J. Chem. Phys. 1989, 90, 5161

[42] Kawaski, H.; Sasaki, S.; Maeda, H. *Langmuir* **1998**, *14*, 773

[43] Kaneko,Y.; Sakai, K.; Kikuchi, A.; Yoshida, R.; Sakurai, Y.; Okano, T. *Macromolecules* **1995**, *28*, 7717

[44] Yoshida, R.; Uchida, K.; Kaneko,Y.; Sakai, K.; Sakurai, Y.; Okano, T. *Nature* **1995**, *374*, 240

[45] Shibayama, M.; Fujikawa, Y.; Nomura, S. *Macromolecules* **1996**, *29*, 6535

[46] Pelton, R. H.; Chibante, P. *Colloids, Surf.* **1986**, *20*, 247

[47] Gao, J.; Hu, Z. *Langmuir* **2002**, *18*, 1360

[48] Martinez-Rubio, M. I.; Ireland, T. G.; Fern, G. R.; Silver, J.; Snowden, M. J. *Langmuir* **2001**, *17*, 7145

[50] Daly, E.; Saunders, B. *Langmuir* **2000**, *16*, 5546

[51] Senff, H.; Richtering, W. *J. Chem. Phys.* **1999**, *111*, 1705

[52] Saunders, B. R.; Vicent, B. *Adv. Coll. Int. Sci.* **1999**, *80*, 1

[53] Pelton, R. *Adv. Coll. Int. Sci.* **2000**, *85*, 1

[54] Zhang, X. Z.; Zhou, R. X. *Langmuir* **2001**, *17*, 12

[55] Zhang, X. Z.; Yang, Y. Y.; Chung, T. S.; Ma, K. X. *Langmuir* 2001, 17(20), 6694

[56] Serizawa, T.; Wakita, K.; Akashi M. *Macromolecules* **2002**, *35(1)*, 10

[57]Hirotsu, S. *Adv. Polym. Sci.* **1993**, *110*, 1

[58] Wu, C.; Zhou, S. *Macromolecules* **1996**, *29*, 4998

[59] Shibayama, M.; Tanaka, T.; Han, C. C. *J. Chem. Phys.* **1992**, *97(9)*, 6842

[60] Shibayama, M.; Ikkai, F.; Inamoto, S.; Nomura, S.; Han, C. C. *J. Chem. Phys.* **1996**, *105(10)*, 4358

[61] Borue, V.; Enikhimovich, I. *Macromolecules* **1988**, *21*, 3240

[62] Vesterinen, E.; Dobrodumov, A.; Tenhu, H. *Macromolecules* **1997**, *30*, 1311

[63] Spevacek, J.; Suchoparek, M. *Macromolecules* **1997**, *30*, 2178

[64] Wang, X.; Wu, C. *Macromolecules*, **1999**, *32(13)*. 4299

[65] Mylonas, Y.; Stailcos, G.; Lianos, P. *Langmuir*, **1999**, *15(21)*, 7172

[66] Vernon, B.; Gutowska, A.; Kim, S. W.; Bae, Y. H. *Macromol. Symp.* **1996**, *109*, 155

[67] Feil, H.; Bae, Y. H.; Feijen, J.; Kim, S. W. *J. Membr. Sci.* **1991**, *64*, 283

[68] Saitoh, T.; Yoshida, Y.; Matsudo, T.; Fujiwara, S.; Dobashi, A.; Iwaki, K.; Suzuki, Y.; Matsubara, C. *Anal. Ch*em. **1999**, *71*, 4506

[69] Go, H.; Sudo, Y.; Hosoya, K.; Ikegamim T.; Tanaka, N. *Anal. Ch*em. **1998**, *70*, 4086

[70] Gehrke, S. H.; Andrews, G. P.; Cussler, E. L. *Chem. Eng. Sci.* **1986**, *41*, 2153

[71] Yoshida, R.; Takahashi, T.; Yamaguchi, T.; Ichiji, H. *J. Am. Chem. Soc.* **1996**, *118*, 5134

[72] Li Y; Hu, Z.; Chen, Y. *J. Appl. Polym. Sci.* **1997**, *63*, 1173

[73] Osada, Y.; Okuzaki, H.; Hori. H. Nature 1992, 355, 242

[74] Osada, Y. *Advances in Polymer Science*; Springer-Verlag; Berlin, 1987; Vol. 81, p1

[75] Stile, R. A.; Burghardt, W. R.; Healy, K. *Macromolecules*, *32*, 7370

[76] *Polyelectrolytes: Science and Technology*, Hara, M., Ed.; Marcel Dekker: New York, 1993

[77] Hariharan, D.; Peppas, N.A. *Polymer* **1996**, *37*, 149

[78] Peppas, N. A.; Mongia, N. K. *Eur. J. Pharm. Biopharm.* **1997**, *43*,51

[79] Peppas, N. A.; Wright, S. L. *Eur. J. Pharm. Biopharm.* **1998**, *46*, 15

[80] Bansil, R.; Pajevic, S.; Konak, C. *Macromolecules* **1995**, *28*, 7536

[81] Melnichenko, Y. B., Klepko, V .V.; Shilov, V. V. *Polymer* **1993**, *34*, 1019

[82] Matsukaa, S. Ando, I., *Macromolecules* **1996**, *29*, 7136

[83] Tatistcheff, H. B.; Fritsch-Faules, I., Wrighton. M. S. *J. Phys. Chem.* **1993**, *97*, 2732

[84] Winlove, C. P.; Parker, K. H.; Oxenhan, R. K. C. *J. Electroanaly. Chem.* **1984**, *170*, 293.

[85] Denuaault, G.; Mirkin, V. M.; Bard, J. A. *J. Electroanaly. Chem.* **1991**, *308*, 27

[86] McLin, M. G.; Angell, C. A. *J. Phys. Chem.* **1996**, 100, 1181

[87] Fan, F.-R. F. *J. Phys. Chem. B*, **1998**, *102*, 9777

[88] Pyo, M.; Bard, J. A. *Electrochimica Acta*, **1997**, *42*, 3077

[89] Hyk, W.; and Ciszkowska, M. *J. Phys. Chem. B* 1999, *103*, 6466-6474

[90] Ciszkowska, M.; Osteryoung, J. G. *J. Phys. Chem.* **1994**, *98*, 3194

[91] Ciszkowska, M.; Guillaume, M. D. *J. Phys. Chem. A* **1999**, 103, 607

[92] Fuller, J.; Breda, A. C.; Carlin, R. T. *J. Electrochem. Soc.* **1997**, *144*, L67

[93] Wightman, R. M. *Anal. Chem.* **1981**, *53*, 1125A

[94] Fleischmann, M.; Pons, S.; Rolison, D. R.; Schmidt, P. P. Eds.; "Ultramicroelectrode:, Datatech Systems, Morganton, NC, 1987

[95] Ciszkowska, M.; Osteryoung, J. G. *J. Phys. Chem.* **1998**, *102*, 291

[96] Ciszkowska, M.; Osteryoung, J. G. *J. Phys. Chem.* **1996**, *100*, 4630

[97] Collinson, M. M.; Zambarano, P. J.; Wang H.; Taussig, J, S. *Langmuir* **1999**, 15, 662

[98] Bard. A. J.; Faulkner, L. R. Electrochemical Methods: Fundamentals and Application, 2nd Edition. John Wiley &sons, Inc. 2001

[99] Ciszkowska, M.; Donten, M.; Stojek, Z. *Anal. Chem.* **1994**, *66*, 4112

[100] Ciszkowska, M.; Osteryoung, J. G. *Anal. Chem.* **1995**, *67*, 1125

[101] Birke, R. L.; Huang, Z. *Anal. Chem.* **1992**, *64*, 1513

[102] Aoki, K.; Osteryoung, J. *J. Electroanaly. Chem.* **1981**, *122*, 19

[103] Shoup, D.; Szabo, A. *J. Electroanal. Chem.* **1982**, *140*, 237

[104] Forouzan, F.; Bard, A. J.; Mirkin, M. V. *Israel J. Chem.* 1997, 37, 155

[105] Graselli, J. G. *Atlas of Spectral Data and Physical Constants for Organic Compounds*; CRC Press: Cleveland OH, 1973.

[106] Orchin, M.; Jaffe, H. H. *Symmetry, Orbitals and Spectra*; Wiley-Interscience: New York, 1971; Chapter 8.

[107] Hyk, W.; Ciszkowska, M. *J. Phys. Chem. B.* **1999**, *103*, 6466

[108] Fan, F.-R. F. *J. Phys. Chem. B*, **1998**, *102*, 9777

[109] Jacob, S. R.; Hong, Q.; Coles, B. A.; Compton, R. G. *J. Phys. Chem. B* 1999, *103*, 2963

[110] Fricke, H. *Phys. Rev.* **1924**, *24*, 575

[111] Waggoner, A. R.; Blum, F. D.; MacElroy, J. M. D. *Macromolecules* **1993**, *26*, 6841

[112] Fujita, H. *Adv. Polym. Sci.* **1961**, *3*,1

[113] Yasuda, H.; Lamaze, C. E.; Ikenberry, L. D. *Die. Makro. Chem.* **1968**, *118*, 19

[114] Cukier, R. I.; *Macromolecules* **1984**, *17*, 252

[115] Cheever, E.; Blum, F. D.; Foster, K. R.; Mackay R. A. *J. Colloid Interface Sci.* **1985**, *104*, 121

[116] Meerwall, E. V.; Mahoney, D.; Iannacchione, G.; Skowronski, D. *J. Colloid Interface Sci.* **1990**, *139*, 437

[117] Wang, J. H. *J. Amer. Chem. Soc.* **1947**, *76*, 4755

[118] Duval, P. F.; Porion, P.; Damme, V. H. *J. Phys. Chem. B* **1999**, *103*, 5730

[119] Lee, H. B.; Jhon, M. S.; Andrade, J, D. *J. Colloid Interface Sci.* **1975**, *51*, 255

[120] Malmsten, R. A.; White, H. S. *J. Electrochem. Soc.* **1986**, *133*, 1067

[121] Hyk, W.; and Ciszkowska, M. *J. Electrochem. Soc.* **2000**, *147(6)*, 2268

[122] Okajima, T; Harada, I.; Nishio, K.; Hirotsu, S. *J. Chem. Phys.* **2002**, *116*, 9068

[123] Kawasaki, H.; Mitou, T.; Sasaki, S.; Maeda, H. *Langmuir* **2000**, *16*, 1444

[124] Cooper, J. B.; Bond, A. M.; Oldham, K. B. *J. Electroanal. Chem.* **1992**, *331*, 877

[125] Tokuhiro, T. *J. Phys. Chem. B* **1999**, *103*, 7097

[126] Koga, S.; Sasaki, S.; Maeda, H. *J. Phys. Chem. B* **2001**, *105*, 4105